ILLINOIS TOLLWAY RESEARCH PROGRAM

UTILIZATION AND LIMITATIONS OF RECYCLED ASPHALT PAVEMENT (RAP) AS ROADWAY EMBANKMENT MATERIAL

DRAFT FINAL REPORT

By

Haifang Wen, PhD, PE, Associate Professor

Mohammadreza Barzegar, Graduate Student

Maziar Mivehchi, Graduate Student

Idil Akin, PhD, Assistant Professor

Balasingam Muhunthan (the late), PhD, PE, Professor

Dept. of Civil & Environmental Engineering
Washington State University

and

Tuncer Edil, PhD, PE, Professor Emeritus

Dept. of Civil & Environmental Engineering

University of Wisconsin-Madison

Submitted to:

Illinois State Toll Highway Authority

January, 2022

DISCLAIMER

The contents of this report reflect the views of the authors who are responsible for the facts and the accuracy of the data presented herein. The contents do not necessarily reflect the official views or policies of Washington State University or the Illinois State Toll Highway Authority. This report does not constitute a standard, specification, or regulation.

ACKNOWLEDGEMENTS

This study was funded by the Illinois State Toll Highway Authority (Illinois Tollway). The authors greatly appreciate the sponsorship of the Authority and especially the input and support from Mr. Ross Bentsen and Ms. Cynthia Williams of Illinois Tollway, Dr. Supraja Reddy and Dr. Sanjeev Bandi of Interra, Inc., Dr. William Vavrik of Applied Research Associates, Inc., and the rest of the project panel. This work could not have been completed without the help of the undergraduate assistants, Mr. Gavin Yip and Mr. Sam Adewale, of Washington State University.

TECHNICAL REPORT DOCUMENTATION PAGE

1. Report No.	2. Government Accession No	3. Recipient's Catalog No
4. Title and Subtitle Utilization and Limitations of Recycled Asphalt Pavement (RAP) as Roadway Embankment Material		5. Report Date December 2021 6. Performing Organization Code
7. Authors Haifang Wen, Mohammadreza Barzegar, Maziar Mivehchi, Tuncer Edil, Idil Akin, and Balasingam Muhunthan		8. Performing Organization Report No.
9. Performing Organization Name and Address Washington Center for Asphalt Technology Department of Civil and Environmental Engineering Washington State University Spokane Street, Pullman, WA 99164		Work Unit No. (TRAIS) Contract or Grant No. RR-20-9224
12. Sponsoring Agency Name and Address Illinois State Toll Highway Authority 2700 Ogden Ave Downers Grove, IL 60515		13. Type of Report and Period Covered 14. Sponsoring Agency Code
15. Supplementary Notes		

16. Abstract

Recycled asphalt pavement (RAP) refers to unprocessed (e.g., milled) or processed (e.g. screened) asphalt mixture obtained from roadways or other resources. The use of RAP is a sustainable practice that potentially could contribute to reduced costs, preservation of the environment, and reduction of greenhouse gas emissions, provided that the engineering performance of the roadways that utilize RAP is not compromised. Reports indicate that some pavements that utilize RAP as embankment material experienced excessive settlement soon after construction. In order to investigate this issue, the research team reviewed design and construction documents. The team then procured RAP samples from five sources used by Illinois Tollway contractors and two conventional soils (as references) for laboratory experiments that included testing for basic soil/RAP characteristics, gradations, moisture-density relationships at different temperatures, permeability, and drainage as well as one-dimensional consolidation tests, dynamic triaxial tests, and conducted settlement analysis. The results show that RAP, considered as permeable material, should not be used directly underneath the pavement drainage layer, within the top five feet of a rigid pavement embankment or eight feet of a flexible pavement embankment, or immediately above underground concrete/metal structures or bedrock. RAP should be compacted to 100% of its maximum dry density in accordance with the standard Proctor test method. It is recommended that the settlement analysis during design should consider the potential settlement of embankment soil from as-compacted condition to saturated condition, as well potential settlement associated with fast-track construction of RAP layer in embankment.

17. Key Words	18. Distribution Statement
Recycled asphalt pavement (RAP), embankment, settlement, triaxial, drainage	

19. Security Classif. (of this report)	19. Security Classif. (of this page)	20. No. of Pages	21. Price

Table of Contents

LIST OF FIGURES

LIST OF TABLES

CHAPTER 1 INTRODUCTION

1.1 Background

Recycled asphalt pavement (RAP) refers to unprocessed (e.g., milled) or processed (e.g., screened) asphalt mixtures obtained from roadways or other resources (FHWA-RD-97148, 2008). Although RAP often is used in hot/warm mix asphalt (HMA/WMA) in asphalt plants, the *in situ* use of RAP offers advantages in terms of reduced costs and/or expedited construction without hauling. These advantages are especially applicable for roadway rehabilitation or widening projects, particularly high traffic tollway projects that have a tight construction schedule.

In the past, the Illinois State Toll Highway Authority (commonly known as the Illinois Tollway) allowed the use of RAP, both unprocessed and processed without expansive aggregate, in roadway embankments as well as for aggregate surfaces in accordance with Illinois Department of Transportation (IDOT) specifications. However, the use of RAP material in roadway embankments per IDOT specifications was loosely specified in terms of maximum aggregate size, gradation, engineering properties, and acceptance qualifications. For instance, the maximum size of RAP particles and its gradation were not specified except within 12 in. from the finished surface of the earth grade. The degree of compaction of RAP currently is based on standard laboratory maximum density and varies from a minimum 95% standard laboratory maximum density (AASHTO T 99 Method C with corrections to large particles) for the top 1.5 ft to a minimum 90% for 3 ft or deeper. The maximum lift thickness is 8 in. and the acceptance of RAP compaction on site is based on nuclear measurements (AASHTO T 191 or modified AASHTO T 310), which do not accurately account for moisture content due to the existence of hydrogen in asphalt.

Although the use of RAP in embankments works well in most instances, a few failures have been reported. For example, in December 2015, unprocessed RAP grindings were used in the reconstruction of the Jane Addams Memorial Tollway (I-90) from Randall Road to Kennedy Expressway in Illinois as pavement embankment material and structural backfill to expedite the construction process. However, by the summer of 2016, severe settlement and pavement cracking issues had occurred, especially at culvert backfill areas. Subsequently, the Illinois

Tollway provided additional specifications for the use of RAP in roadway embankments or structural backfill through a special provision. Those specifications now include that RAP, when used in embankments or fill, must be processed material, must pass the 1.5-in. sieve, must be placed only at the ambient temperature of 40°F or higher, and must be covered with 3 ft of earth soil. Also, the lift thickness has been reduced from 8 in. to 6 inches. The specified quality acceptance of RAP is based on dynamic cone penetrometer measurements, with a required penetration rate of 1.5 in./blow or less.

RAP consists of discrete aggregate particles from coarse to fine and therefore acts like conventional granular soils that are affected by moisture, load level, etc., and compresses under loading. However, the behavior of RAP is complicated by the presence of the asphalt coating on the aggregate. Unlike conventional soils in most cases, the behavior of asphalt is viscoelastic and temperature-sensitive such that the modulus or stiffness of the asphalt decreases as the temperature increases (Roberts et al., 2009). In terms of compaction at a high temperature, the asphalt can deform, especially if the coating of the particles is uneven, thereby reducing the distance or voids between the RAP particles, whereas at a relatively low temperature, the asphalt becomes stiff and cannot be deformed easily, creating voids between particles. Therefore, the maximum dry density (MDD) of RAP decreases when RAP is compacted at low temperatures (e.g., during the late fall or winter) (Montemayor, 1998). When RAP is placed and compacted at a low temperature, the maximum dry density of RAP in an embankment or fill also would be low, which leads to less strength and more settlement.

In terms of modulus/stiffness and permanent deformation at high temperatures, due to the viscous behavior of asphalt, RAP has lower resilient modulus or stiffness values and higher plastic deformation values than conventional soils (Wen et al., 2008; Wen & Wu, 2011). In addition, due to the presence of asphalt, RAP is affected by the loading rate. At a high loading rate (e.g., high traffic speed), the modulus or stiffness of RAP is greater than that of conventional soils or aggregate (Wen et al., 2008; Wen & Wu, 2011; Attia & Abdelrahman, 2010). At a low loading rate or static loading (e.g., overburden pressure), RAP exhibits viscous behavior and tends to creep (secondary compression) over a long period of time (Cosentino et al., 2012; Soleimanbeigi et al., 2014; Viyanant et al., 2007; Soleimanbeigi & Edil, 2015), especially at high temperatures (e.g., during summer). Researchers have conducted uniaxial compression tests and triaxial compression tests and found that the creep strain of RAP under static loading is the

primary driving factor for the settlement or permanent deformation of embankment material or fill (Viyanant et al., 2007; Soleimanbeigi et al., 2014; Soleimanbeigi & Edil, 2015; Yin et al., 2017). Furthermore, the compaction temperature greatly affects the creep strain and compression rate (Soleimanbeigi & Edil, 2015; Yin et al., 2017). When RAP samples are compacted at a high temperature (e.g., during construction in summer), they are thermally preloaded and the creep rate is reduced. The opposite is true when RAP samples are compacted at a low temperature (e.g., in late fall or winter). In addition, dynamic loading from traffic may induce settlement, especially at the top of an embankment or fill.

Based on these considerations, a systematic approach is needed that addresses the settlement issues of RAP when it is used as embankment material.

1.2 Objectives

The primary objective of this proposed research is to determine the limits for using RAP as roadway embankment material. The work will result in the development of draft specifications for the required material and its placement.

1.3 Organization of Report

This report consists of six chapters. The first chapter introduces the background and objectives of the research. Chapter 2 presents findings of a literature review of related topics as well as the current practice of highway agencies based on survey results. Chapter 3 covers the forensic investigation of construction projects that used RAP in embankments and experienced excessive settlement. Chapter 4 describes the study materials and the laboratory tests that were conducted to determine the performance of RAP in embankments. Chapter 5 presents the test and analysis results. Chapter 6 provides conclusions, recommendations for further study, and proposed revisions to current special specifications.

CHAPTER 2 LITERATURE REVIEW AND SURVEY RESULTS

In order to understand the state-of-the-art and state-of-the-practice regarding the use of RAP in embankments, the research team reviewed the literature on this topic. The results are synthesized herein. In addition, the research team surveyed highway agencies to obtain information regarding their practices when using RAP in embankments.

2.1 Literature Review

2.1.1 Introduction

According to a survey conducted by the National Asphalt Pavement Association, nearly 82.2 million tons of RAP were used in new asphalt pavement roadways during the 2018 construction season. Most of that RAP was used in HMA, but only 2 million tons were used in embankments and backfill during the decade from 2009 to 2018 (Williams et al., 2019). This relatively insignificant use of RAP in subsurface construction can be attributed to its much greater value when used in HMA compared to its use in embankments and backfill.

Typically, RAP materials have 4.5% to 8.5% binder by the mass of the mix. The RAP binder has hardened and oxidized during its previous service life (Sandin, 2008) and, unlike conventional embankment soils, the aggregate particles of RAP are coated with aged binder. Asphalt binder exhibits time- and temperature-dependent behavior and thus the properties of RAP could be very different from those of conventional soils or aggregate used for geotechnical applications. Therefore, the use of RAP in embankments or backfill material requires a comprehensive assessment of its engineering properties. Previous studies have investigated various mechanical and hydraulic properties of RAP materials used in base layers, sub-base layers, embankments, and backfill and have compared the results for RAP with those for conventional soils and aggregate. Researchers also have investigated the effects of climatic conditions on these properties. As such, the purpose of this literature review is to summarize the engineering properties of RAP that is to be used in embankments and structural backfill materials based on the findings from previous studies.

2.1.2 RAP Properties

In this section, the quality of RAP as embankment and structural backfill material is assessed and compared to conventional materials used in embankment construction. The essential properties of RAP materials also are discussed.

2.1.2.1. Sources of RAP

The primary sources of RAP are from milling (or called grinding) and full-depth pavement removal (Copeland, 2011). Milling often takes place during pavement rehabilitation projects. The process involves machinery that grinds, picks up, and fills trucks with the resultant RAP. Figure 1 shows a stockpile of milled RAP (or called RAP grindings). The considerable pressure from milling machinery can lead to crushed aggregate and changes in the gradation of milled RAP compared to the original aggregate gradation used in HMA before milling (West, 2015).

FIGURE 1. Unprocessed RAP from a single stockpile (Copeland, 2011)**.**

Full-depth pavement removal consists of ripping the asphalt layer into slabs and processing the slabs into small particles. Figure 2 shows recycled pavement slabs produced from

full-depth pavement removal. Compared to milled products, RAP obtained from full-depth removal is prone to contamination of the underlying soil (Copeland, 2011).

FIGURE 2. Road slabs produced from full-depth demolition (West, 2015)**.**

2.1.3. Gradation and Variability of RAP

The screening and/or processing (i.e., crushing) of RAP can improve the consistency of RAP materials but also changes their gradation and properties (McDaniel and Anderson, 2001). Processing RAP materials that are produced from multiple sources is essential to improve the consistency of blended RAP, but also results in the final grain size distribution of RAP that is finer than that of milled-off RAP materials that did not undergo processing. Processed RAP often is used in HMA rather than in embankments or backfill materials.

Sandin (2008) investigated milled-off RAP and processed RAP stockpiles in the state of Florida and found that milled-off RAP particles are coarser than processed ones. Table 1 and Figure 3 provide summaries of the Sandin study results (Sandin, 2008). Table 1 shows that the nominal maximum aggregate sizes of the milled and processed particles are, on average, 0.93 in. and 0.5 in., respectively, and Figure 3 presents the average grain size distribution of the RAP. Figure 4 presents the results of another study that show the gradations of RAP and recycled pavement material (RPM) obtained from different states along with RAP limits found in the literature (Edil et al., 2012). The difference between RAP and RPM is that RPM includes the materials underneath the asphalt layer, such as the base or sub-base layer materials. Due to the

binder coating on the aggregate, RAP fines have low plasticity compared to fines in conventional soils (Sharma & Sivapullaiah, 2016).

TABLE 1. RAP Gradation Parameters (Sandin, 2008)

	Milled			**Processed (Crushed)**		
	Avg	Min	Max	Avg	Min	Max
Number of samples tested	52	-	-	43	-	-
NMAS, in.	0.93	0.5	1.5	0.5	0.37	1.0
Percent Passing #4	45%	29%	64%	59%	30%	72%
Percent Passing #200	0.6%	0.2%	1.6%	0.5%	0.1%	1.8%
D_{10}*, in.	0.022	0.011	0.056	0.015	0.008	0.075
C_u**	13	5	23	13	4	22
C_c***	1.8	0.7	4.2	1.2	0.4	2.9

Note: NMAS is nominal maximum aggregate size; * D_{10} is the effective size of particles that corresponds to 10% finer in the particle size distribution graph; ** C_u is the coefficient of uniformity; and *** C_c is the coefficient of curvature.

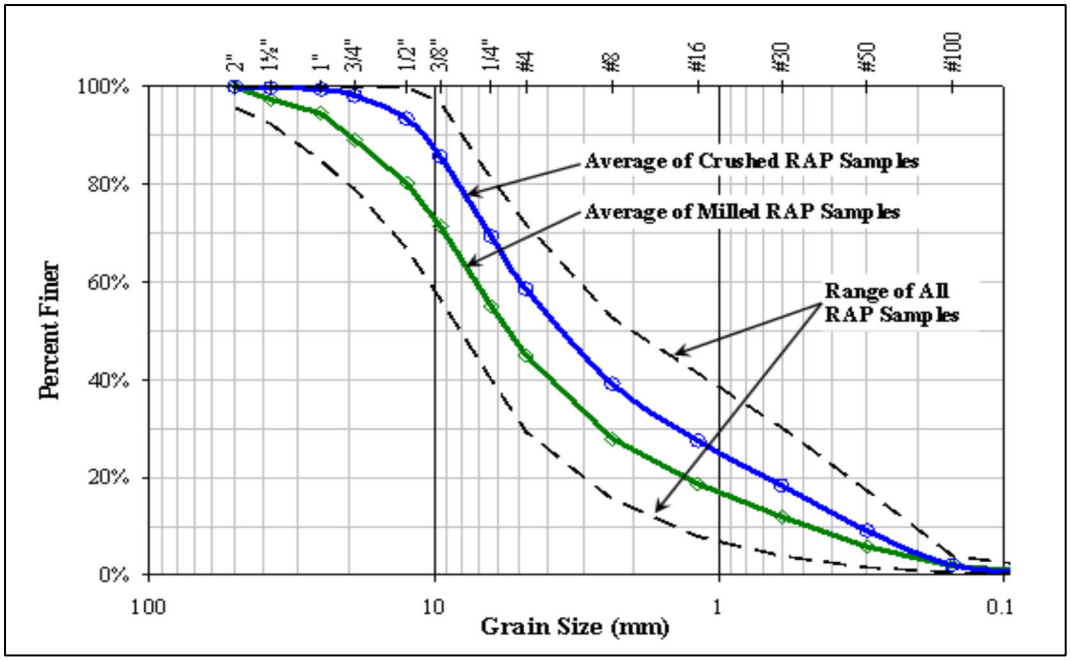

FIGURE 3. Average grain size distribution of reclaimed asphalt pavement (RAP) in Florida (Sandin, 2008)**.**

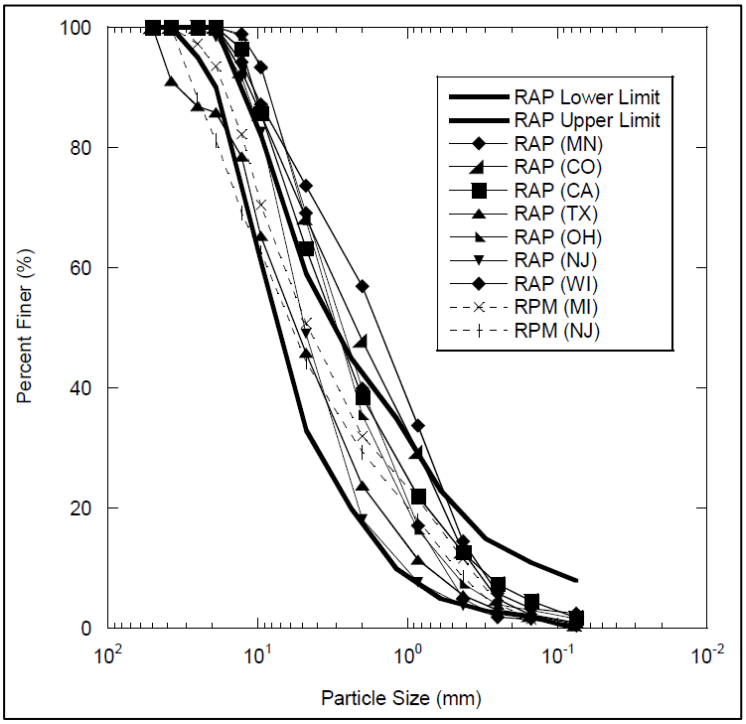

FIGURE 4. Reclaimed asphalt pavement (RAP) and recycled pavement material (RPM) gradations from different sources (Edil et al., 2012)**.**

2.1.4. Density and Moisture Content of RAP

The optimum moisture content (OMC) and maximum dry density (MDD) of RAP depend on the RAP gradation and source. Figure 5 shows the results for measured dry density vs. moisture content from various RAP stockpiles in Florida (Cosentino et al., 2003). When the moisture content changes, the dry density of RAP remains relatively constant, indicating that the dry density of RAP is relatively insensitive to moisture content (Cosentino et al., 2003; Montemayor, 1998). Edil et al. (2012) also investigated the OMC vs. MDD for RAP from different sources, as shown in Figure 6. They concluded that the existing binder in RAP will prevent water from easily reaching the aggregate particles, resulting in a relatively low OMC for RAP. Cosentino et al. (2012) found that the field density of RAP/soil mixtures can be higher than the MDD obtained from the modified Proctor test. Ping et al. (2003a; 2003b) also studied moisture density curves for A-3 soil that was compacted using different methods and found that the field density values typically were higher than the laboratory density values based on the standard or modified Proctor test. Therefore, specifying 100% MDD based on the modified Proctor method can be considered appropriate.

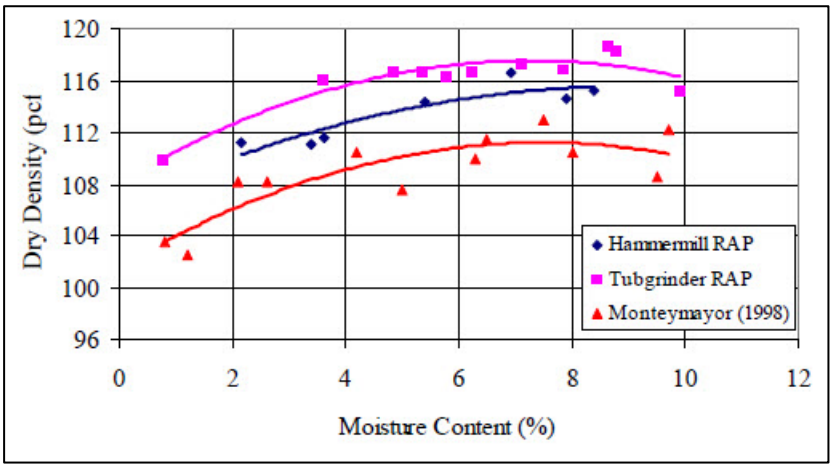

FIGURE 5. Dry density vs. moisture content for RAP materials measured by modified Proctor method (Cosentino et al., 2003)**.**

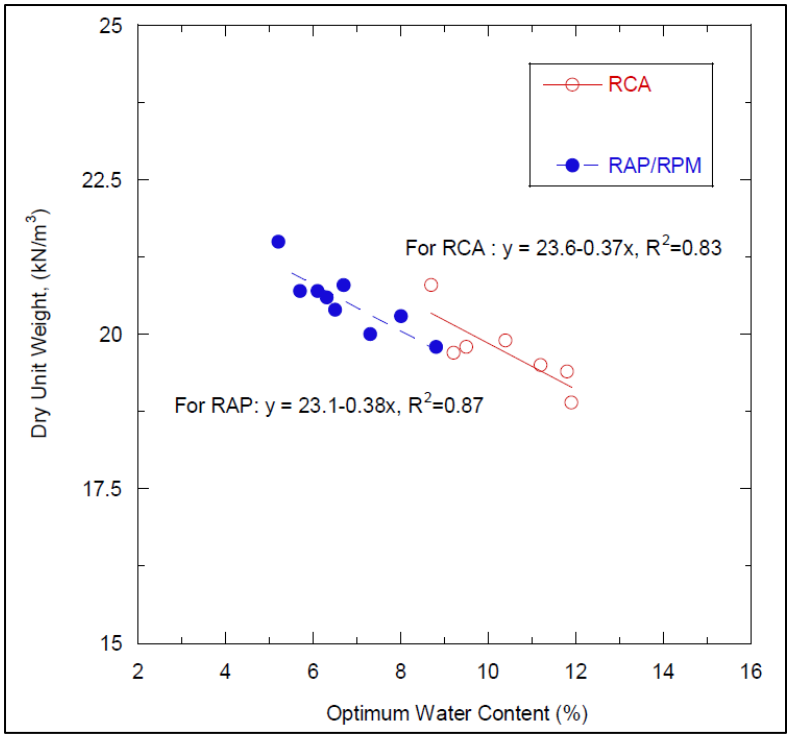

FIGURE 6. Relationship between optimum moisture content and maximum dry density for RAP/RPM and recycled concrete aggregate (RCA) (Edil et al., 2012)**.**

2.1.5. Mechanistic Properties

Researchers have studied several different mechanical properties of RAP, including the California bearing ratio (CBR), limerock bearing ratio (LBR), resilient modulus (M_r), friction angle (Φ'), and cohesion (c'). Some studies have compared the mechanical properties of 100% RAP with soils and natural aggregate whereas other studies have varied the RAP content in the sample to find an optimum RAP content based on the mechanical properties.

2.1.5.1. Friction Angle (Φ') and Cohesion (c')

Shear strength is an important engineering property, especially for materials used in layers beneath the surface. Arulrajah et al. (2013) reported that the internal friction angle of RAP is around 45.0°. This value is higher than that of typical sand and gravels (38.4°) (Holtz et al. 2015). Based on studies of RAP blended with fine sand, Cosentino et al. (2003) observed that the friction angle increases with an increase in the RAP percentage, as shown in Figure 7. On the other hand, the cohesion was found to increase initially and reach a maximum value before decreasing with the RAP percentage (Figure 7). A similar trend was found in studies that

investigated RAP blended with different aggregates (Bennert & Maher, 2005; El & Attia, 2010; Garg & Thompson, 1996; Kim & Labuz, 2007).

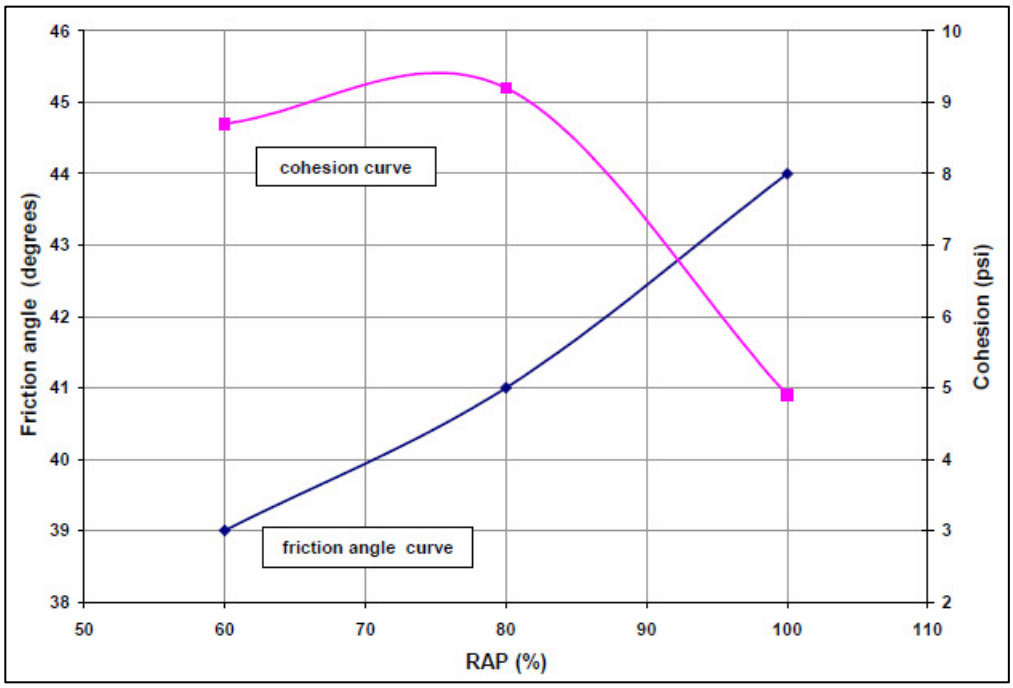

FIGURE 7. Variation of friction angle and cohesion with RAP content (Cosentino et al., 2003).

Bennert et al. (2000) and Doig (2000) reported cohesion of 2.32 psi for RAP samples. Soleimanbeigi et al. (2014) reported cohesion of 1.74 psi and Piratheepan et al. (2013) reported cohesion of 1.23 psi for RAP material. This large variation in reported cohesion values, especially from triaxial tests, may be due to the different asphalt contents of the RAP samples (Thakur & Han, 2015). In general, researchers have reported the friction angle of RAP to be between 42° (Soleimanbeigi et al., 2014) and 52° (Bejarano, 2001) and cohesion less than 2.32 psi (Doig, 2000) based on direct shear tests. Although the variation in cohesion values is significant, the trend of a decrease in cohesion with an increase in RAP content is evident in most studies (Bennert et al. 2000; Cosentino et al., 2003; Doig, 2000; Garg & Thompson, 1996; Thakur & Han, 2015). Note that this cohesion is the initial cohesion, and in the field the cohesion of RAP increases over the long term (Cosentino et al., 2003).

2.1.5.2. California Bearing Ratio, Limerock Bearing Ratio, and Resilient Modulus (M_r)

The CBR is the ratio of the penetration resistance of a material to that of standard crushed stone and is a measure of the strength and its bearing capacity under loading (Thakur & Han, 2015). Based on the literature, the measured CBR values for 100% RAP samples range from 11% to 33% (Bennert & Maher, 2005; Cosentino et al., 2012; Guthrie et al., 2007; Taha et al., 1998). Thakur and Han (2015) reported that CBR test results are affected mainly by the RAP source and moisture content. Thus, they recommend conducting an independent CBR test for each RAP source. For conventional embankment soils, the CBR decreases with an increase in plasticity, clay content, and fine particles, as shown in Table 2 (Christopher et al., 2010). The Iowa Department of Transportation specifies a minimum CBR of 10 for a soil to be used in embankments (Schaefer et al., 2008). Based on the CBR alone, RAP can be considered suitable for use in embankments. However, the CBR may not reflect the characteristics of settlement.

TABLE 2. Field California Bearing Ratios of Some Conventional Embankment Soils
(Christopher et al., 2010)

USCS Soil Classifications	CBR
Silty Sand (SM)	20-40
Clayey Sand (SC)	10-20
Low Plasticity Silt (ML)	5-15
Low Plasticity Clay (CL)	5-15
High Plasticity Silt (MH)	4-8
High Plasticity Clay (CH)	3-5

Similar to the CBR, the LBR, which uses limerock as the standard material, is another measure of the strength of a sample relative to standard limestone. The Florida DOT (FDOT) has specified a minimum LBR of 100 for materials used in the base layer and a minimum LBR of 40 for materials used in the subgrade and fill layers (Cosentino et al., 2008). Sandin (2008) measured the LBRs for various RAP types and sources in Florida; the LBRs for 100% RAP samples were between 7 and 44, with an average of 17 (Sandin, 2008). As a comparison, Bandara and Rowe (2003) determined the LBRs of conventional subgrade soils obtained from 25

different highway sections in Florida. These soils consisted mostly of clean fine sand and silty fine sand and the resultant LBRs were between 23 and 49, with an average of 40 (Bandara & Rowe, 2003), which are higher than the LBRs of RAP reported by Sandin (2008). Cosentino et al. (2008) reported that the fractionation of RAP would reduce the LBR. However, in their study, a 50/50 blend of RAP materials with natural aggregate provided an acceptable LBR for use in sub-base layers in Florida. The asphalt content also affected the LBR results considerably whereby the LBR of the RAP samples decreased with an increase in the asphalt content (Cosentino et al., 2008).

The use of CBR and LBR test results to evaluate fill materials was found to have limitations, however, as the results do not adequately reflect field performance (Bennert & Maher, 2005; Camargo et al., 2013). More recent research has investigated the use of resilient modulus values of blended or 100% RAP aggregate samples. The resilient modulus is a measure of the stiffness of the sample under repeated loads in a triaxial test that simulates traffic load conditions in the field. Studies have concluded that RAP materials have higher resilient modulus values compared to conventional soils and crushed aggregate (Alam et al., 2010; Attia & Abdelrahman, 2010; Kim et al., 2007, Wen et al., 2010, 2011, Edil et al. 2012). Moreover, researchers have found that the resilient modulus increases with an increase in the RAP content of blended RAP/aggregate (Abdelrahman et al., 2010; Bennert et al., 2000; Cosentino et al., 2003; MacGregor et al., 1999), as shown in Figure 8. Note, however, that the resilient modulus reflects the behavior of fill material under dynamic loading, but it does not address the long-term settlement of fill material under static loading.

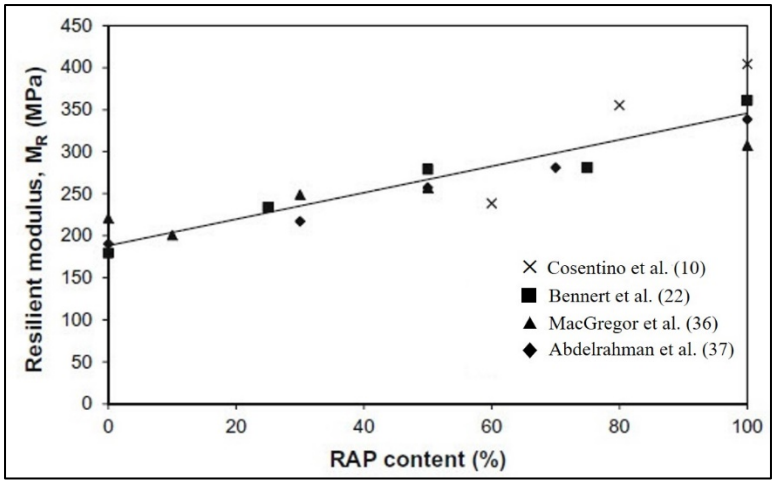

FIGURE 8. Increase in resilient modulus with increasing RAP content in RAP with soil/aggregate blend (Thakur & Han, 2015)**.**

2.1.5.3. Climatic Effects

Temperature, moisture, and freeze-thaw cycles are the three primary climatic parameters that affect the engineering properties of RAP. As stated, RAP includes aged asphalt binder that coats the aggregate particles and, because asphalt binder is viscoelastic, the asphalt binder will manifest different behaviors under different climate conditions.

Soleimanbeigi et al. (2015) measured the resilient modulus of compacted RAP samples at temperatures ranging from 44.6^0F to 122.0^0F. Based on the results shown in Figure 9 (a), when the temperature increases, the resilient modulus decreases and the plastic strain of the compacted RAP sample increases. Other researchers also have noticed this same phenomenon (Wen et al., 2010, 2011). However, for AASHTO A-5 soil, the resilient modulus is not affected by the compaction temperature, as expected (Figure 9 (a)). In addition, Figure 9 (b) shows that increasing the compaction temperature during sample preparation induces thermal preloading to the sample, which in turn, increases the resilient modulus of the RAP sample. Moreover, thermal preloading is shown to increase the shear strength and stiffness of the compacted RAP samples and decrease the plastic strain. Consequently, the construction of RAP fill is recommended for warm seasons (Soleimanbeigi et al. 2015).

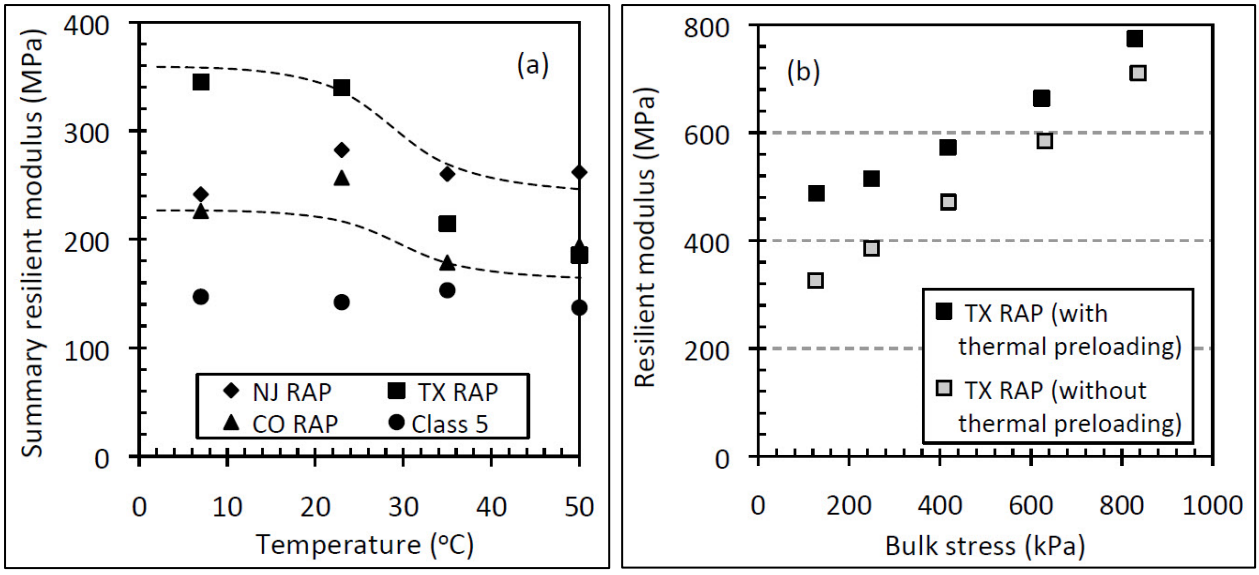

FIGURE 9. Changes in resilient modulus of different RAP samples with (a) temperature and (b) bulk stress with thermal preloading (Soleimanbeigi et al., 2015)**.**

Wen et al. (2011) studied variations in resilient modulus values with water content for samples with different RAP contents, as presented in Figure 10. They measured the resilient modulus values in the range of -4% OMC to +2% OMC and concluded that, similar to conventional soils and aggregate, the resilient modulus will decrease with an increase in water content for all samples. Kim et al. (2007) measured the resilient modulus for blended RAP/aggregate samples at 65% OMC and 100% OMC to evaluate the effects of water content on the resilient modulus. Their test results showed an increase in the resilient modulus value when the water content was decreased (or dried) from the OMC to 65% OMC. Noureldin and Abdelrahman (2013) also reached the same conclusion regarding the effects of moisture content on the resilient modulus of RAP materials.

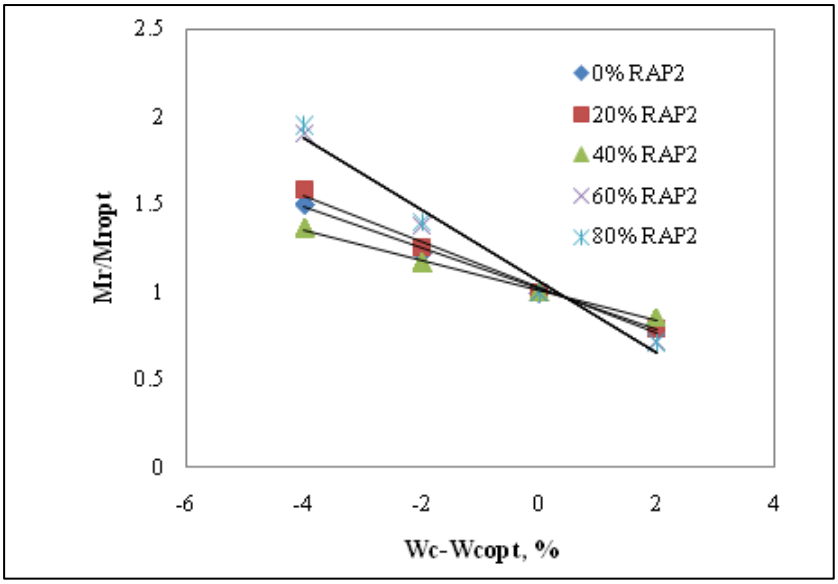

FIGURE 10. Effect of water content on resilient modulus (M_r) values of RAP samples (Wen et al., 2011)**.**

Soleimanbeigi et al. (2015) investigated the effect of freeze-thaw cycles on the resilient modulus of compacted RAP samples. After 20 freeze-thaw cycles, the resilient modulus values of the compacted RAP samples had decreased by more than 20%, although the values were still higher than those of conventional aggregate. Other studies also have shown that freeze-thaw cycles will reduce the stiffness and strength of materials (Arm, 2001; Rosa, 2017). This reduction in resilient modulus and strength is due to the expansion of the soil or RAP structure as well as an increase in the pore water pressure and the volume of the soil during the freezing process. Arm (2001) and Rosa (2017) noted that the increase in pore water pressure during freezing will generate forces large enough to break aggregate, which leads to degradation and a reduction in stiffness.

2.1.5.4. Hydraulic Properties

The hydraulic conductivity (permeability) of RAP is a significant property that controls moisture drainage. Moreover, permeability and water retention characteristics can vary based on the RAP gradation (Lafleur et al., 1989). The literature reports mixed results in terms of RAP's hydraulic conductivity or permeability. Poon and Chan (2006), MacGregor et al. (1999), and Bennert and Maher (2008) studied the permeability of mixtures with different RAP contents. Their results indicate that permeability decreases with an increase in RAP content. However, other researchers have reported that, due to RAP's hydrophobicity as a result of asphalt coating

(Edil et al., 2012; Rahardjo et al., 2011), RAP tends to have higher saturated hydraulic conductivity (k_{sat}) values than aggregate (Nokkaew et al., 2012). Thus, for a given gradation, RAP tends to provide a better drainage layer than aggregate (Edil et al., 2012; Hoppe et al., 2015). In addition, Cosentino et al. (2003) reported good drainage for 100% RAP and blended RAP samples. Cosentino et al. (2013) evaluated the permeability of milled and processed RAP samples blended with limerock, cemented coquina, and crushed concrete. Their results showed that using processed and milled RAP significantly increases the permeability of the mixture, e.g., 1.2×10^{-3} in./s for 100% milled RAP, 7×10^{-6} in./s for 100% processed RAP, and 4.7×10^{-7} in./s for 100% limerock, which are significantly higher values than for fine-grained soil, e.g., 1×10^{-7} in./s for marine soil (Cosentino et al., 2012; Nagaraj et al., 1991). Mijic et al. (2020) evaluated the hydraulic conductivity of RAP samples using a bubble-tube constant head parameter and found higher hydraulic conductivity for RAP samples compared with conventional aggregate. Moreover, they found that the effective particle size (D_{10}) had a significant effect on the hydraulic conductivity of RAP samples. They also observed an increase in hydraulic conductivity of RAP materials with a decrease in fine aggregate and an increase in the total binder content of the sample. Due to the large variability regarding the permeability of RAP found in the literature, McGarrah (2007) recommended determining permeability for each RAP source separately.

2.1.5.5. Creep and Permanent Deformation

2.1.5.5.1. Introduction to Soil Settlement

Soil settlement occurs in three stages: (1) immediate or elastic, (2) primary consolidation, and (3) secondary compression or creep (Bergaya et al., 2013). The immediate/elastic and primary consolidation stages occur within a short period immediately after construction, whereas creep settlement could continue long term. Elastic settlement occurs during or immediately after construction (Kong, 2016). Primary consolidation settlement occurs due to the dissipation of excess pore pressure and the associated volume change of the soil (Zou et al., 2016). Secondary compression (sometimes called one-dimensional creep) is a continuation of the volume change that is due to micro shear strain. Creep also can occur due to deviatoric or shear stress. Creep is the accumulation of time-dependent macro shear strain under sustained shear stress and is controlled by the viscosity of the soil structure (Mitchell & Soga, 2005). As shown in Figure 11,

creep settlement is significant when the soil is subjected to high or long-term stress. Under high deviatoric stress, the material may be subject to creep rupture, as illustrated in Figure 11. Note that researchers have used different parameters to characterize settlement, including (1) the slope of the secondary creep strain vs. time curve, namely the strain rate ($\dot{\varepsilon}$), (2) the slope of the strain rate vs. time curve, namely the rate of the strain rate (m), which covers the elastic, primary, secondary, and tertiary stages, and (3) the slope of the creep compliance in the secondary stage vs. time curve. Creep compliance is the creep strain divided by stress, or the creep strain per unit stress.

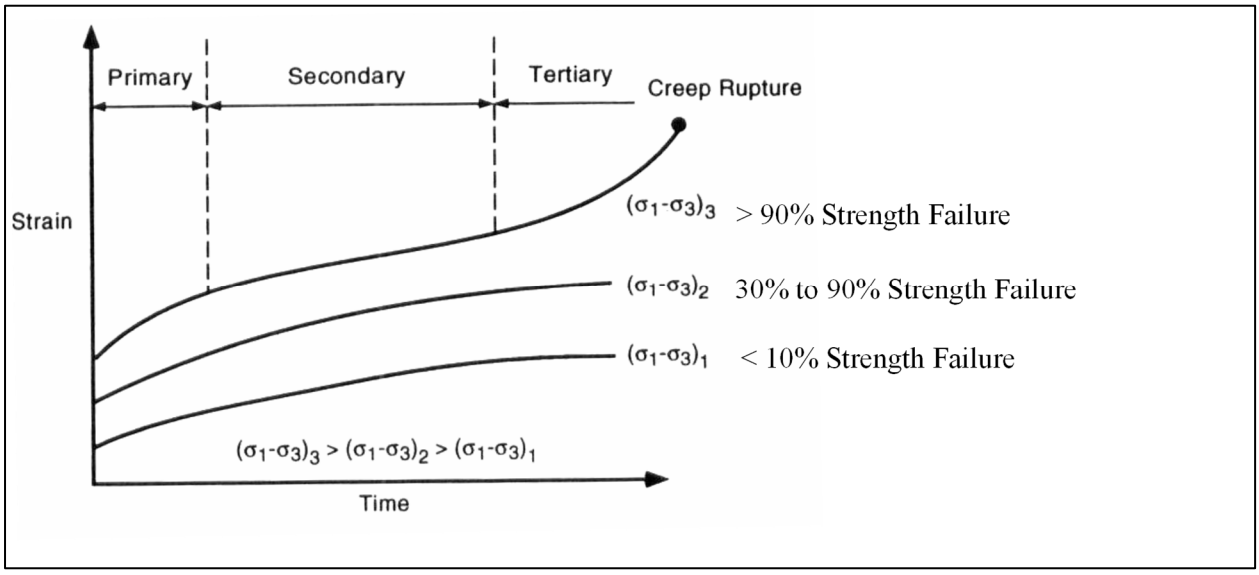

FIGURE 11. Creep modes under constant deviatoric stress (Mitchell & Soga, 2005)**.**

Coarse-grained soils reach a stable strain level under constant loading. However, RAP exhibits continuous deformation under constant loading according to Augusten et al. (2004), which is similar to cohesive and organic soils, i.e., clays and silts with fine grains. The occurrence of this phenomenon in RAP, i.e., acting like cohesive soil while known as a coarse-grained material, is due to the presence of the asphalt binder. The asphalt binder that coats the aggregate particles has viscoelastic properties and, therefore, RAP continues to deform under a constant load.

2.1.5.5.2. Comparison of Creep of RAP to Conventional Fill Soils

Mitchell and Soga (2005) developed an empirical model that describes the time-dependent deformation behavior of soil (the slope of the line in Figure 11) in the primary and

secondary stages of creep. They concluded that this model, presented here as Equation 1, can be applied to various soil types and is most applicable in the stress range from 30% to 90% of strength failure.

$$\dot{\varepsilon}_{(t)} = Ae^{\alpha D}\left(\frac{t_1}{t}\right)^m \quad (1)$$

where $\dot{\varepsilon}_{(t)}$ is the strain rate as a function of time; A is a constant; D is the deviatoric stress; α is the slope of the linear portion of the logarithmic strain vs. stress plot; t_1 is an arbitrary reference time; t is time; and m is the absolute value of the slope of the straight line on the log strain rate vs. log time plot. The value of the creep parameter, m, indicates the creep behavior over time. Based on Figure 12, if the m parameter is below 1, the strain rate will increase over time, and failure is more likely to occur (Mitchell and Soga, 2005).

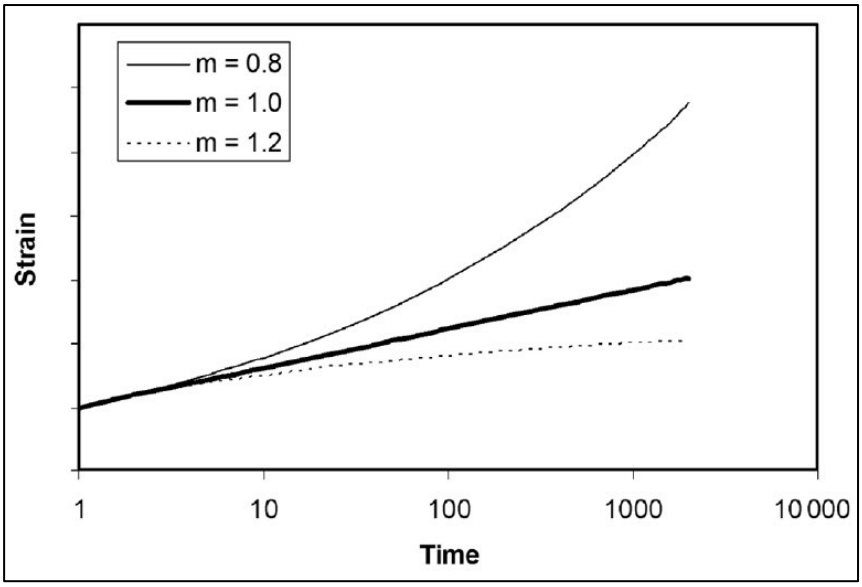

FIGURE 12. Creep shape, as predicted by Mitchell and Soga's empirical model (Mitchell & Soga, 2005)**.**

Viyanant et al. (2007) investigated the creep behavior of 100% RAP samples under drained conditions (because of the high permeability of RAP) at different confining pressures. At all stress levels, increasing the confining pressure led to a delay in creep rupture. Table 3 presents the range of the creep parameter, m, for the Viyanant et al. (2007) study RAP materials and conventional soils. The maximum value of m for RAP was calculated as 0.9, indicating the risk that creep rupture could occur for 100% RAP samples under certain conditions.

TABLE 3. Creep Parameter *m* for Different Soils and Fill Materials (Viyanant et al., 2007)

Material	*m*
Ice (-18℃) (Ting, 1983)	0.4-0.5
Frozen sand (-18℃) (Ting, 1983)	0.75-0.85
San Francisco Bay mud (Singh & Mitchell, 1969)	0.75
Haney clay (Campanella & Vaid, 1974)	0.6-0.8
Atchafalaya levee clay (Lacasse & Berre, 2005)	0.5-0.8
Norwegian clays (Lacasse & Berre, 2005)	0.8-0.9
Sand (Augustesen et al., 2004)	0.9-1.0
RAP (Viyanant et al., 2007)	0.3-0.9

Cleary (2005) and Dikova (2006) studied the creep behavior of RAP and RAP blended with sand, respectively, using two consolidometers and one pneumatic loading device. Cleary (2005) also modeled creep compliance using the Maxwell and Voigt models, explained by Huang (2004), to predict settlement based on the empirical model recommended by Mitchell and Soga (2005). Figure 13 shows the creep compliance (creep strain divided by stress, or creep strain under unit stress) with time, as reported by Cleary (2005). As the RAP content increases, the slope of the creep compliance vs. time (in log scale) curve increases, showing additional significant creep behavior for specimens with higher RAP content. On the other hand, adding about 20% A-3 sand reduced the slope by 30% compared with that for 100% RAP. For all the tested samples, the long-term creep decreased with an increase in confining pressure (Cleary, 2005).

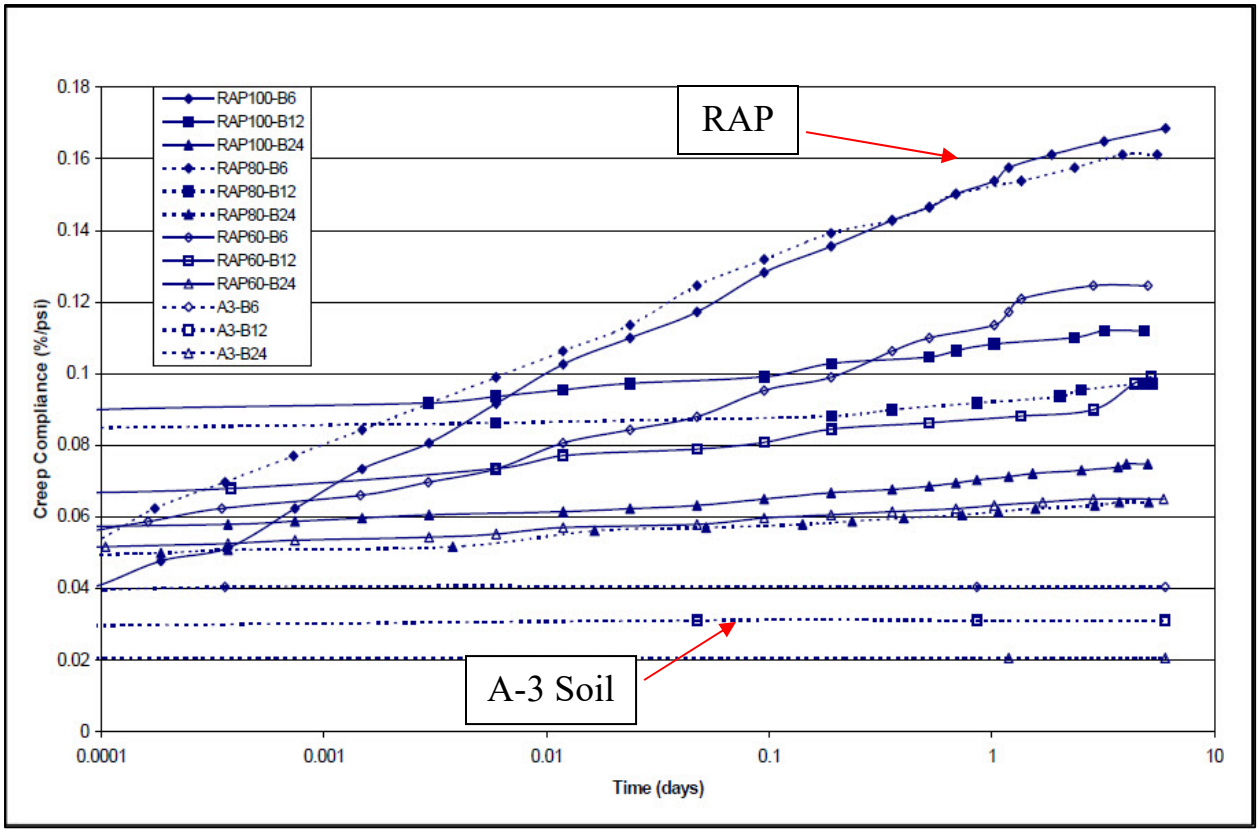

FIGURE 13. Creep compliance vs. log(time) for all samples with 6 psi, 12 psi, and 24 psi creep pressure (Cleary, 2005)**.**

Soleimanbeigi et al. (2014) conducted one-dimensional (1-D) compression tests to evaluate the compressibility of RAP and compared the results with those for conventional sands. Table 4 presents the secondary compression ratios for the slope of the creep strain vs. log-time curve, $\dot{\varepsilon}$, during the secondary creep stage for typical soils as well as RAP. The slope for RAP is higher than that for sands and is lower than that of clay. In addition, Figure 14 shows that the $\dot{\varepsilon}$ of the RAP material increases with an increase in vertical stress. Such an increase in the $\dot{\varepsilon}$ with vertical stress indicates that the creep of RAP is more sensitive to the depth of the fill compared to sand.

TABLE 4. Secondary Compression Ratios of Different Soils Compared to RAP

Material	Secondary Compression Ratio
Berthierville clay (Mesri & Castro, 1987)	0.0185
California tar sand (Mesri & Castro, 1987)	0.0014
Micaceous Antelope Valley sand (Lade & Liu, 1998)	0.0011
Lake Michigan beach sand (Mesri et al., 1990)	0.0004
Wisconsin outwash sand (Soleimanbeigi et al., 2014)	0.0003
RAP (Soleimanbeigi et al., 2014)	0.0067

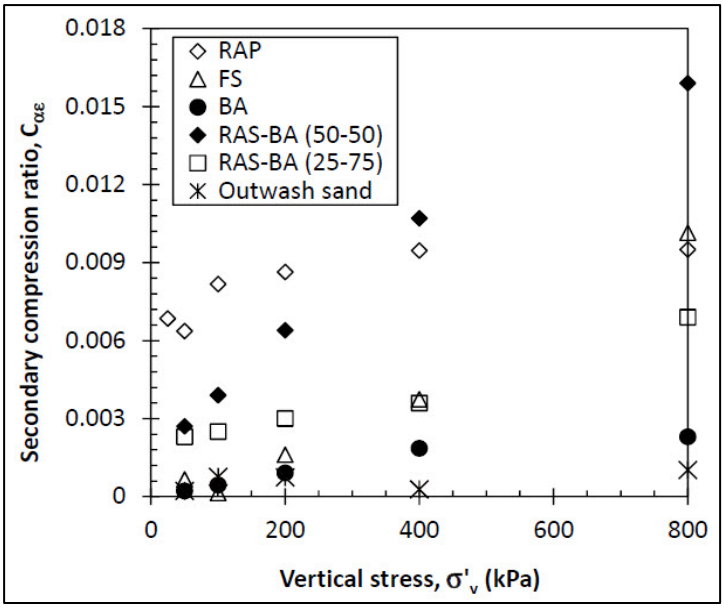

FIGURE 14. Change in secondary compression ratio of different materials with change in vertical stress (FS: foundry slag, BA: bottom ash, RAS: recycled asphalt shingles) (Soleimanbeigi et al., 2014**).**

2.1.5.5.3. Effect of Temperature on Creep of RAP

Soleimanbeigi et al. (2012) observed that the temperature in embankments varies from -41°F to 95°F. Therefore, the temperature of RAP is a key factor that would affect creep performance. Yin et al. (2017) compacted RAP samples at 71.6°F and then evaluated the creep performance of the RAP samples with 4.3% binder at 71.6°F, 95°F, and 122°F. They found that the creep strain and strain rate for the compacted RAP samples increased, and the time to rupture decreased with an increase in the test temperature. Following recommendations by Soleimanbeigi and Edil (2015), Yin et al. (2017) studied the effect of temperature and compaction on creep, respectively. The first scenario was to compact the sample at room temperature and measure the creep at elevated temperatures, and the second scenario was to compact the sample at elevated temperatures and measure the creep at room temperature; i.e., the two scenarios measured the effect of thermal preloading. Figure 15 (a) and (b) present plots of the axial strain rate ($\dot{\varepsilon}$) vs. temperature for each scenario, respectively. The slope of each plot is defined as the coefficient of thermal creep, $C_{\varepsilon T}$. The $C_{\varepsilon T}$ for the first scenario (strain rate vs. creep test temperature) is 0.061 and for the second scenario (strain rate vs. compaction temperature) is -0.061/℃. The values for thermal creep indicate that thermal preloading (i.e., RAP compacted at elevated temperatures) reduces the strain rate (or creep slope). Consequently, based on this thermal preloading investigation, the construction of structural fill is recommended to take place during warm seasons.

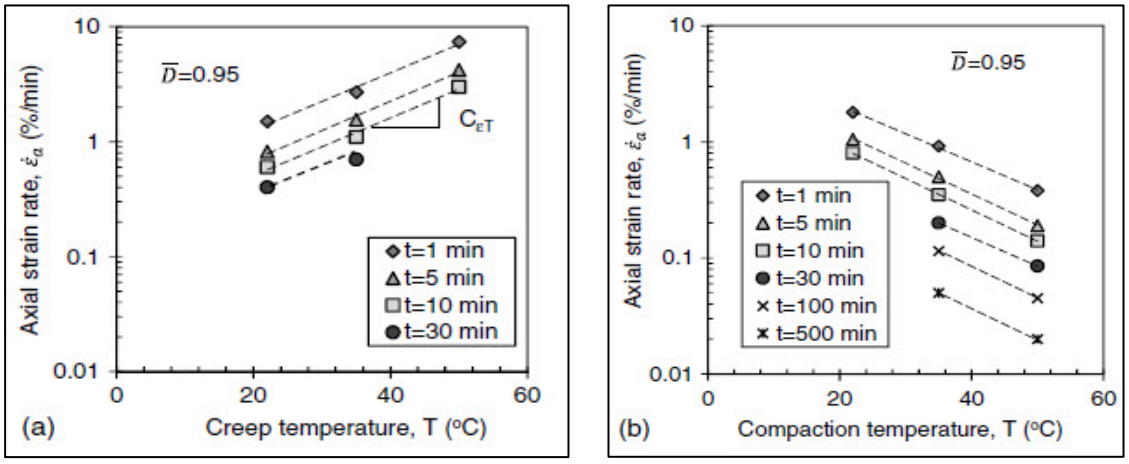

FIGURE 15. Axial strain vs. temperature for (a) effect of creep test temperature and (b) effect of sample compaction temperature (Yin et al., 2017)**.**

2.1.5.5.4. Effect of Asphalt Content in RAP on Creep

Cosentino et al. (2003) investigated the creep of 100% RAP, 80% RAP with 20% A-3 soil, and 100% A-3 soil samples and reported that the strain rate ($\dot{\varepsilon}$) decreased from 100% RAP to 80% RAP and 100% A-3 soil. The strain rate ($\dot{\varepsilon}$) decreased by about half an order of magnitude when the RAP content was decreased from 100% to 80 percent. The strain rate of 80% RAP decreased by an order of magnitude when the RAP percentage was reduced to 0% (i.e., 100% A-3 soil) (Cosentino et al., 2003). In addition, Cosentino et al. (2003) found that creep deformation increased significantly for materials with greater than 3% asphalt content (Cosentino et al., 2012). Kazmee et al. (2016) compared the permanent deformation of RAP with other large-size unconventional subgrade aggregate, such as dolomite and rubblized concrete, and found higher rutting susceptibility for RAP. Kazmee et al. (2016) concluded that the asphalt film thickness and depth of the water table also significantly affect permanent deformation. Wen et al. (2010) reported that RAP samples exhibit greater permanent deformation than conventional Grade 2 gravel, but the permanent deformation decreases significantly when the RAP sample is stabilized with fly ash, as shown in Figure 16 (Wen et al., 2010).

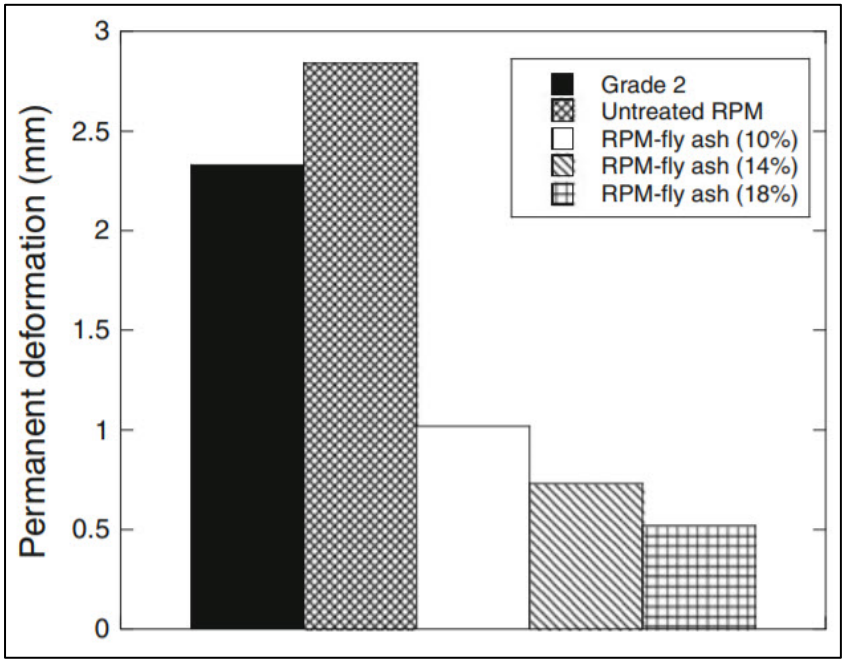

FIGURE 16. Permanent deformation of Grade 2 gravel, untreated RAP, and fly ash-treated RAP (RPM) samples (Wen et al., 2010)**.**

2.1.5.5.5. Effect of Dynamic Loading on Performance Deformation

In addition to the settlement due to creep that results from overburden pressure or deadload, additional permanent deformation can be caused by dynamic traffic loading. Several researchers have investigated the permanent strain and deformation of blended RAP samples using triaxial cyclic load tests, which are similar to the resilient modulus test (Bennert et al., 2000; Wen et al., 2011; El & Attia, 2010; Kim & Labuz, 2007; Garg & Thompson 1996). All these studies concluded that the permanent strain of RAP samples due to dynamic loading would increase with an increase in RAP content and number of loading cycles, as shown in Figure 17 (Thakur & Han, 2015). Therefore, traffic loading can be a significant factor that affects RAP embankments in terms of settlement.

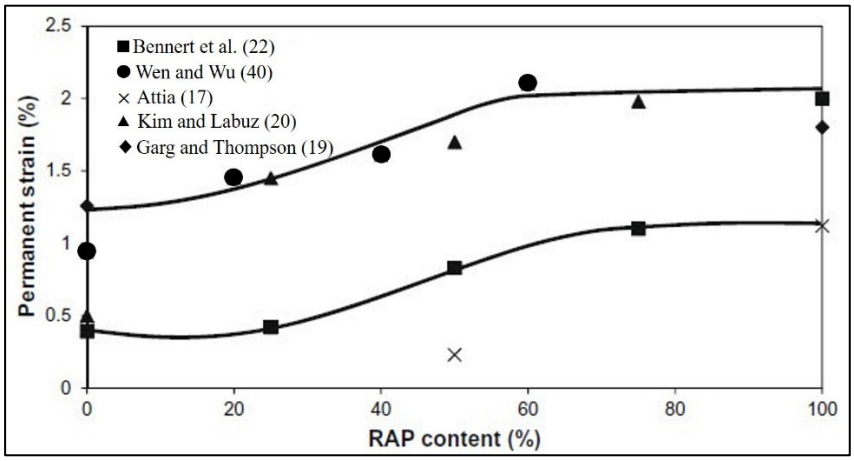

FIGURE 17. Change in permanent strain of RAP/aggregate blends with increase in RAP content (Thakur & Han, 2015)**.**

2.1.6 RAP in Structural Backfill

Natural or recycled materials can be used as backfill if they meet the specification criteria. Backfill material should have a good drainage system with high hydraulic conductivity, which limits the use of fines in backfill (Elias et al., 2001; Rathje et al., 2006). Vennapusa et al. (2015) measured the saturated hydraulic conductivity (k_{sat}) of RAP and compared it with that of conventional structural backfill soils. They reported equal or greater saturated hydraulic conductivity for RAP materials compared with conventional backfill soils, as shown in Figure 18. Soleimanbeigi et al. (2014) conducted rigid wall hydraulic conductivity tests to measure the hydraulic conductivity of RAP samples and concluded that RAP's hydraulic conductivity is four times that of conventional embankment soils, indicating that adequate drainage capacity is

achievable for RAP's use in structural fill materials. Berg et al. (2009) recommended using not more than 15% fines for reinforced backfill. However, based on a 2015 survey conducted by the Wisconsin DOT (WisDOT), among 48 DOTs, the allowable fine content for abutment backfill was reported to be up to 25% (Vennapusa et al., 2015). Vennapusa et al. (2015) also compared the gradation of RAP material with that of both conventional structural backfill soils and a range of most erodible soils provided by Briaud et al. (1997), as shown in Figure 19. The RAP material is significantly coarser than the conventional backfill soils. All the backfill soils were classified as sandy soils, whereas the RAP was classified as gravel.

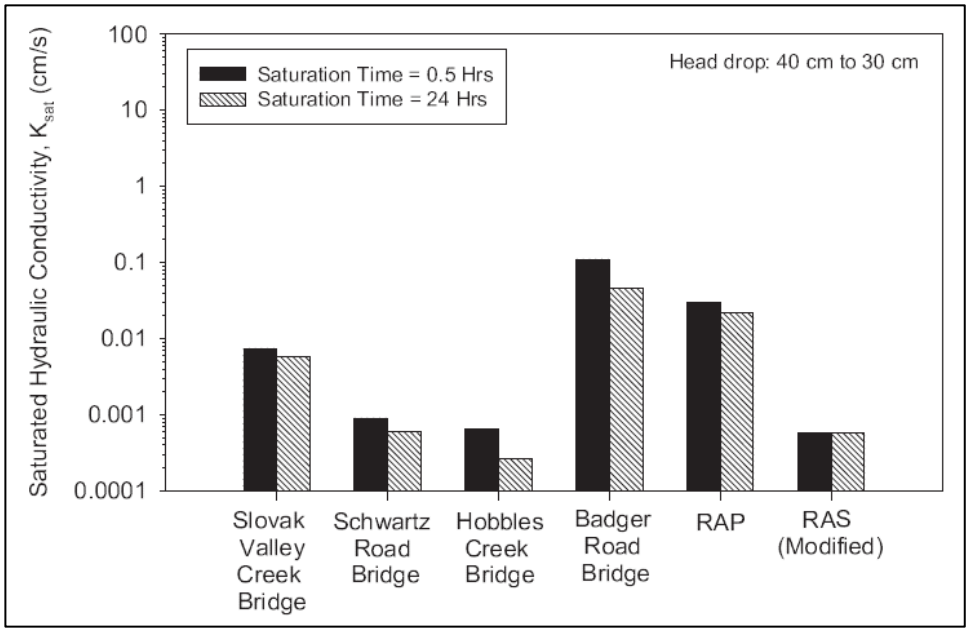

FIGURE 18. Saturated hydraulic conductivity of conventional backfill soils and RAP (Vennapusa et al., 2015)**.**

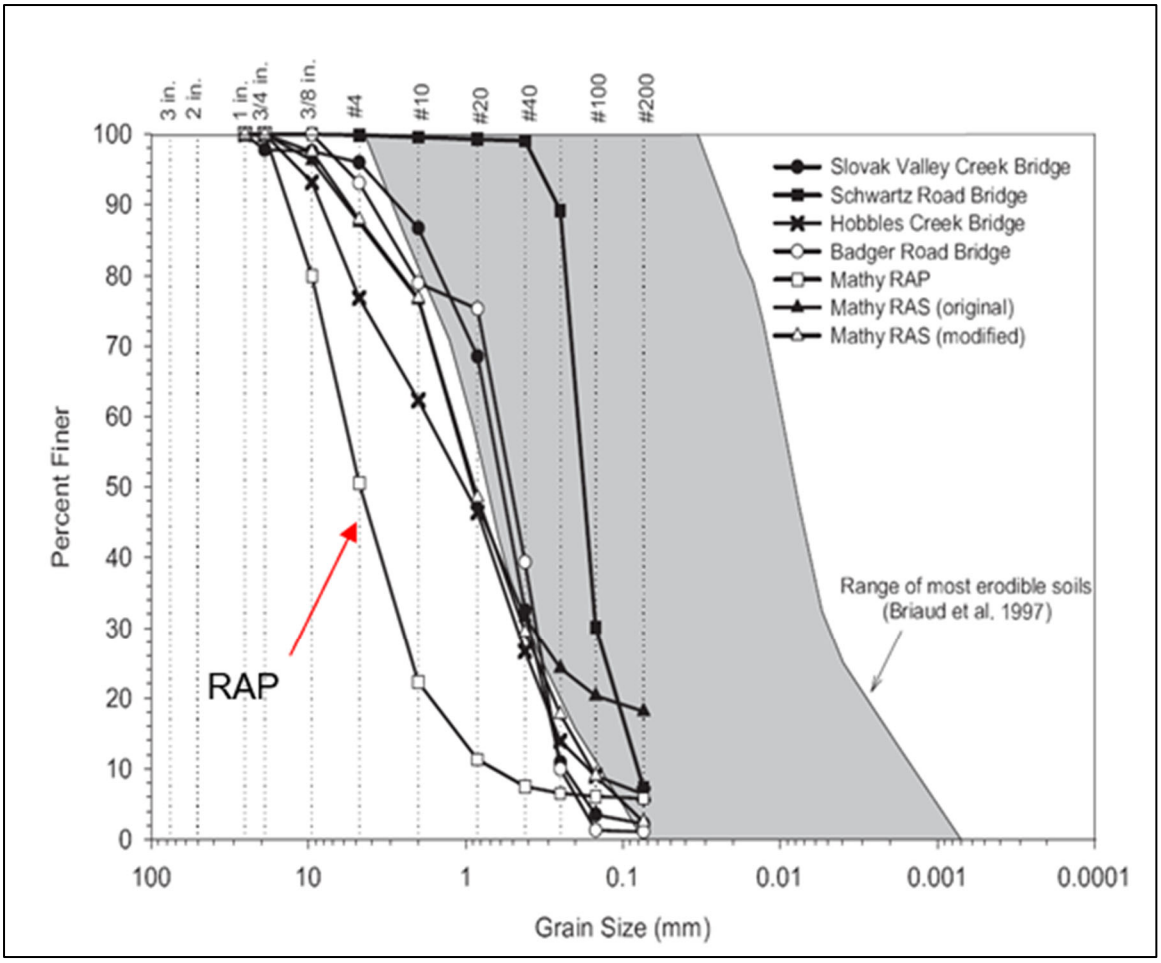

FIGURE 19. Gradation of RAP, conventional backfill soils, and range of most erodible soils (Vennapusa et al., 2015)**.**

Other important parameters for materials used in backfill include adequate internal and interface friction angles (Berg et al., 2009; Elias et al., 2001; Rathje et al., 2006). The friction angle of RAP material varies between 42° and 52°, and the minimum friction angle recommended by both AASHTO and the Federal Highway Administration for backfill material is 34° (AASHTO, 2011; Berg et al., 2009). RAP also exhibits acceptable drainage and low plasticity, which makes it favorable for use in backfill (Soleimanbeigi et al., 2016). The only concern regarding the use of RAP material is its deformation and creep performance (Soleimanbeigi et al., 2014; Soleimanbeigi & Edil, 2015).

Vennapusa et al. (2015) tested RAP materials and compared the results and properties with results obtained from *in situ* conventional backfill soil material. They were unable to measure the drained friction angle for RAP materials due to creep failure at 15% strain under

saturated conditions. Vennapusa et al. (2015) also conducted collapse tests using RAP samples that had been compacted at the bulk moisture content and recorded vertical strain levels of 4% to 5%, which indicates that about 4.72 in. to 5.91 in. of settlement can occur in a 9.84-ft backfill. Consequently, the post-construction deformation of RAP materials can lead to failure; thus, Vennapusa et al. (2015) did not recommend the use of RAP as backfill material.

Soleimanbeigi et al. (2016) investigated the properties and performance of RAP as backfill material along with alternatives. They measured the properties of RAP compacted at elevated temperatures, similar to work by Yin et al. (2017). Although compaction at elevated temperatures did not consistently affect the interface friction angle, it improved the shear strength, reduced the permanent deformation and creep susceptibility, and decreased the volume change during creep. Therefore, construction of structural backfill using RAP during warm weather would be instrumental in reducing settlement. However, Soleimanbeigi et al. (2016) recommended that the applied deviator stress should be below 70% of the compressive strength to mitigate creep-related problems.

2.2 Survey of State Highway Agencies

The research team for this study sent out a questionnaire to all the highway agency members of the AASHTO Committee of Materials and Pavements. A total of 32 state DOTs responded. Since many DOTs start with the same first letter, we use state abbreviations to distinguish them. IL DOT followed up by sending a memo regarding the use of RAP in the Aggregate Subgrade Improvement provision. Based on the responses, the research team contacted several state DOTs for interviews, including the DOTs of AZ, FL, IN, MT, NY, PA, and UT. AZ DOT responded to interview questions via email and the other six DOTs responded via video/conference calls. Below is a summary of the survey results. Note that not every DOT responded to all the questions and that the total number of respondents for one question may not be the same for all the DOTs surveyed.

(1) Use of RAP as embankment fill by state agencies

Eleven DOTs (in CO, FL, ID, IL, IN, MD, MT, NM, NY, WA, and WV) allow the use of RAP as embankment fill and seventeen states do not. The reasons given for not using RAP in embankments are listed below and illustrated in Figure 20 (the number of responses is shown in each slice).

a. RAP is used in HMA and/or base/sub-base layers because RAP is more valuable in these layers than in embankments (7 responses).
b. RAP has shown difficulties associated with compaction, density control, and/or environmental concerns (3 responses from DOTs of AZ, MI, and UT).
c. No interest from industry (2 responses from DOTs of KS and ME).
d. Specifications are under revision to allow the use of RAP (2 responses from DOTs of AZ and UT).
e. Limited RAP for use (2 responses from the DOTs of DC and IA).
f. Legal barriers; considering revision to specifications to allow the use of RAP due to abundant RAP stockpiles (1 response from DOT of PA).

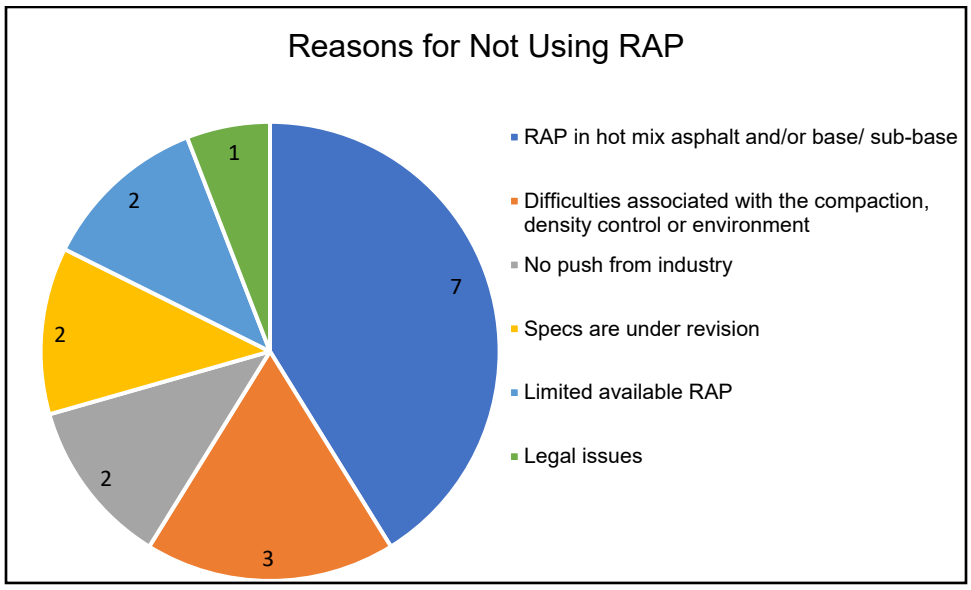

FIGURE 20. State transportation agencies' reasons for not using RAP as embankment material.

Note that a single state DOT may provide more than one reason highlighted in Figure 20. Based on interviews with DOT personnel, the use of RAP in embankments is much needed in metro areas where RAP stockpiles are abundant and fill materials are difficult to find nearby. States such as MT and UT in particular allow relatively low RAP content in HMA and have expressed the need to use RAP in embankments. The CO DOT allows the use of RAP in embankments, but does not allow RAP in the upper 2 ft of the final subgrade elevation. In addition, some agencies, such as the NY DOT, allow the use of RAP in embankments according

to specifications, but avoid using RAP in practice for the reasons listed in item (b) above. FL DOT limits the use of RAP in embankments by mixing RAP with natural soil (1 RAP: 2 soil); also, the RAP layer and soil layer can be alternated instead of mixing them. The WA DOT allows 100% RAP in embankments 3 ft below the subgrade elevation and limits the asphalt percentage to 25% within 3 ft of the subgrade elevation.

(2) Maximum size of RAP particles and percentage of fines allowed in RAP

Figure 21 shows the maximum size of RAP particles specified by some state DOTs; the range is from 3/4 in. up to 12 in., as follows:

a. ¾ in. (1 response from DOT of MD)
b. 1.5 in. (4 responses)
c. 2 in. (1 response from NY DOT)
d. 3½ in. for top 12 in., 6 in. for 12 in. to 24 in. below the subgrade, and 12 in. deeper than 2 ft (1 response from FL DOT)
e. 6 in. (1 response from MT DOT)
f. 12 in. and may revise down to 6 in. (1 response from CO DOT)

Most states do not specify the percentage of fines allowed in RAP, except IN DOT, which has a limit of maximum 10% fines.

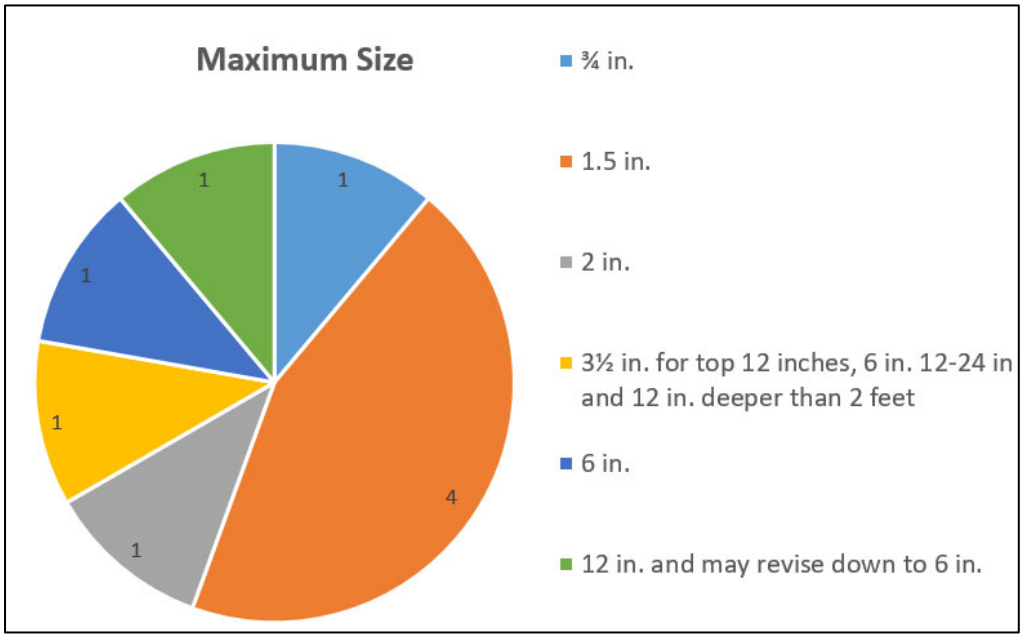

FIGURE 21. Maximum size of RAP particles specified by several state DOTs.

(3) Maximum lift thickness for placement of RAP as embankment fill.

The maximum allowed compacted lift thickness for RAP as embankment fill is between 6 in. and 8 in. and is fairly consistent among state DOTs. However, NY DOT specifies that the lift thickness must be dependent on the type of compaction equipment. FL DOT specifies a maximum 12-in. compacted lift thickness of mixed RAP and soil. WA DOT limits the lift thickness to 4 in. within the top 2 ft of subgrade and 8 in. below a 2-ft subgrade elevation.

(4) Control of degree of compaction during construction.

Nine state DOTs have indicated that they use the MDD determined from laboratory or field (test strip) tests to control the degree of compaction. Four state DOTs (MA, OR, WA and WV) use a pass pattern (or roller pattern) to establish the maximum density. Five states use AASHTO T 180, the Modified Proctor test, to determine the MDD of RAP fill, and another five states use AASHTO T 99, the Standard Proctor test, instead. For agencies that use a percentage of MDD to control the degree of compaction, 95% MDD is often specified for either the standard Proctor or modified Proctor test. However, FL DOT specifies 100% for the Standard Proctor test. NY DOT specifies 90% for the Standard Proctor test in embankments below the subgrade, but 95% for the subgrade (20 in. below the bottom of the sub-base or base). CO DOT uses a one-point T-180 wet density value and requires compaction up to 100% of that value. The DOT of MD specifies that the density should be a minimum 97% of the maximum density established from the test strip.

Twelve states use a nuclear density gauge to measure density on site. Recognizing the inaccuracies of density readings taken from nuclear density gauges, however, NY DOT avoids the use of nuclear density gauges, although they are allowed, and instead uses a sandcone/volumeter. The MT DOT uses offset correction as recommended by the nuclear gauge manufacturer to correct the gauge's density readings. ADOT exclusively uses the sandcone method instead of the nuclear density method to measure the density of RAP.

(5) Control of moisture content of RAP fill measured during construction.

Only five states measure the moisture content of RAP fill. Because the hydrogen in asphalt binder is recognized as moisture by nuclear density gauges, moisture readings taken by nuclear density gauges are not accurate. FL DOT uses a speedy moisture test method by means

of a calcium carbide gas pressure moisture tester. DOTs of CO and NY use an oven dry-back method (60ºC maximum).

(6) Performance tests in the laboratory and on site

The NM DOT specifies the use of *R*-values in laboratory tests of embankment materials. Seven agencies stated that they use proof-rolling on site during construction to accept the embankment's construction quality, which includes RAP quality acceptance. Agencies specify either compaction equipment or a dump truck for proof-rolling. For example, IN DOT specifies the use of a dump truck for at least 15 tons for every 5 ft in height of the embankment with deflection less than 0.5 inch. CDOT specifies that pneumatic tire equipment shall be used for proof-rolling with a minimum load of 18 kips per axle. CO DOT does not set criteria for embankment performance acceptance and instead calls for engineering judgement. NY DOT specifies the use of a pneumatic tire roller for proof-rolling without specific tonnage and deflection criteria.

IN DOT uses a dynamic cone penetrometer for embankment performance acceptance and specifies a minimum number of blows to penetrate the lift thickness. The number of blows depends on the classification of the material and lift thickness. IN DOT also uses a lightweight deflectometer when aggregate is used for embankment construction. According to an interview with an IN DOT engineer, IN DOT plans to use a lightweight deflectometer for all embankment and base layer construction acceptance in the near future.

(7) Placement temperature limitations

Few states specify a placement temperature. The MD DOT requires that the earthwork must be above freezing. NY DOT prohibits earthwork between Nov. 1 and April 1; however, winter earthwork may be requested and approved when the temperature is 32ºF or higher.

(8) Distresses in RAP embankments

Only NY DOT reported discernible distress, such as shoving/rutting/pumping, in RAP embankments. During the interview, an NY DOT engineer indicated that RAP is believed to be susceptible to long-term creep, or being "too live", and attributes the distress to the presence of RAP material and heavy traffic. UT DOT reported that the RAP layer tends to become

impermeable after construction and that water becomes trapped on top of the RAP layer; therefore, a drainage layer is needed.

When asked how to prevent distress in RAP embankments, state transportation agencies responded as follows and as shown in Figure 22.

a. Limit asphalt content by blending with natural/mineral soils, e.g., 50% (4 responses).
b. Ensure proper construction (e.g., compaction, lift thickness) (5 responses).
c. Control the gradation (2 responses).
d. Place in warmer weather to obtain limited bonding in lifts (1 response).

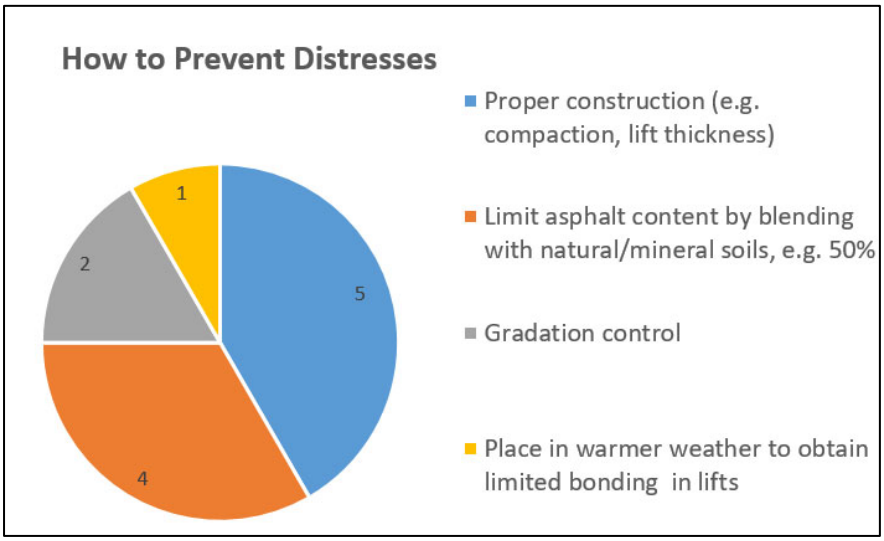

FIGURE 22. Ways that different state transportation agencies prevent distress.

(9) Use of RAP in structural backfill

Fewer (six) agencies allow the use of RAP as structural backfill compared with using RAP in embankments. The reasons given for not allowing use of RAP in structural backfill include:

a. Difficulty in compaction and testing (4 responses)
b. Creep (3 responses)
c. Drainage (2 responses)
d. Environmental contamination (2 responses)
e. No interest from industry (2 responses)

The MD DOT indicated that a couple of its projects have used RAP as pipe backfill but exhibited long-term settlement issues. The IA DOT allows the use of RAP in structural backfill only, but not in embankments, due to RAP's low volume.

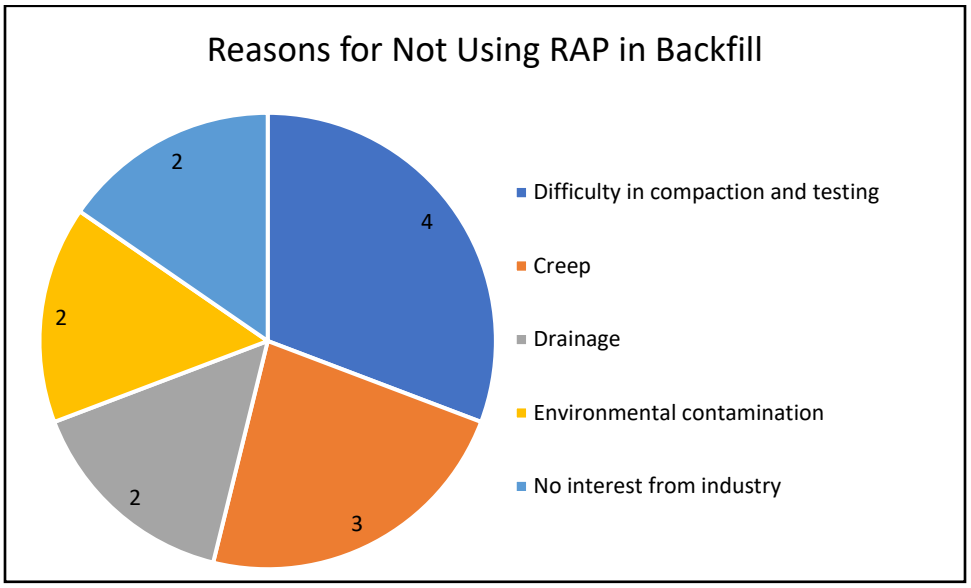

FIGURE 23. State transportation agencies' reasons for not using RAP in backfill.

Based on the literature review and survey results, many questions remain to be answered with regard to the use and quality of RAP as embankment and backfill, such as the maximum size of RAP particles allowed, specifications for dry density, field control of compaction and compaction measurements, field control of moisture, performance measurements in the laboratory and field, construction temperature, long-term settlement assessment, etc.

CHAPTER 3 FORENSIC INVESTIGATION

In order to understand past settlement issues that are presumed to be associated with the use of RAP, the research team conducted forensic investigations and reviewed the design and construction documents of Illinois Tollway construction projects that were reported to have excessive settlement when RAP was used in an embankment. The documents reviewed include project plans, specifications, pavement design reports, geotechnical reports, field inspection and testing results, non-conformance reports, and interviews with engineers, depending on available sources. Two major construction projects were reviewed especially closely: the I-90 Jane Addams Memorial Road (Contract I-14-4206) and the IL Rte. 390 Elgin O'Hare Expressway under various contracts. Note that much of the design and construction information for both projects was not available for review.

3.1. Jane Addams Memorial Tollway

The I-90 Jane Addams Memorial Tollway reconstruction project was undertaken between 2014 and 2017 and extended from Randall Road to the Kennedy Expressway in Cook County in Illinois. The pavement structure consists of a 13-in. doweled concrete layer, 3-in. WMA, 3-in. RAP cap of 6-in. porous granular embankment (PGE), and A-6 subgrade and embankment, as described in Table 5. Figure 24 shows that fabric-lined, trenched 6-in. diameter pipe underdrains also were installed to collect water from the PGE layer (the underdrain is highlighted in the red box). Due to delays, the contractor requested the use of unprocessed asphalt grindings for the embankment to expedite the construction. After the completion of the outside lanes in December 2015 and the shoulder in spring 2016, excessive settlement and pavement cracks had occurred by the summer of 2016. These areas were repaired by the end of 2016. The retaining wall areas (Retaining Walls # 1, #4, and #5) of excessive settlement and pavement cracking as well as the corrective actions taken are discussed in detail in the following sections.

TABLE 5. Pavement Structure of I-90 Jane Addams Memorial Tollway

Thickness, in.	Layer
13.0	Jointed plain concrete pavement (15-ft joint spacing, 1.5-in. dowels @ 12-in. centers)
3.0	WMA
3.0	RAP cap
9.0	Porous granular embankment (minus 4 in.)
N/A	A-6 subgrade (CBR = 6)

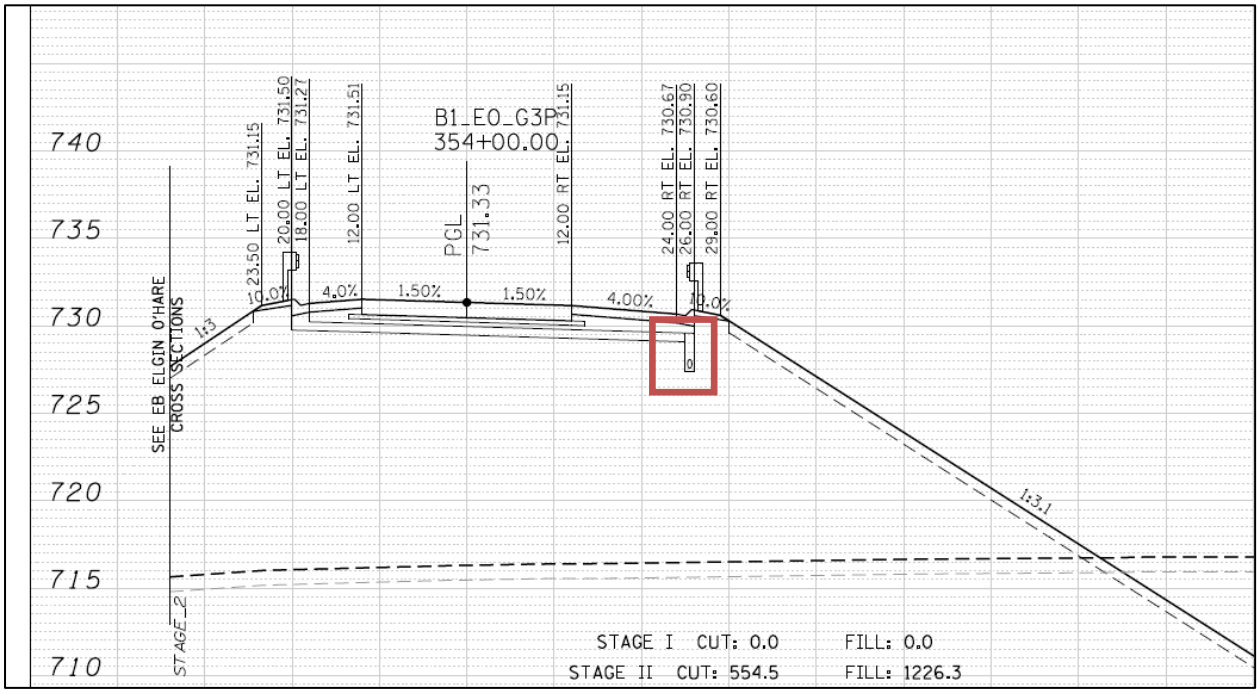

FIGURE 24. Cross-section with drainage system at I-90 Jane Addams Memorial Tollway.

3.1.1 Retaining Wall #1 Area

3.1.1.1 Settlement

The settlement of the pavement next to Retaining Wall #1 took place in the westbound lanes from Station 3217+60 to Station 3221+65, as shown in Figure 25 (highlighted in red box).

A pile-supported box culvert is located at approximately Station 3219. In 2016, an average settlement of 4.75 in. was reported in this area. The pavement over the culvert had more settlement compared to the area adjacent to the culvert. According to the forensic boring information (No. SB-11), shown in Figure 26, the top 5.5 ft of the embankment was constructed with RAP, with clay fill underneath. Estimates of the settlement provided in geotechnical reports (at both the design stage and forensic stage) show minimal settlement, e.g., 0.47 in. in the forensic geotechnical report, as shown in Figure 27. Note that the soil settlement estimates, which were determined in accordance with IDOT's soil settlement analysis method, did not include settlement of the embankment soil or RAP.

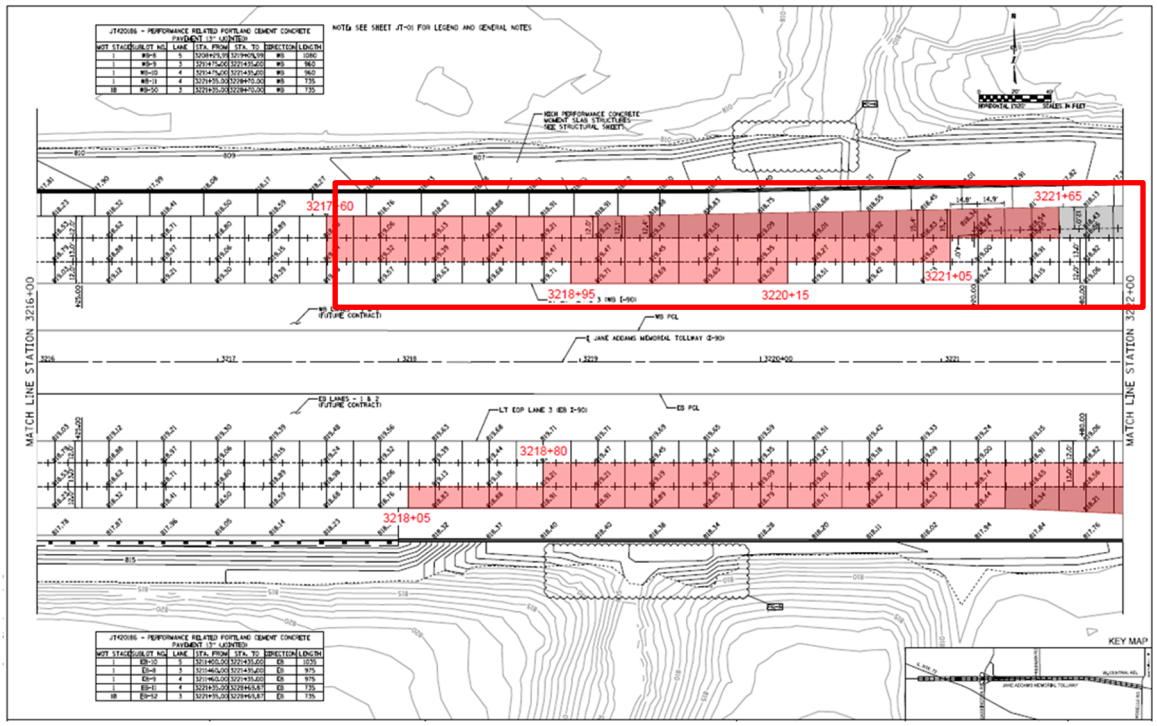

FIGURE 25. Failure locations next to Retaining Wall #1.

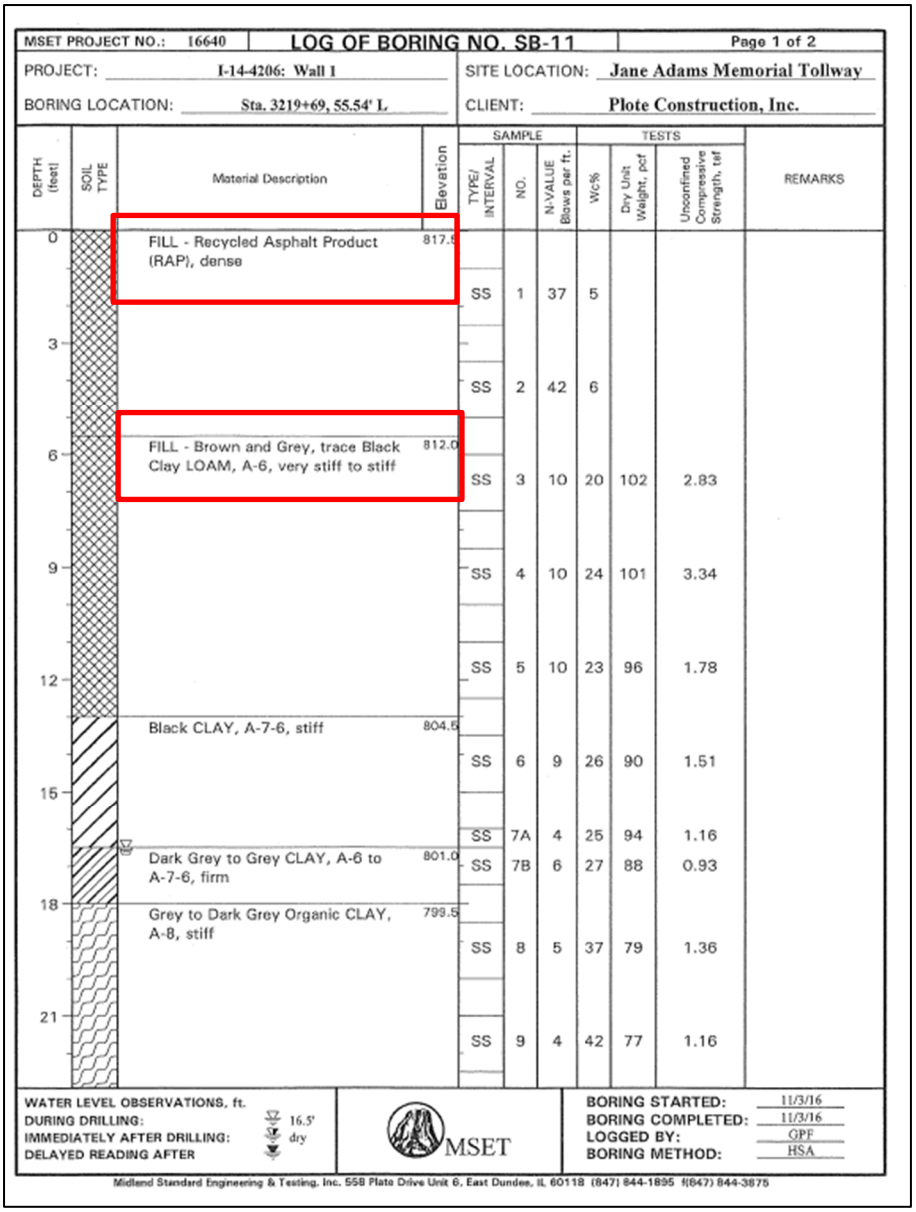

FIGURE 26. Boring profile next to Retaining Wall #1.

3.1.1.2 Corrective Actions

After significant settlement and pavement cracks had occurred, a series of repairs were performed in the specified area around Retaining Wall #1. First, the concrete pavement structure above the embankment was removed, followed by 1 ft of RAP embankment undercut. The remaining RAP in the embankment was recompacted to achieve maximum density using a roller pattern, and the maximum density after compaction was measured using a nuclear gauge. Subsequently, the compacted RAP was proof-rolled. Ground stabilization fabric was placed with

PGE in the undercuts prior to the aggregate subgrade placement. Since these corrective actions have taken place, no noticeable settlement has been reported.

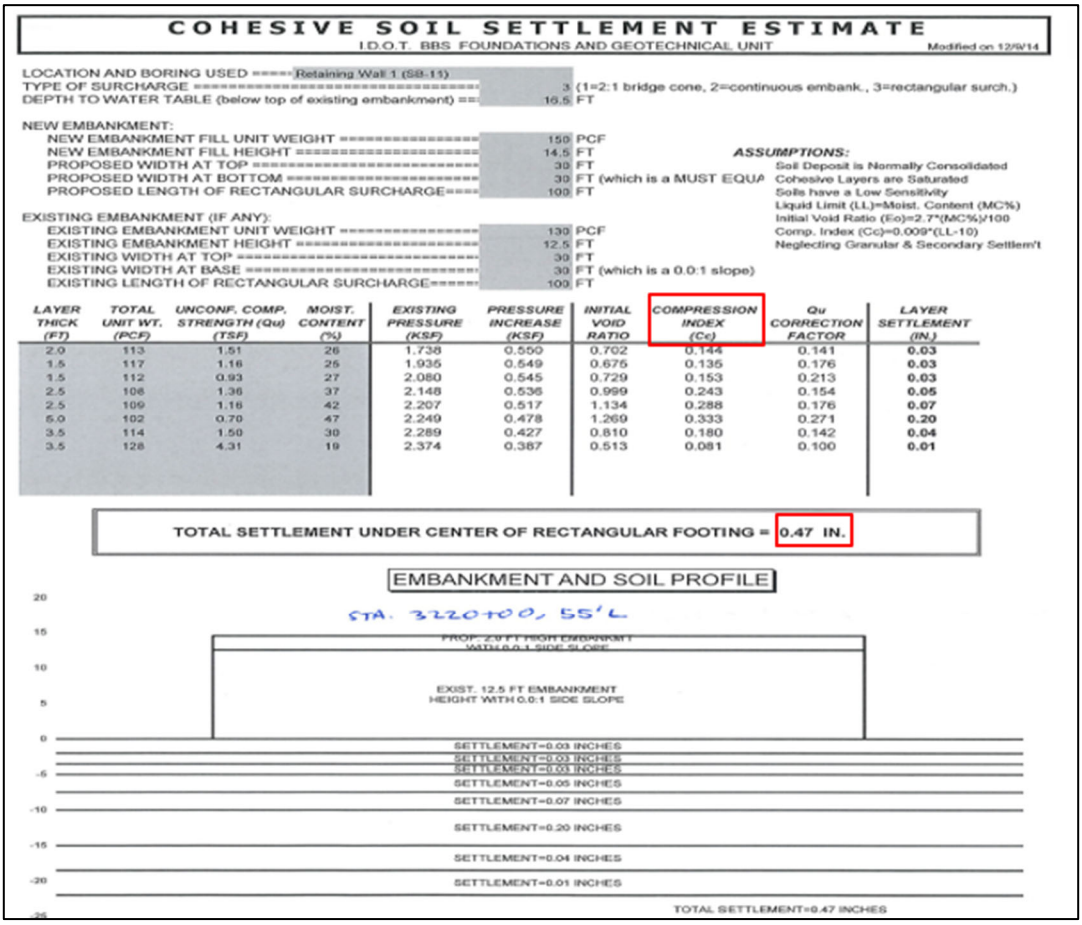

COHESIVE SOIL SETTLEMENT ESTIMATE

I.D.O.T. BBS FOUNDATIONS AND GEOTECHNICAL UNIT — Modified on 12/9/14

LOCATION AND BORING USED ===== Retaining Wall 1 (SB-11)
TYPE OF SURCHARGE ========== 3 (1=2:1 bridge cone, 2=continuous embank., 3=rectangular surch.)
DEPTH TO WATER TABLE (below top of existing embankment) == 16.5 FT

NEW EMBANKMENT:
NEW EMBANKMENT FILL UNIT WEIGHT ========== 150 PCF
NEW EMBANKMENT FILL HEIGHT ========== 14.5 FT
PROPOSED WIDTH AT TOP ========== 30 FT
PROPOSED WIDTH AT BOTTOM ========== 30 FT (which is a MUST EQUA
PROPOSED LENGTH OF RECTANGULAR SURCHARGE==== 100 FT

EXISTING EMBANKMENT (IF ANY):
EXISTING EMBANKMENT UNIT WEIGHT ========== 130 PCF
EXISTING EMBANKMENT HEIGHT ========== 12.5 FT
EXISTING WIDTH AT TOP ========== 30 FT
EXISTING WIDTH AT BASE ========== 30 FT (which is a 0.0:1 slope)
EXISTING LENGTH OF RECTANGULAR SURCHARGE==== 100 FT

ASSUMPTIONS:
Soil Deposit is Normally Consolidated
Cohesive Layers are Saturated
Soils have a Low Sensitivity
Liquid Limit (LL)=Moist. Content (MC%)
Initial Void Ratio (Eo)=2.7*(MC%)/100
Comp. Index (Cc)=0.009*(LL-10)
Neglecting Granular & Secondary Settlem't

LAYER THICK (FT)	TOTAL UNIT WT. (PCF)	UNCONF. COMP. STRENGTH (Qu) (TSF)	MOIST. CONTENT (%)	EXISTING PRESSURE (KSF)	PRESSURE INCREASE (KSF)	INITIAL VOID RATIO	COMPRESSION INDEX (Cc)	Qu CORRECTION FACTOR	LAYER SETTLEMENT (IN.)
2.0	113	1.51	26	1.738	0.550	0.702	0.144	0.141	0.03
1.5	117	1.16	25	1.935	0.549	0.675	0.135	0.176	0.03
1.5	112	0.93	27	2.080	0.545	0.729	0.153	0.213	0.03
2.5	106	1.36	37	2.148	0.536	0.999	0.243	0.154	0.05
2.5	109	1.16	42	2.207	0.517	1.134	0.288	0.176	0.07
5.0	102	0.70	47	2.249	0.478	1.269	0.333	0.271	0.20
3.5	114	1.50	30	2.289	0.427	0.810	0.180	0.142	0.04
3.5	128	4.31	19	2.374	0.387	0.513	0.081	0.100	0.01

TOTAL SETTLEMENT UNDER CENTER OF RECTANGULAR FOOTING = 0.47 IN.

EMBANKMENT AND SOIL PROFILE

STA. 3220+00, 55' L

PROP. 2.0 FT HIGH EMBANKMT WITH 0.0:1 SIDE SLOPE

EXIST. 12.5 FT EMBANKMENT HEIGHT WITH 0.0:1 SIDE SLOPE

SETTLEMENT=0.03 INCHES
SETTLEMENT=0.03 INCHES
SETTLEMENT=0.03 INCHES
SETTLEMENT=0.05 INCHES
SETTLEMENT=0.07 INCHES
SETTLEMENT=0.20 INCHES
SETTLEMENT=0.04 INCHES
SETTLEMENT=0.01 INCHES

TOTAL SETTLEMENT=0.47 INCHES

FIGURE 27. Settlement estimation for pavement next to Retaining Wall #1.

3.1.2 Retaining Wall #4 Area

3.1.2.1 Settlement

The settlement for Retaining Wall #4 occurred in the eastbound lanes at Station 3218+05 to Station 3224+05. A pile-supported box culvert is located at approximately Station 3221, as shown in Figures 28 and 29. In 2016, the pavement in this area was reported to have experienced about 3 in. of settlement. The pavement over the culvert showed more settlement compared to the area adjacent to the culvert. According to the forensic boring information (SB Nos. 1, 3, 5, and 7), shown in Figure 30, the top 4 ft to 5 ft of the embankment were constructed with RAP,

with clay fill underneath, although the settlement analysis given in the forensic geotechnical reports estimated a minimal settlement of 0.22 in., as shown in Figure 31.

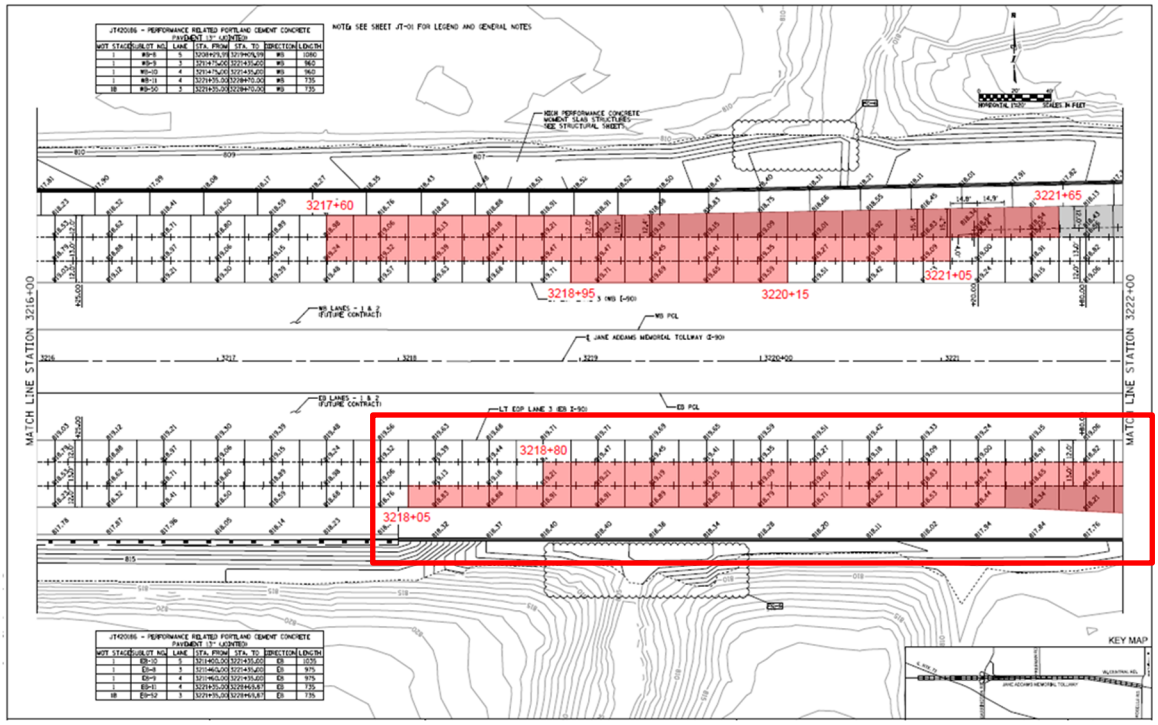

FIGURE 28. Failure locations next to Retaining Wall #4 (Station 3216+00).

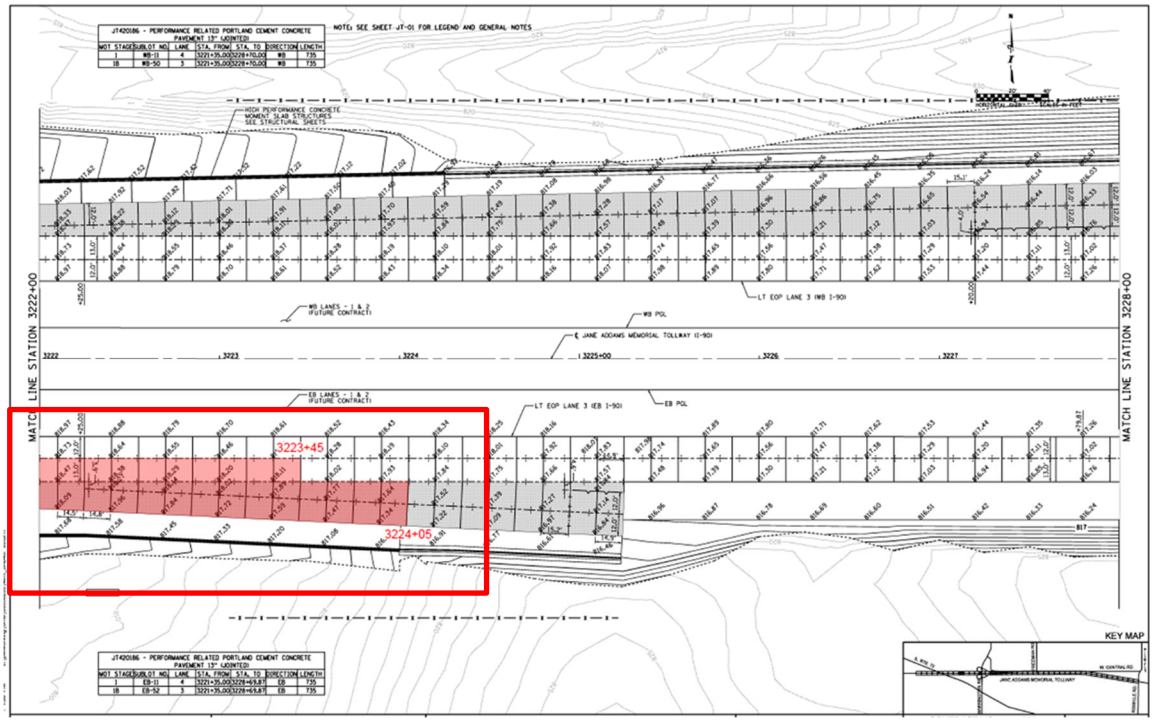

FIGURE 29. Failure locations next to Retaining Wall #4 (Station 3222+00).

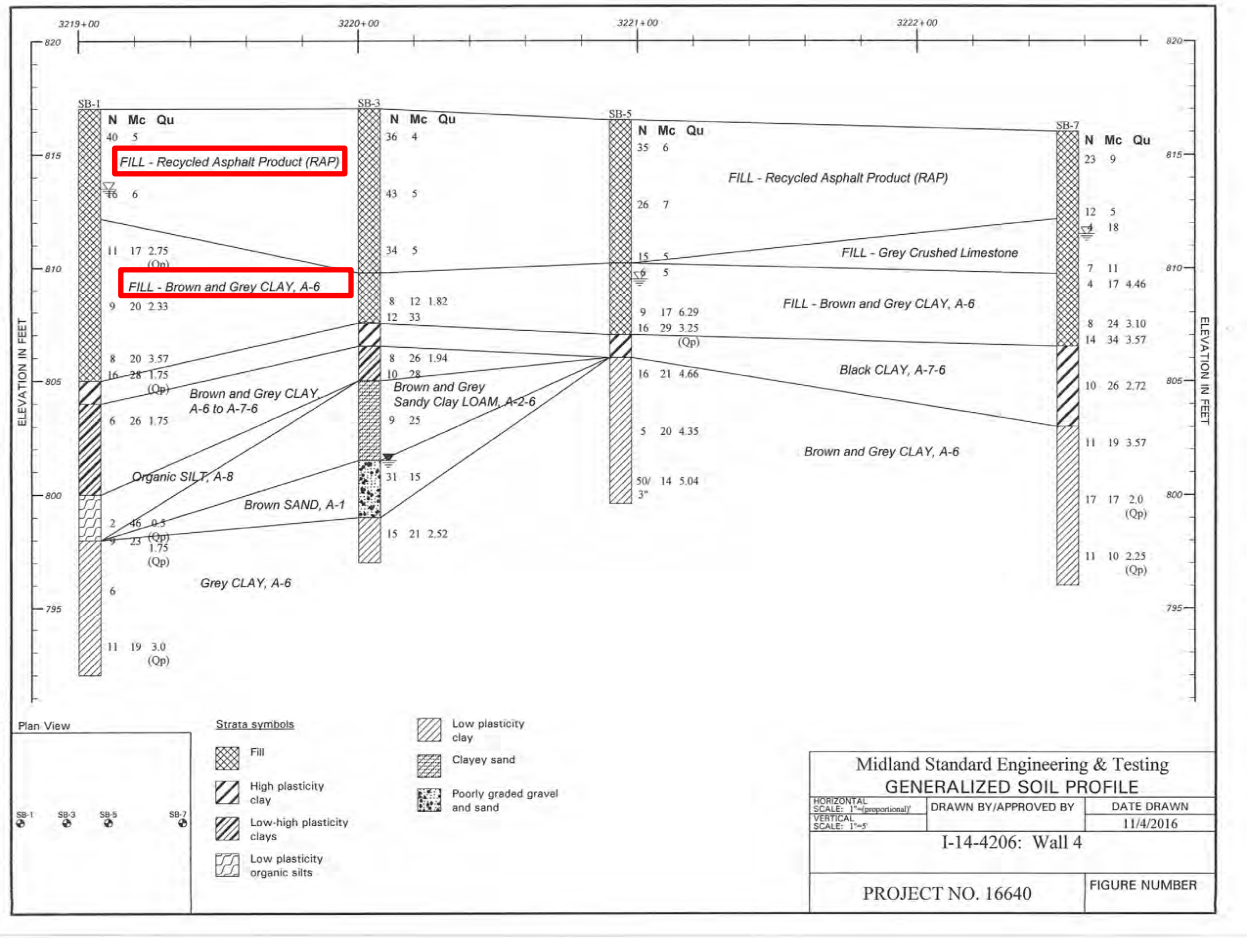

FIGURE 29. Boring profile next to Retaining Wall #4.

3.1.2.2 Corrective Actions

After significant settlement had occurred in the Retaining Wall #4 area, similar to the area next to Retaining Wall #1, a series of repairs were performed. First, the existing pavement structure above the embankment was removed, followed by 1 ft of RAP embankment undercut. The RAP fill that was excavated as well as the RAP that was left in place below the undercut were reported to be in a rather loose condition throughout. The remaining RAP in the embankment was recompacted to achieve maximum density using a roller pattern and the nuclear density method and was proof-rolled. Ground stabilization fabric was placed with PGE in the undercuts prior to the aggregate subgrade placement. Since these corrective actions have taken place, no noticeable settlement has been reported.

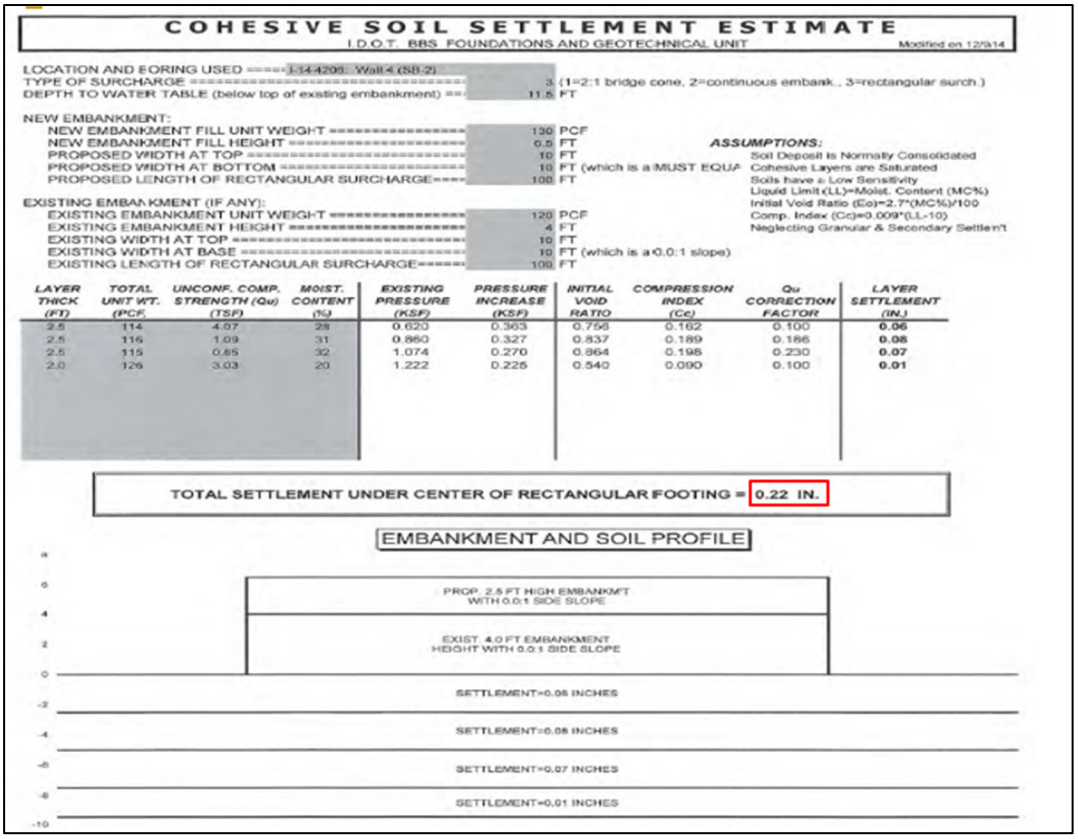

FIGURE 30. Settlement estimation for Retaining Wall #4.

3.1.3 Retaining Wall #5 Area

3.1.3.1 Settlement

The settlement of the pavement next to Retaining Wall # 5 occurred in the eastbound lanes from Station 3336+00 to Station 3337+75, as shown in Figures 32 and 33. A pile-supported box culvert is located at approximately Station 3337. The settlement was not measured because an asphalt layer was constructed over the concrete pavement as a temporary repair measure. The pavement over the pile-supported culvert exhibited more settlement compared to the area adjacent to the culvert. According to the forensic boring information (Nos. SB 1-5), shown in Figure 34, the top 6 ft of the embankment was constructed with RAP, with clay fill underneath. The estimates of the settlement provided in the geotechnical reports (both at the design stage and forensic stage) show minimal settlement, e.g., 0.33 in. in the forensic geotechnical report, as shown in Figure 35. However, these soil settlement estimates, which are in accordance with the

IDOT soil settlement analysis method, again did not include settlement in the embankment that contains soil and RAP.

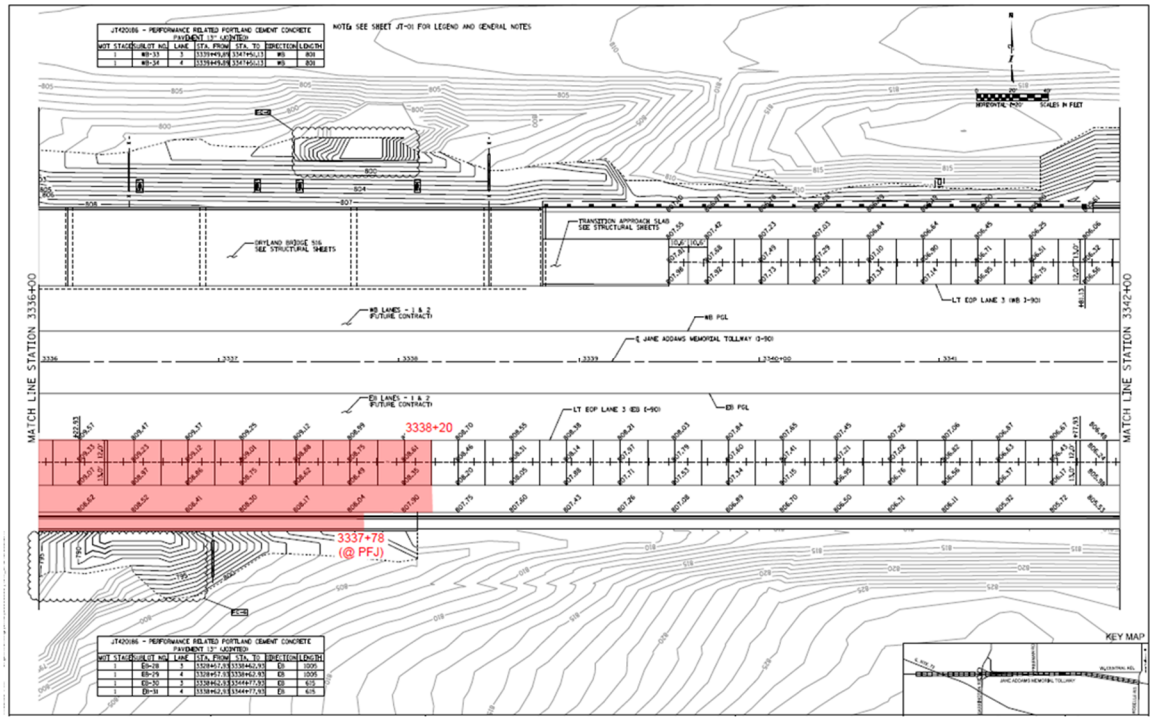

FIGURE 31. Failure locations next to Retaining Wall #5 (Station 3336+00).

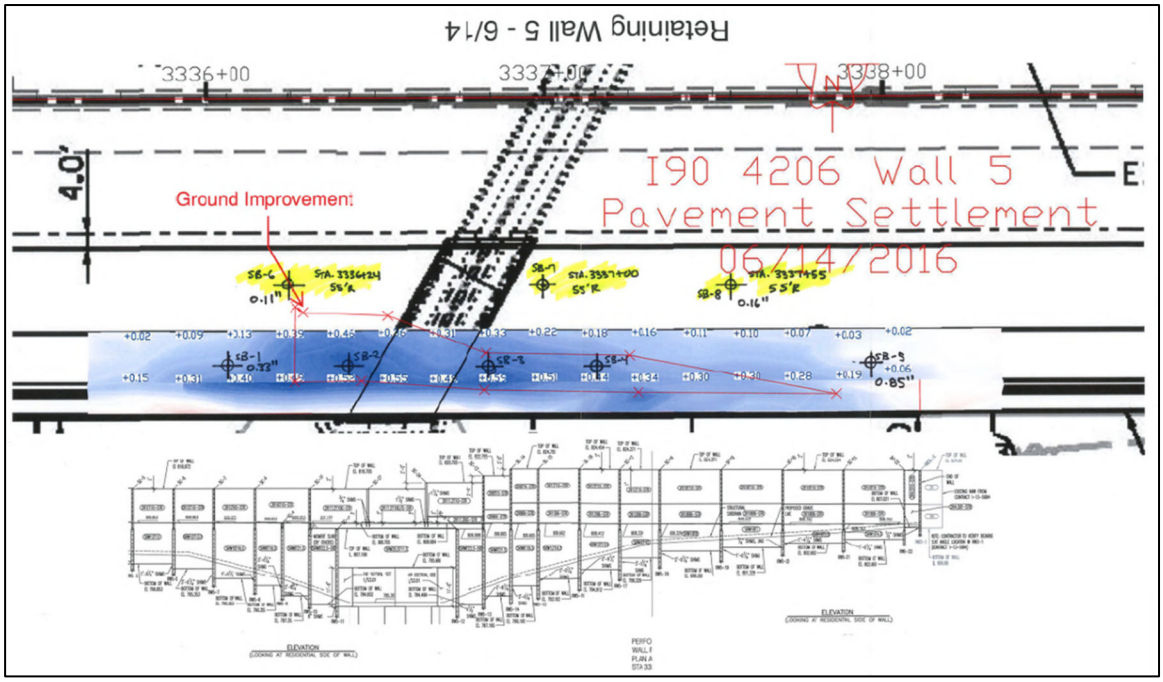

FIGURE 32. Failure locations next to Retaining Wall #5 (Station 3336+00 – Station 3338+00).

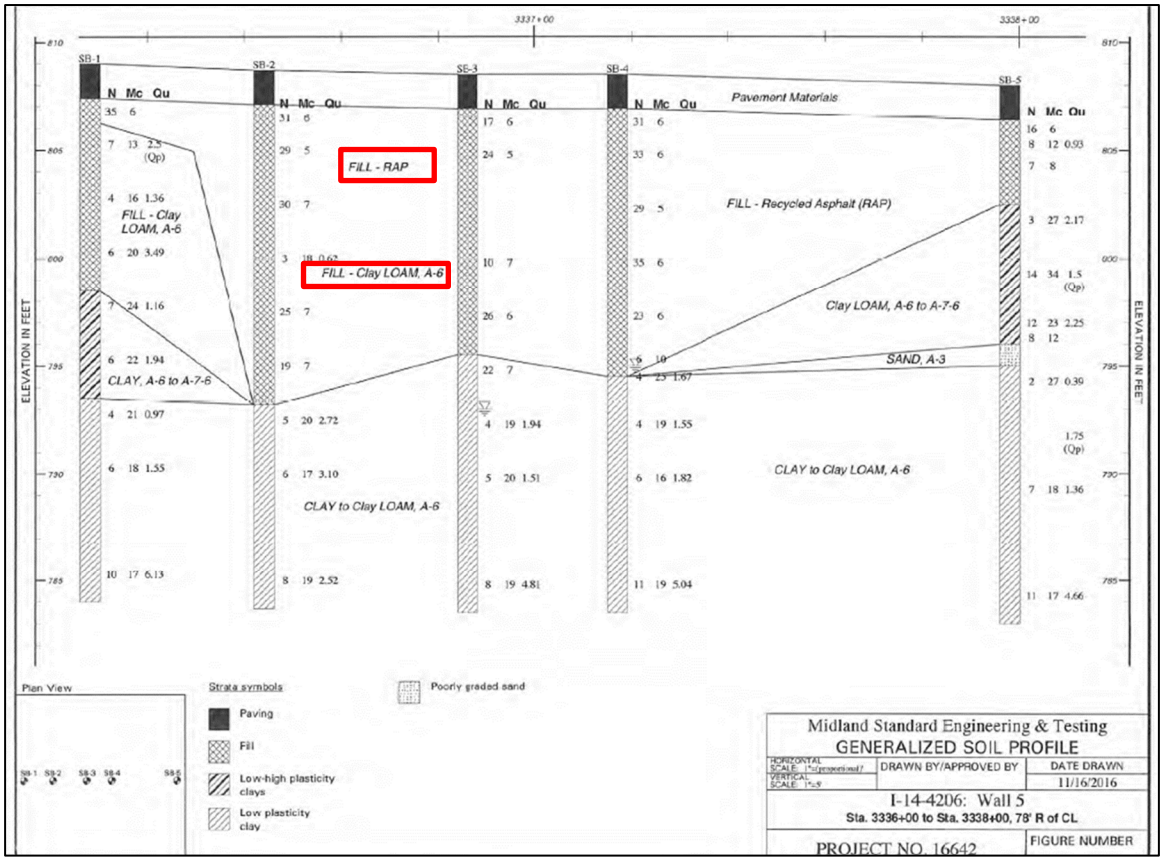

FIGURE 33. Boring profile next to Retaining Wall #5.

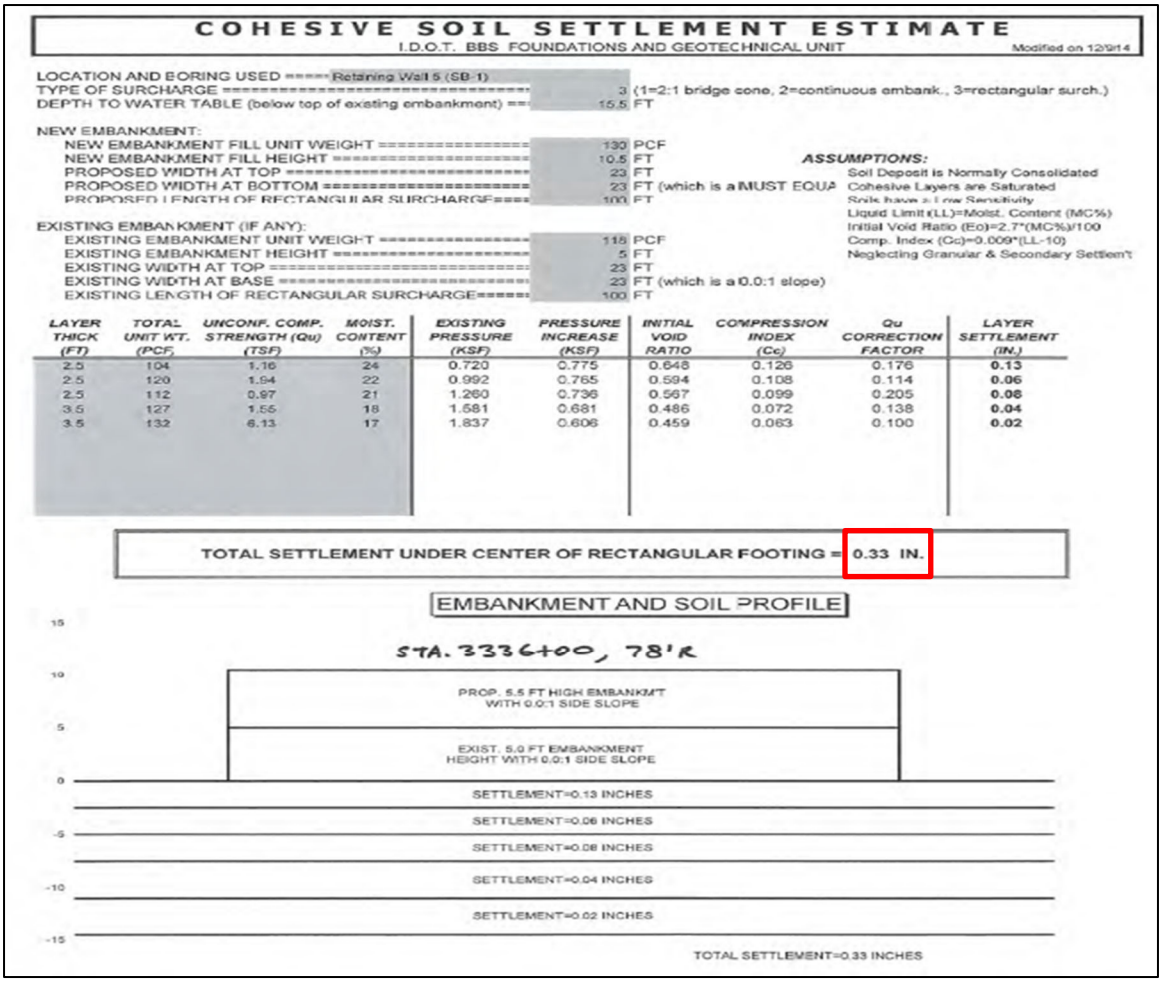

FIGURE 34. Settlement estimation for Retaining Wall #5.

3.1.3.2 Corrective Actions

After significant settlement and pavement cracking had occurred, a series of repairs were performed in the specified area around Retaining Wall #5. First, the existing pavement structure above the embankment was removed, followed by 2 ft of RAP embankment undercut. The remaining RAP in the embankment was recompacted to achieve maximum density using a roller pattern and the nuclear density method and was proof-rolled. Ground stabilization fabric was placed with PGE in the undercuts prior to the aggregate subgrade placement. Since these corrective actions have taken place, no noticeable settlement has been reported.

3.2 IL-390 Elgin O'Hare Expressway

3.2.1 Actual Site and Pavement Layer Profile Information

The IL Rte. 390 Elgin O'Hare Expressway project, under various contracts, also experienced settlement when RAP was used in the embankment. Figures 36 through 39 show the five locations of the settlement. All of the pavement structures consisted of a 10.5-in. concrete layer, 3-in. WMA sub-base, and a 3-in. RAP cap of 6-in. PGE layer. The special provision for embankments specifies that, when RAP is used in an embankment, the RAP shall comply with IDOT's policy guidelines, *Reclaimed Asphalt Pavement for Aggregate Applications*, which requires the asphalt grindings to be processed. Also, embankment fill materials that may be permeable need to be covered with 3 ft of low-permeability soil. However, a significant amount of information, such as settlement measurements, etc., was not available, nor was information about whether any repairs had taken place. A review of the field compaction results indicates that the *in situ* RAP density met or exceeded the 95% maximum density specified by the Standard Proctor method. Figure 40 provides an example of the field compaction test results.

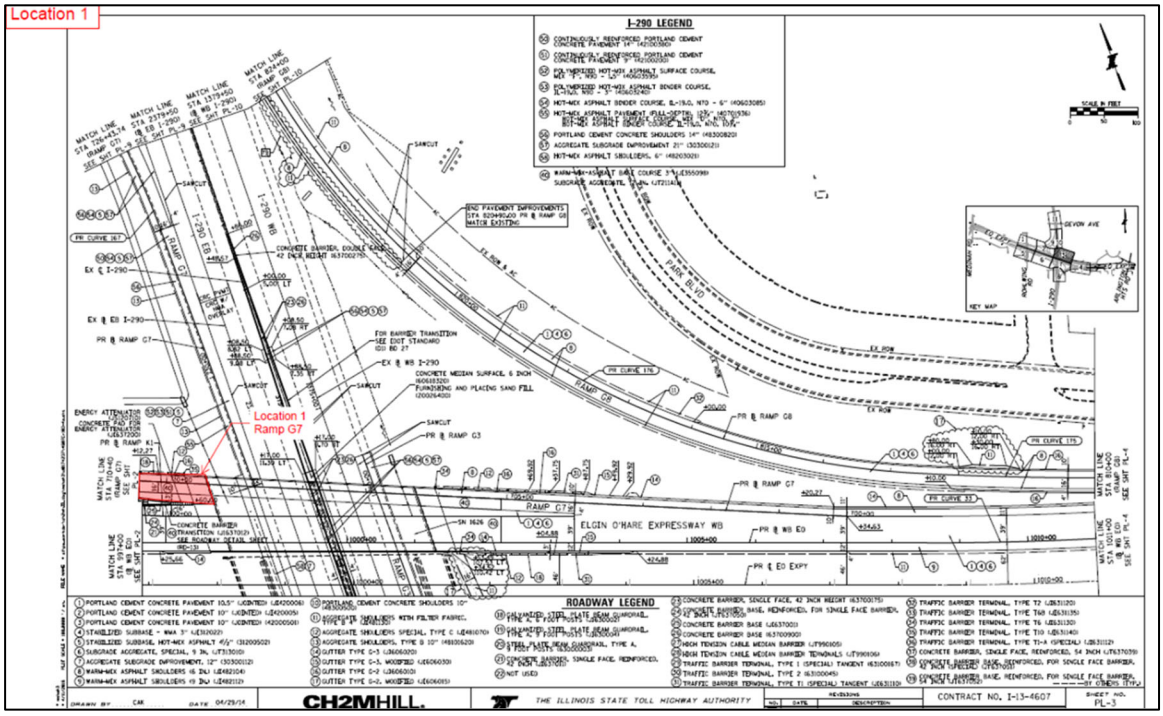

FIGURE 35. Location 1 of settlement at Elgin O'Hare Expressway.

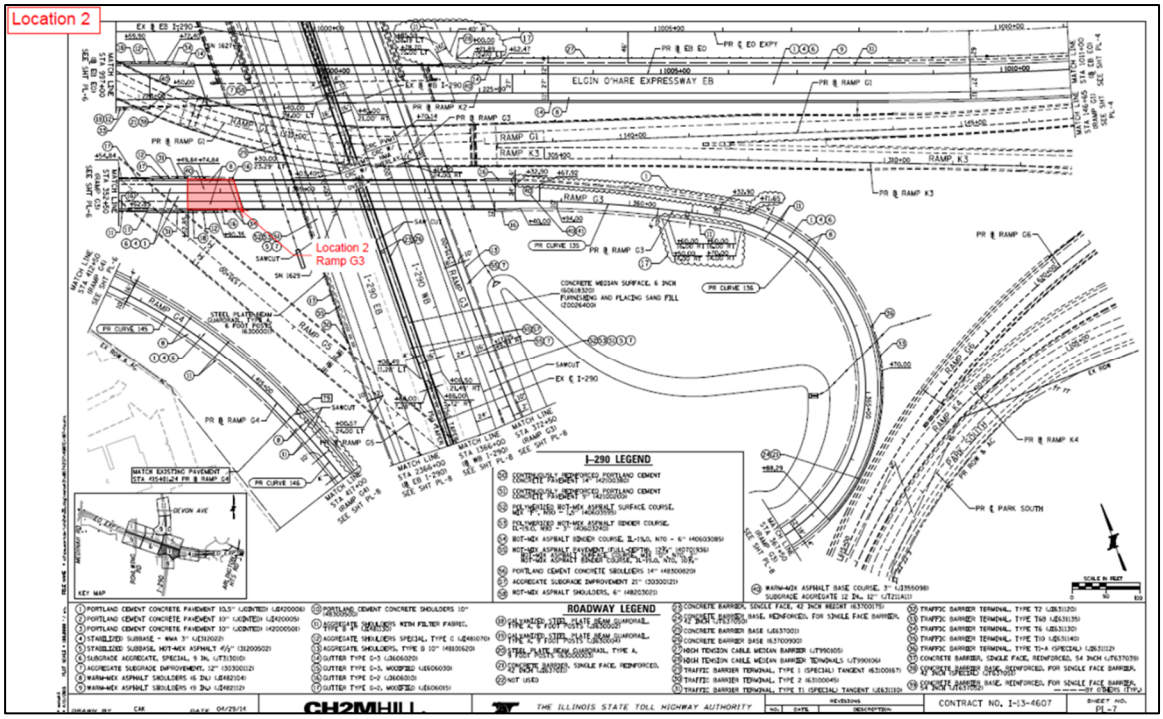

FIGURE 36. Location 2 of settlement at Elgin O'Hare Expressway.

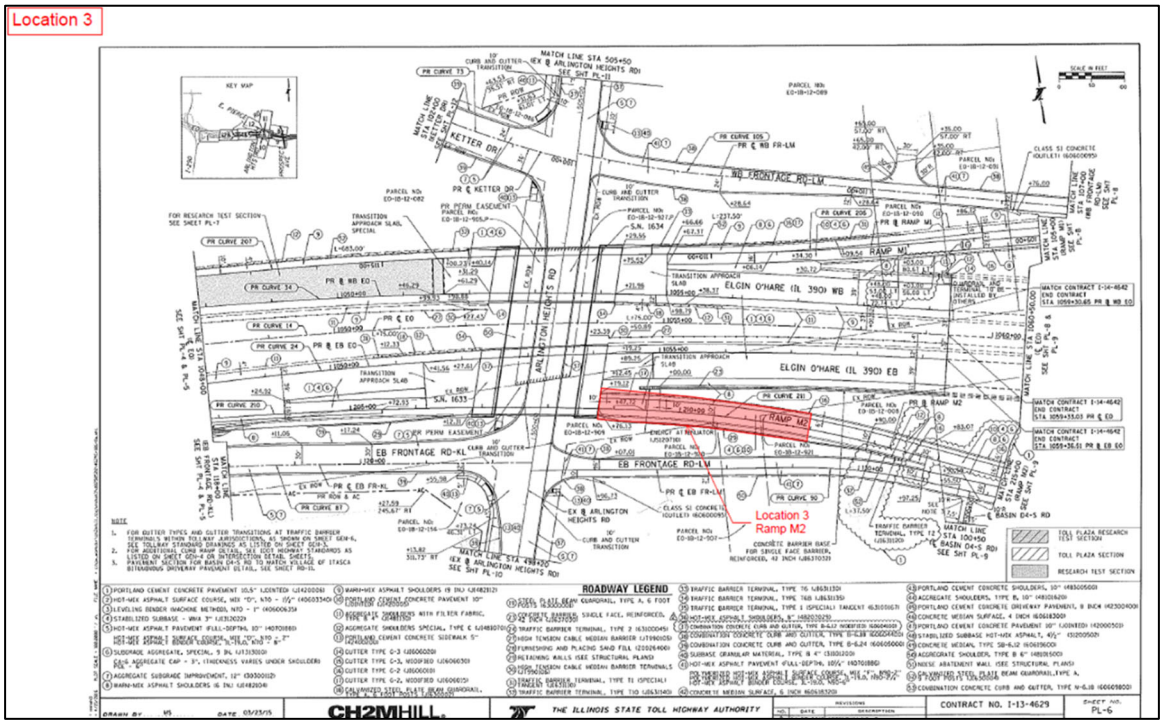

FIGURE 37. Location 3 of settlement at Elgin O'Hare Expressway.

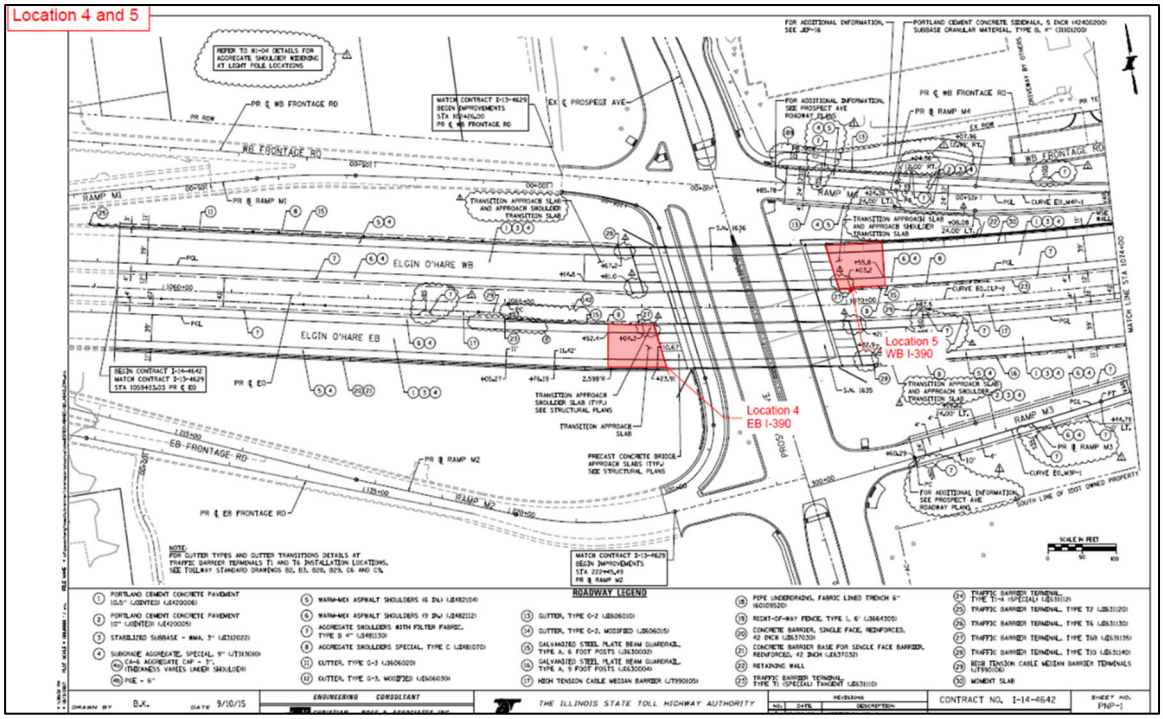

FIGURE 39. Locations 4 and 5 of settlement at Elgin O'Hare Expressway.

TABLE 6. Summary of Specifications for Locations 1 through 5 on Elgin O'Hare Expressway

Location	Contract Number	Route Number	Construction Date	Settlement Area	Settlement Limits (Estimated)	Pavement Structure	Cross Section	Embankment Height Fill	Adjacent Structure	Structure Slope
1	I-13-4607	Elgin O'Hare Expressway (IL Rte. 390) at I-290 interchange	Apr - Sept 2015	Ramp G7	Station 709+40 to Station 710+40	PCC 10.5 in. +3 in. WMA sub-base + subgrade aggregate special 9 in.	Slope	22 ft	Bridge	Slope
2	I-13-4607	Elgin O'Hare Expressway (IL Rte. 390) at I-290 interchange	Jun 2015	Ramp G3	Station 353+50 to Station 354+30	PCC 10.5 in. + 3 in. WMA sub-base + subgrade aggregate special 9 in.	Slope	13 ft	Bridge B1629	Slope
3	I-13-4629	Elgin O'Hare Expressway west access	Nov 2016 – Feb 2017	Ramp M2	Station 208+70 to Station 212+00	PCC 10.5 in. + 3 in. WMA sub-base + subgrade aggregate special 9 in.	Retaining Wall (North)	23 ft	Bridge 1633	Mechanically-stabilized earth
4	I-14-4642	Elgin O'Hare Expressway west access		EB AND WB next to Bridge 1636	EB: Station 1066+40 to Station 1067+20 WB: Station 1069+80 to Station 1070+50	PCC 10.5 in. + 3 in. WMA sub-base + subgrade aggregate special 9 in.	Slope for EB Retaining Wall for WB (South)	28 ft	Bridge 1636	Mechanically-stabilized earth
5	I-14-4642	Elgin O'Hare Expressway West Access		EB next to Bridge 1639	Station 1095+00 to Station 1098+20	PCC 10.5 in. + 3 in. WMA sub-base + subgrade aggregate special 9 in.	Retaining Wall (South)	1 ft	Bridge 1639	

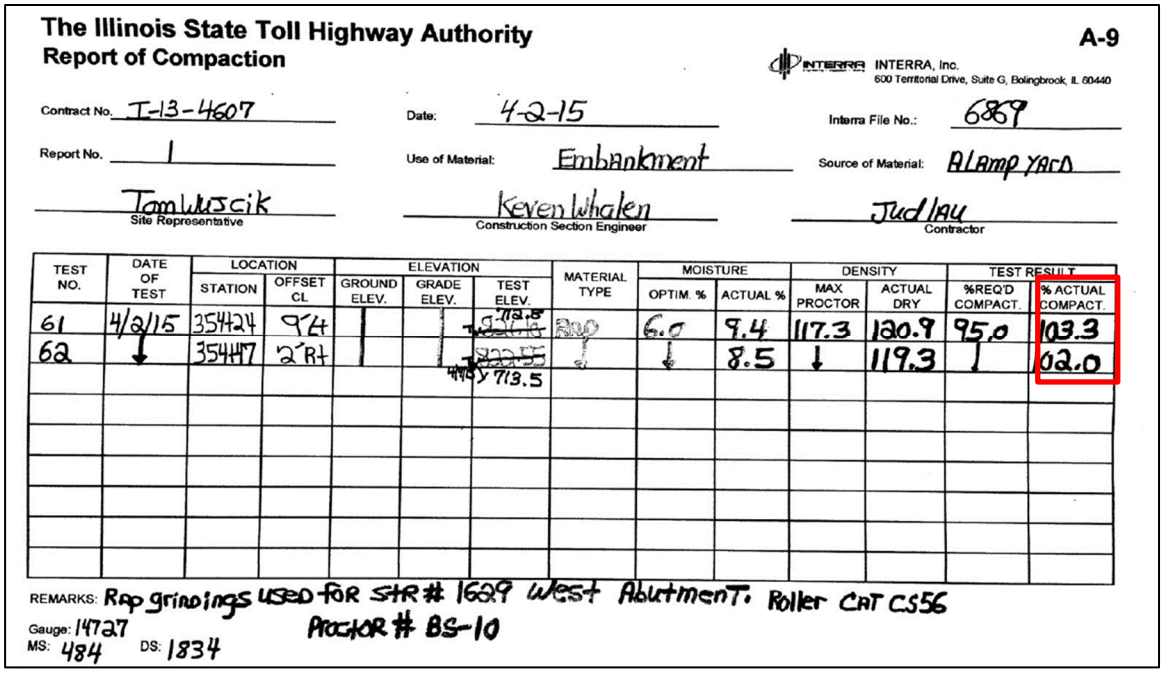

The Illinois State Toll Highway Authority
Report of Compaction

A-9

INTERRA, Inc.
600 Territorial Drive, Suite G, Bolingbrook, IL 60440

Contract No. I-13-4607 Date: 4-2-15 Interra File No.: 6869

Report No. 1 Use of Material: Embankment Source of Material: RAMP YARD

Tom Wiscik
Site Representative

Keven Whalen
Construction Section Engineer

Jud Iau
Contractor

TEST NO.	DATE OF TEST	LOCATION		ELEVATION			MATERIAL TYPE	MOISTURE		DENSITY		TEST RESULT	
		STATION	OFFSET CL	GROUND ELEV.	GRADE ELEV.	TEST ELEV.		OPTIM. %	ACTUAL %	MAX PROCTOR	ACTUAL DRY	%REQ'D COMPACT.	% ACTUAL COMPACT.
61	4/2/15	354424	97' Lt			713.5	RAP	6.0	9.4	117.3	120.9	95.0	103.3
62	↓	354417	2' Rt			713.5	↓	↓	8.5	↓	119.3	↓	102.0

REMARKS: Rap grindings used for STR # 1609 West Abutment. Roller CAT CS56
Proctor # BS-10

Gauge: 14727
MS: 484 DS: 1834

FIGURE 38. Example of compaction inspection test results.

3.3 Summary of Forensic Investigation

The geotechnical settlement analyses, for both the design stage and forensic stage, predicted minimal settlement, yet excessive settlement was observed soon after construction, especially for the I-90 Jane Addams Memorial Tollway. In these analyses, the embankment (soil or RAP) settlement was not included. Most of the distressed pavement sections on the I-90 Jane Addams Memorial Tollway were removed and undercut by 1 or 2 feet. The bottom of the undercut was compacted and the undercut was replaced with a PGE layer. No further noticeable settlement has been reported after this repair.

CHAPTER 4 MATERIALS AND TESTING

In order to study the performance of RAP in embankments, the research team conducted laboratory tests of RAP and compared the results to conventional embankment soils that have been used by Illinois Tollway. As no excessive embankment settlement has been reported when conventional embankment soils are used in embankments, conventional soils are considered the benchmark for comparative purposes.

4.1 Characterization of RAP and Natural Soils

4.1.1 Sampling

Illinois Tollway and Interra, Inc. (Illinois Tollway's support team) collected two conventional embankment soils and five unprocessed asphalt grindings and shipped them to Washington State University. The two embankment soils are referred to as EMB1 and EMB2 and the five RAP samples are referred to as RAP1, RAP2, RAP3, RAP4, and RAP5. Figures 41 and 42 present photographs of the as-received embankment soils and RAP samples, respectively. In addition to testing the unprocessed RAP grindings that passed the 2-in. sieve, these RAP samples were screened through a 1.5-in. sieve, which is consistent with the current Illinois Tollway special provision for RAP, in order to study the effect of the maximum particle size of RAP on settlement. In addition, the team included a mixture of unprocessed RAP2 and EMB1 (50:50) as a potential measure to improve the performance of RAP as embankment material; this mixture was added to the study at a later stage and is referred to as the 'soil + RAP mix'.

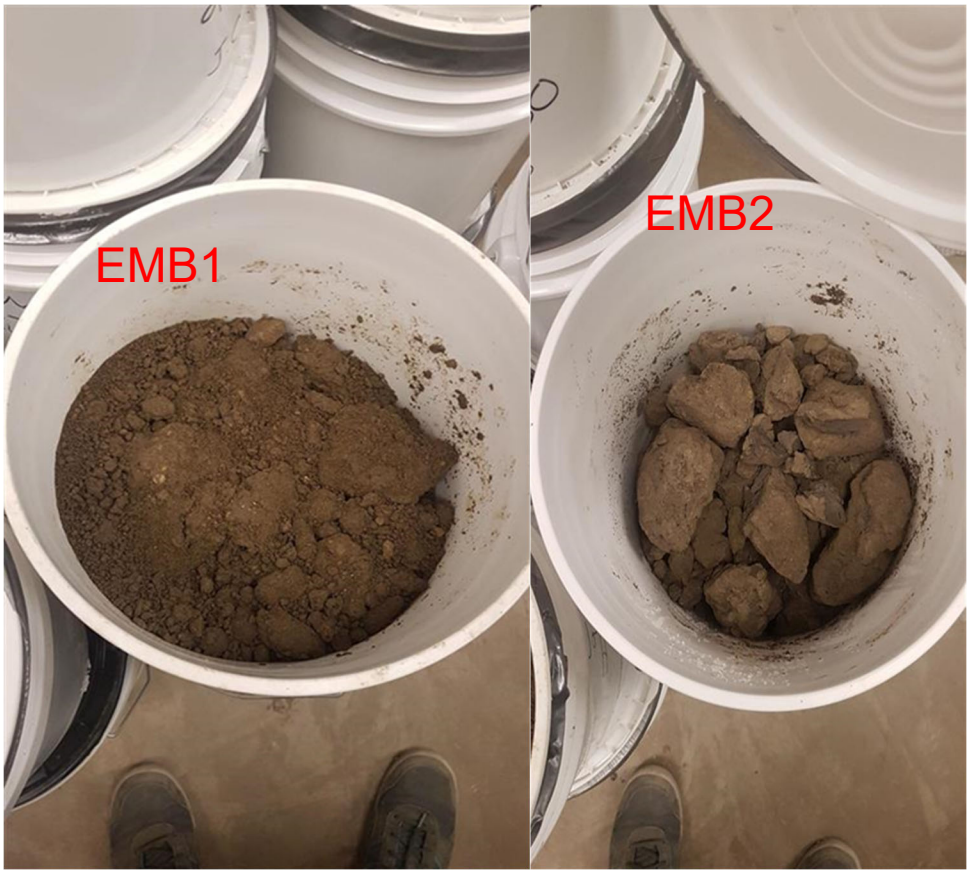

FIGURE 39. Embankment soils: EMB1 and EMB2.

FIGURE 40. RAP samples.

4.1.2 Gradations and Soil Characteristics

The RAP samples were dried at 140°F overnight and sieved according to AASHTO T 27-20 (*Sieve Analysis of Fine and Coarse Aggregate*). A few individual large particles of RAP grinding were present and screened through the 2-in. sieve, because the largest mold diameter used in laboratory tests is 6 in. and the ratio of the mold diameter to particle size should not be more than 3:1. Figure 43 presents the RAP and soil gradations that were determined in accordance with AASHTO T 27 and 88. The RAP samples are shown to be coarser than the two soils. EMB1 and EMB2 were characterized based on AASHTO T 89 and T 90 and classified as AASHTO A-6 and A-4, respectively. Table 7 presents the plastic limit, liquid limit, and the plasticity index values of the two soils. Using a magnet, the research team found approximately 16%, 3%, 2%, 0%, and 0% steel slag (or iron-containing materials) in RAP1, RAP2, RAP3, RAP4, and RAP5, respectively, based on the total mass of the RAP samples.

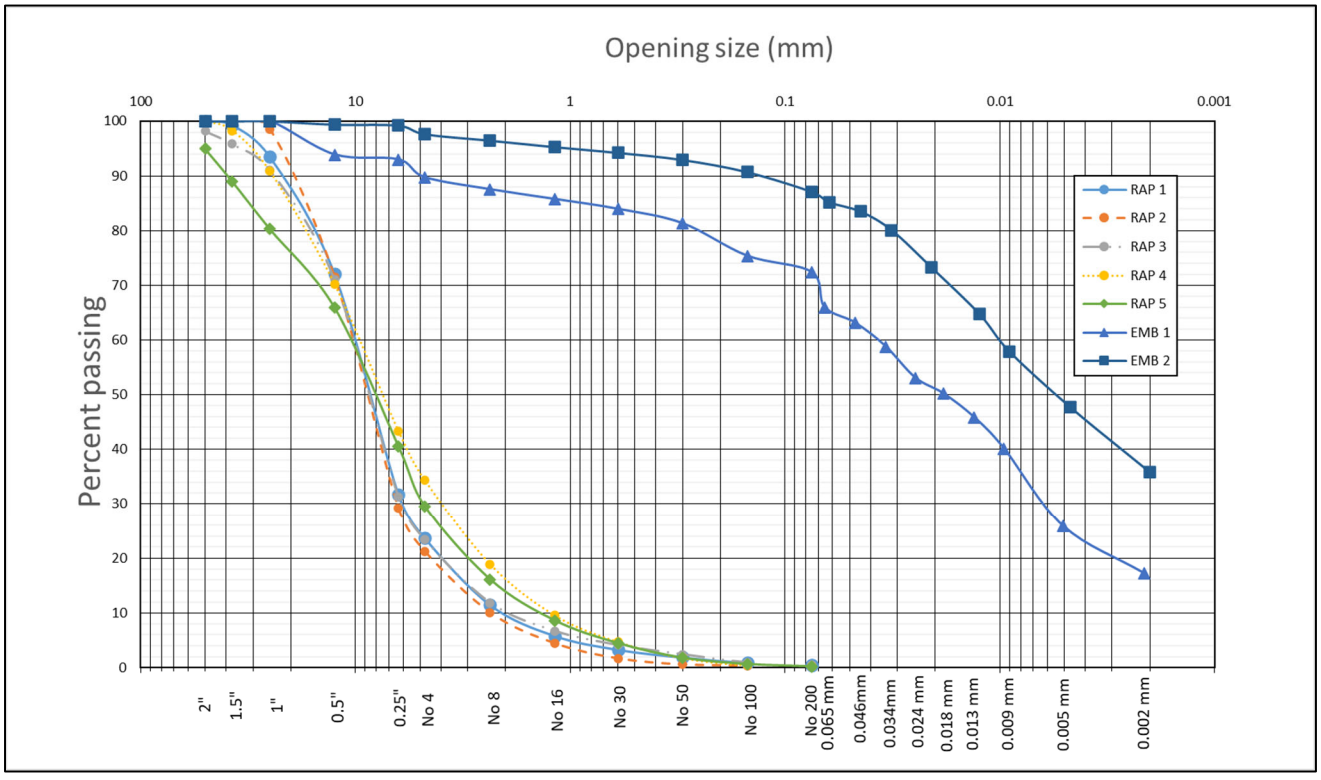

FIGURE 41. Gradations of the five study RAP samples and two embankment soil samples.

TABLE 7. Soil Characteristics

	EMB1	EMB2
Plastic Limit (%)	23	17
Liquid Limit (%)	36	27
Plasticity Index	13	10

4.1.3 RAP Asphalt Content

Two methods, the ignition oven method (AASHTO T 308) and the quantitative extraction of asphalt binder from HMA (AASHTO T 164 Method A) were used to determine the asphalt contents of the RAP samples. The ignition oven method reported unreasonably high asphalt contents, e.g., more than 8%, probably due to the lack of aggregate correction factors. Therefore, the research team used the results from the extraction method. Dichloromethane was used as the solvent and the asphalt content was calculated based on Equation (2). Table 8 presents a summary of the asphalt contents of the RAP samples.

$$AC\% = \frac{(W_1 - W_2) - (W_3 + W_4)}{W_1 - W_2} \times 100 \quad (2)$$

where

AC% = asphalt binder content, %;

W_1 = mass of test portion;

W_2 = mass of water in test portion;

W_3 = mass of extracted mineral aggregate; and

W_4 = mass of mineral matter in the extract.

TABLE 8. Asphalt Content of RAP Samples

Material	Asphalt Content (%)
RAP1	5.82
RAP2	5.00
RAP3	5.69
RAP4	5.42
RAP5	6.33

4.1.4 Moisture-Density Relationship

The standard Proctor compaction test was conducted to determine the OMC and MDD or density in accordance with AASHTO T 99 Method C. This procedure uses a 5.5-lb rammer and 12-in. drop height. Particles retained on the ¾-in. sieve were removed prior to compaction. The samples then were compacted in three layers in a 4-in. mold using 25 blows per layer. The wet density was calculated using Equation (3). Based on the wet density and average moisture content, the dry density was calculated based on Equation (4).

$$W_1 = (A-B)/V \quad (3)$$

where

W_1 = wet density;
A = mass of compacted specimen and mold;
B = mass of mold; and
V = volume of mold.

$$W = \frac{W_1}{w+100} \times 100 \quad (4)$$

where

W = dry density; and
w = moisture content of the specimen by percentage.

In order to evaluate the effect of the construction season on the density, loose RAP samples were conditioned at four temperatures (32ºF, 40ºF, 70ºF, and 100ºF) for each of the five RAP samples. A loose sample for each moisture content was divided into five parts, and each part was stored in a plastic bag. These plastic bags of loose materials were conditioned in an environmental chamber for 8 h, 8 h, and 5 h at 32ºF, 40ºF, and 100ºF, respectively, based on trial and error. 70ºF was considered to be room temperature. Prior to compaction, each bag was removed from the environmental chamber and the materials were compacted into one layer as soon as possible before another bag was removed from the chamber. For the 32ºF compaction, due to the quick loss of temperature during the time from the removal of the bags to the completion of compaction for each layer, the RAP samples were set to 30ºF instead, based on trials.

4.1.4.1 Correction for Optimum Moisture Content and Maximum Dry Density

As specified by AASHTO T 99, corrections to the OMC and MDD values were necessary for particles retained on the ¾-in. sieve. The OMC and MDD values obtained from the compaction tests were corrected in accordance with the adjustment Equations (5) through (8).

$$MC_T = (MC_f \cdot P_f + MC_C \cdot P_C) / 100 \quad (5)$$

where

MC_T = corrected moisture content of test sample, expressed as a decimal;
MC_f = moisture content of fine particles that pass the 19.00-mm (3/4-in.) sieve, expressed as a decimal;
MC_C = moisture content of oversized particles retained on the 19.00-mm (3/4-in.) sieve, expressed as a decimal that can be assumed to be 0.02 for most construction applications;
P_f = percentage of fine particles, by weight; and
P_C = percentage of coarse particles, by weight.

$$D_d = 100\ D_f\ k / (D_f \cdot P_C + k \cdot P_f) \quad (6)$$

where

D_d = corrected total dry density, kg/m^3;
D_f = dry density of fine particles, kg/m^3; and
K = 1000 × bulk specific gravity of coarse particles, kg/m^3.

$$P_f = 100\ M_{DF} / (M_{DF} + M_{DC}) \quad (7)$$

$$P_C = 100\ M_{DC} / (M_{DF} + M_{DC}) \quad (8)$$

where

M_{DF} = mass of fine particles; and
M_{DC} = mass of coarse particles.

In addition to the two soils and five unprocessed RAP samples, a mix of soil and RAP ('soil + RAP') also was later tested for OMC and MDD based on the standard Proctor test method. Moreover, for information purposes, RAP3 was tested in accordance with AASHTO T 180 (modified Proctor) at different test temperatures based on the results of the survey of highway agencies that use MDD in the modified Proctor test in their specifications. The results are presented in Chapter 5.

4.2 One-Dimensional Consolidation Tests

4.2.1 Introduction

1-D consolidation tests were conducted according to AASHTO T 216. In this test protocol, each load increment is maintained until the change in deformation is relatively negligible (typically 24 hours). During the consolidation process, the specimen height is measured at different time increments. The collected data can be used to compare the effective stress and void ratio or strain and the various coefficients of consolidation.

Initially, the 1-D consolidation tests were conducted using a traditional soil consolidation device, called GeoJac, as shown in Figure 44. However, this set-up was suitable only for fine soils because the diameter of the samples prepared for the GeoJac device was limited to 2.5 in., which is too small for RAP particles. In addition, the GeoJac device cannot be placed in an environmental chamber for temperature control, which is critical for RAP samples. In order to compare soil and RAP, a test that uses the same device for both is preferable. Therefore, the GeoJac test set-up was tried initially, but then dismissed.

FIGURE 42. First test set-up (GeoJac) for one-dimensional consolidation testing.

The second set-up involves equipment developed at WSU specifically for this project. This set-up, shown in Figure 45, uses pneumatic pressure and is capable of applying different loads on a steel plate placed on top of the sample. Samples were prepared in 6-in. diameter

molds. The pressure to be applied was verified using a digital load cell prior to testing. The deformation was measured using digital dial gauges. Prior to the tests, a seating load (1 psi) was applied to ensure close contact between the steel plate on top of the sample and the sample. Both the soils and RAP samples were tested in this set-up for comparative purposes to remove any effects from the device.

FIGURE 43. Second test set-up (equipment fabricated at WSU) for one-dimensional consolidation testing.

4.2.2 Test Procedure

The 1-D consolidation tests followed AASHTO T 216. The soils and RAP samples were compacted to 95% MDD at the OMC and also under saturated conditions for the soils only. The samples were 6 in. in diameter and 6.9 in. in height. For the saturated condition of soil samples, due to the sample size, each sample that was originally compacted to 95% MDD at the OMC was exposed to water from the top of the sample, and then vacuum suction pressure was applied from the bottom of the sample, which is equivalent to compressive pressure. No surcharge was applied

to the top of the sample and no swelling was noticed during saturation. Using this method, more than 95% saturation was reached.

During the 1-D consolidation tests, five stress levels, 1.8 psi, 3.6 psi, 7.2 psi, 14.4 psi, and 29 psi, were applied for 24 h at each pressure level. The data were recorded at 0.1, 0.25, 0.5, 1, 2, 4, 8, 15, 30, 60, 120, 240, 480, and 1440 minutes. The RAP samples were tested at two different temperatures, room temperature (70ºF) and 100ºF. The 100ºF temperature simulates extreme summer temperatures in an embankment. Before running the test at 100ºF, the samples were conditioned in an environmental chamber at 100ºF for two hours. The soils were tested only at room temperature because they were not expected to be as sensitive to temperature as the RAP samples. In addition, 1-D consolidation tests were conducted at the single stress level of 14.5 psi for an extended period (7 days). The pressure level of 14.5 psi represents the overburden pressure in the middle of a RAP embankment of 25 ft, which is the greatest height that RAP has been used in an embankment, based on the review of project documents.

4.3 Direct Shear

In order to measure the resistance of the soils and RAP samples to shear, two different test set-ups were tried. The GeoJac, which is the set-up used in a traditional geotechnical laboratory, is capable of direct shear tests of soils only and, as aforementioned, cannot be used for RAP samples due to RAP's large particle size. Therefore, a large direct shear device (6 in. in diameter) was fabricated for this study, as shown in Figure 46. Using this device, normal pressure can be applied through a pneumatic air cylinder. The shear force is applied via a closed-loop servo-hydraulic test machine, called a GCTS system, which records the shear force and displacement over time during the test. The samples for this test were compacted to 95% MDD at OMC in the 6-in. mold. Each sample was 6 in. in height and the shear plane was located in the middle of the sample.

The shear tests followed AASHTO T 236 under unconsolidated and drained conditions. The confining pressure was controlled to be 4.27 psi, 8.54 psi, and 12.81 psi. The shear displacement was set as 0.04 in./min. Because no apparent peak shear loads occurred, especially for the RAP samples, the shear pressure at 10% shear strain was used as the shear strength.

FIGURE 44. Direct shear test set-up.

In order to verify whether the manufactured device set-up and data collection procedure were effective, clean dry sand was used as the verification sample. Dry sand should have no or minimal cohesion between its particles, and only friction between particles is resistant to shear pressure. Based on the data collected, the cohesion and friction forces were determined to be 0 psi and 44.98º, respectively, as shown in Figure 47, which confirms the theory of zero cohesion for dry sand. Therefore, the fabricated shear device was found to be effective.

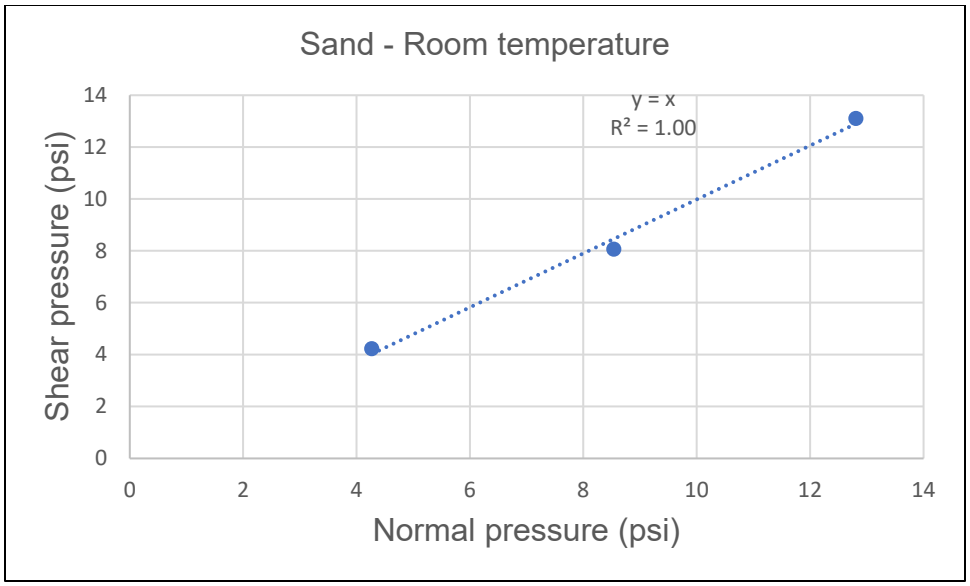

FIGURE 45. Direct shear test results for sand.

4.4 Permeability

4.4.1. Constant Head Test

Given the gradations of the RAP samples, fewer than 10% of the RAP particles passed the No. 200 sieve. Therefore, the constant head method was chosen to determine permeability in accordance with AASHTO T 215. Figure 48 shows the constant head permeameter with a diameter of 6 in. that was used to conduct the permeability tests. Because all five RAP samples had similar gradations, only RAP2 was tested due to time limitations (note that this test was added later in this study). Particles larger than 3/4 in. were removed and the percentage of oversized particles was recorded. Samples were compacted in the permeability cylinder in thin layers to a height about 0.8 in. above the upper manometer outlet. As shown in Figure 48, the distance between the bottom of the permeameter and the upper manometer outlet is about 8 in.; thus, the total sample height of 8.8 in. allowed the top surface of the sample to reach 0.8 in. above the upper manometer outlet. The weight of the samples that were added to each layer was calculated based on 90% MDD. The coefficient of permeability was calculated using Equation (9).

$$K = \frac{QL}{Ath} \tag{9}$$

where

K = coefficient of permeability;

Q = quantity of water discharged;
L = distance between manometers, which is 6 in. in this study;
A = cross-sectional area of specimen, which equals 28.26 in.^{2} in this study;
t = total time of discharge; and
h = difference in head on manometers.

FIGURE 46. Constant head/falling head permeability test equipment.

4.4.2 Falling Head Permeability Test

For the two soil samples and the soil + RAP mix, because more than 10% passed the No. 200 sieve, the falling head test (ASTM D5084) was conducted. The samples were prepared to 95% MDD at the OMC with a 6-in. diameter and 4.5-in. height. Vacuum pressure was applied from the bottom to saturate the sample and remove air. According to Equation (10), four different levels of water were used for the measurements.

$$k = \frac{a.L}{A.\Delta t} \ln\left(\frac{\Delta h_1}{\Delta h_2}\right) \quad (10)$$

where

k = hydraulic conductivity (m/s);

L = length of specimen (m);

Δt = interval of time (s);

A = cross-sectional area of specimen (m^2);

Δh_1 = head loss across the specimen at t_1 (m); and

Δh_2 = head loss across the specimen at t_2 (m).

4.4.3. Tube Permeability

In order to simulate a drainage system in the pavement of the I-90 Jane Addams Memorial Tollway, a 12-in. diameter PVC tube was fabricated and filled with PGE, RAP3, and EMB1, layered from top to bottom, as shown in Figure 49, which is the same order as field conditions. Weep-holes were drilled into the PVC tube wall at the bottom of the PGE layer to allow water to drain out. The layers of RAP3 and EMB1 were compacted to 95% MDD at the OMC. Each layer had an equal height of 6 inches. Figure 50 shows the RAP and rocks (PGE layer) in the permeability tube.

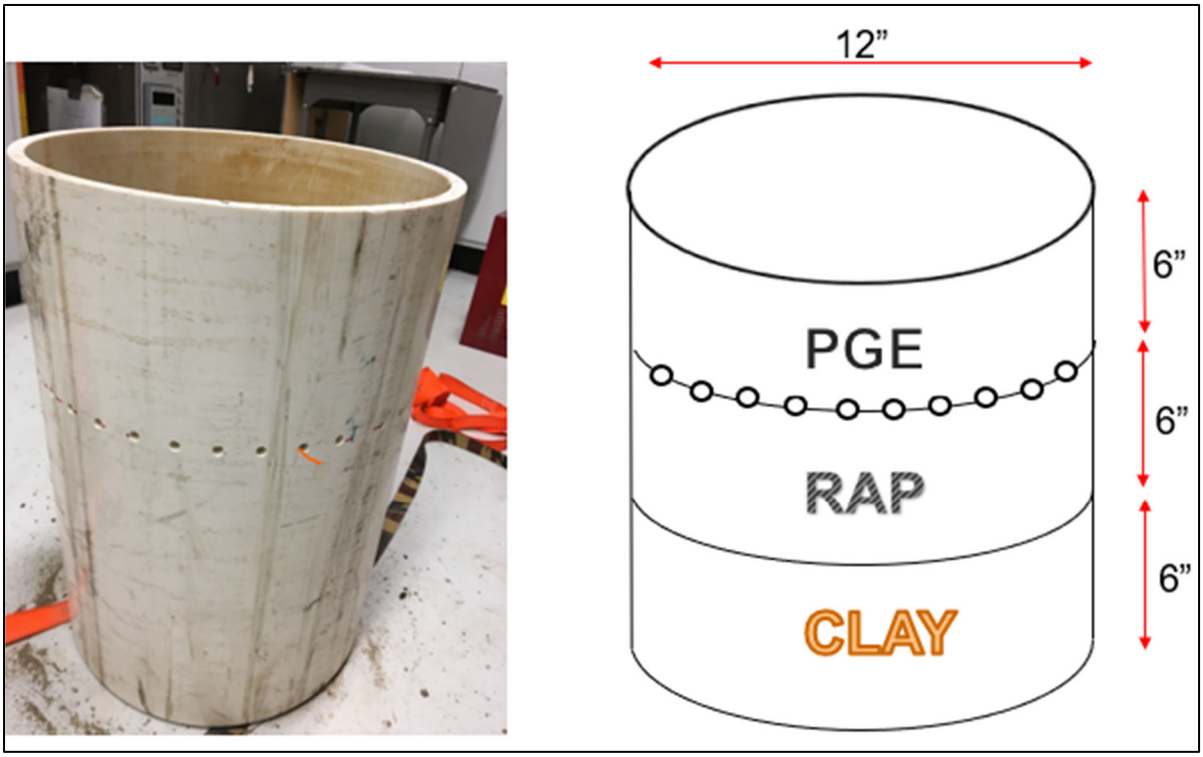

FIGURE 49. Permeability tube and schematic of tube fill.

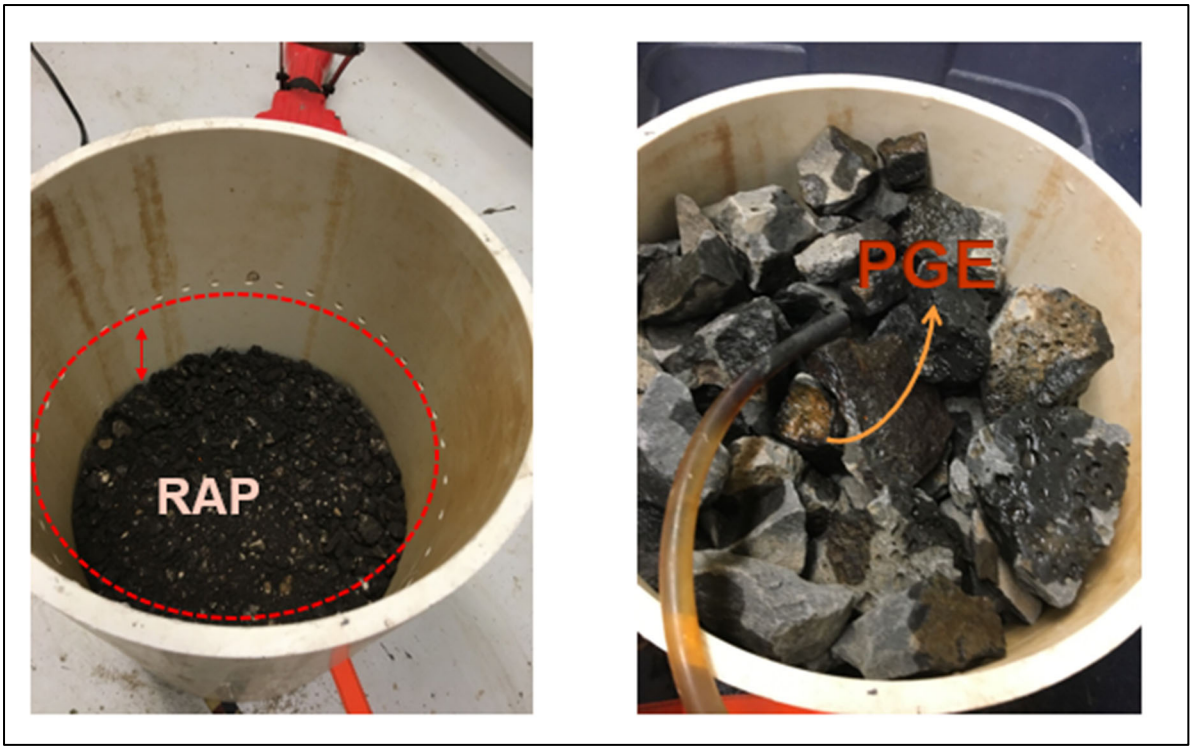

FIGURE 47. RAP and rocks (porous granular embankment, or PGE) in permeability tube.

Water was introduced to the sample with a flow rate of 0.33 lb/min, based on results from the Drainage Requirement in Pavements (DRIP) program, as shown in Figure 51. The weight of the sample in the tube was measured periodically.

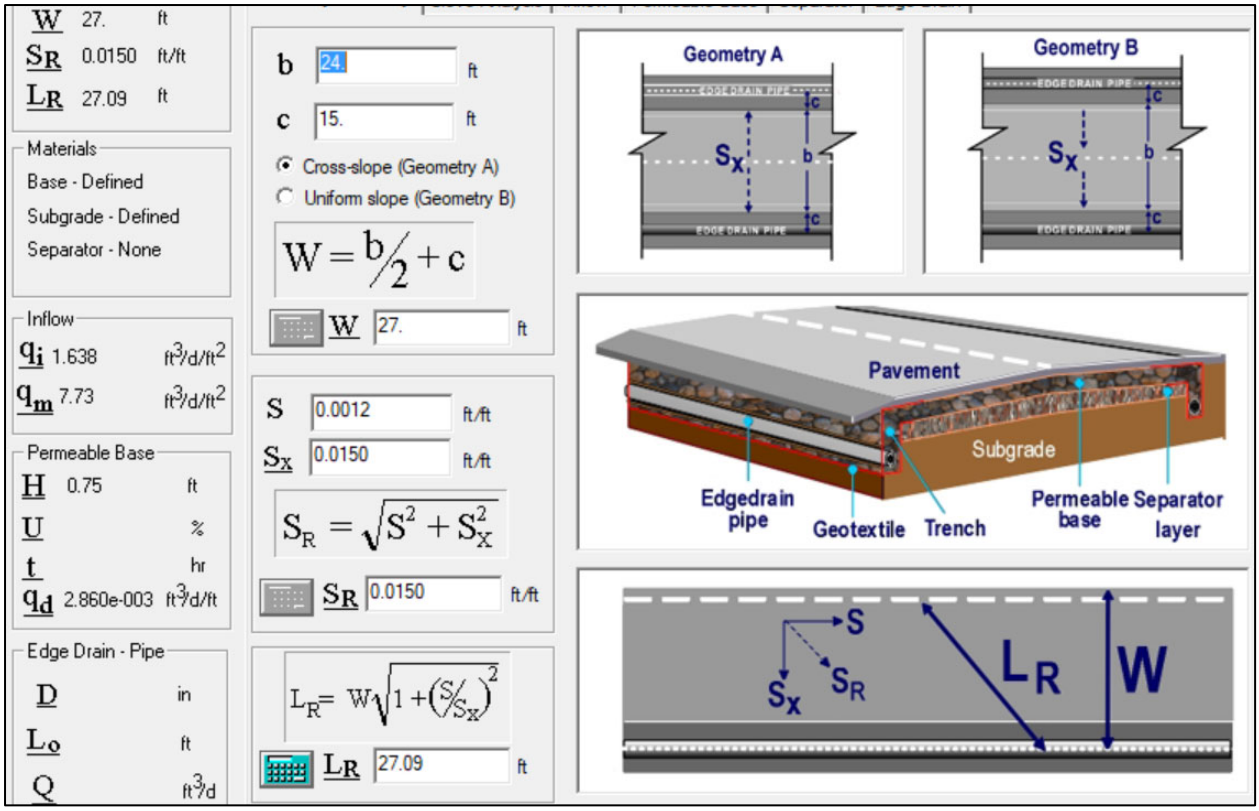

FIGURE 48. DRIP program output for flow rate calculations.

4.5 Dynamic Triaxial Testing

Dynamic triaxial tests were conducted to simulate the impact of traffic loading on the soils and RAP samples in an embankment. Samples were prepared in accordance with the compaction procedure given in AASHTO T 307-99 (2017). The material was compacted in a split mold with a diameter of 6 in. for six layers, with each layer a height of 2 in. to make a target height of 12 inches. The mass of each layer was determined using the corrected OMC and 95% MDD in accordance with the protocol.

Samples were placed in the triaxial cell of the GCTS loading system, shown in Figure 52, for testing, following AASHTO T 307-99. Two linear variable differential transducers (LVDTs) were used to measure the axial deformation over 6-in. spacing. The deformation also was measured by an overhead frame LVDT. A triaxial chamber was used to provide an air-tight environment so that the target confining pressure could be reached during the test. The water valves for drainage were kept open during the tests.

FIGURE 49. Triaxial test set-up.

In order to determine the stress levels to be applied, the pavement structure of the I-90 Jane Addams Memorial Tollway was analyzed using EverFE, a finite element program. Figures 53 and 54 respectively show the traffic loading pattern and applied stress used for analysis. Based on the results, the confining pressure at the bottom of the base layer was determined to be 4.35 psi, the seating load was determined to be 2.9 psi, and the cyclic load to be 2.9 psi. Axial loading was applied using haversine-shaped loading, a 0.1-s load pulse followed by a 0.9-s rest period, as shown in Figure 55.

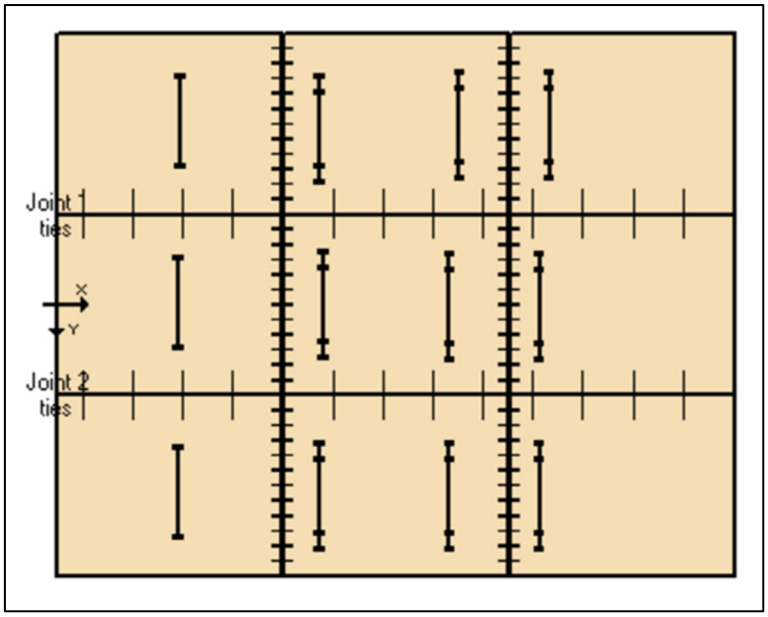

FIGURE 50. EverFE design vehicles: wheel loading pattern.

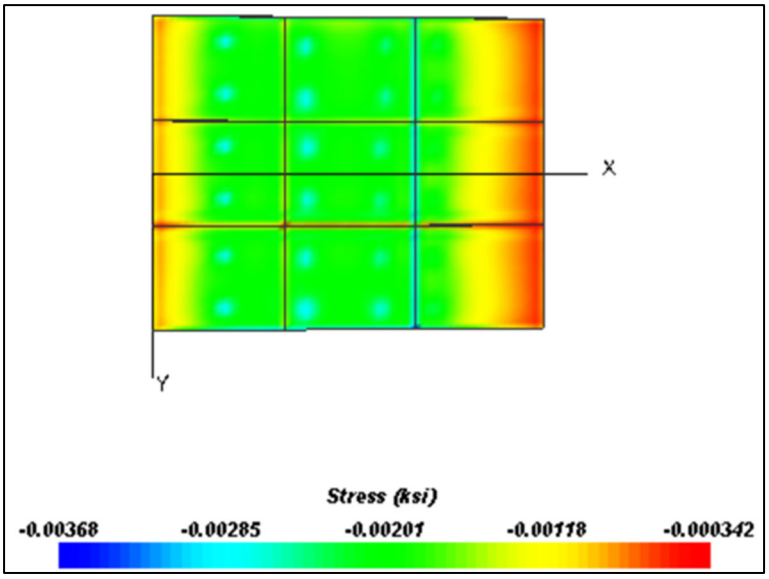

FIGURE 51. Stress levels based on EverFE analysis.

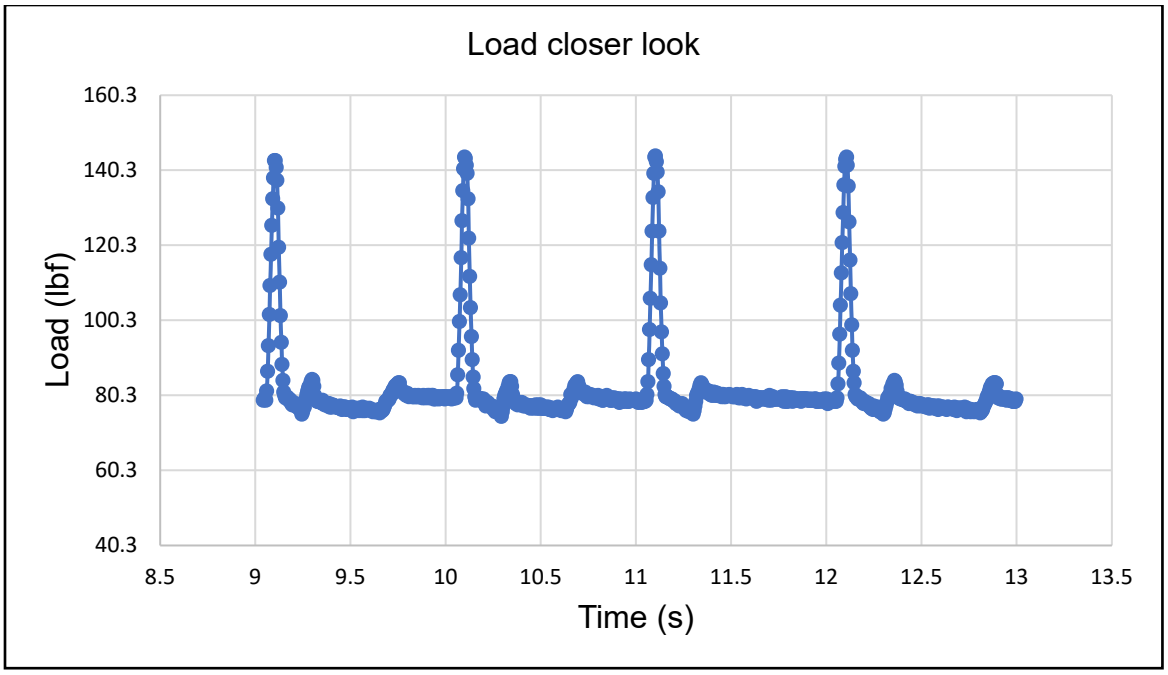

FIGURE 52. Load pattern for triaxial tests.

4.6 Summary of Tests

Table 9 presents a summary of the test schedule for all the tests conducted in this study, including:

- Characterization of the tested materials
- Proctor tests
- 1-D consolidation tests, including various conditioning, gradation, and loading criteria
- Direct shear tests
- Triaxial tests
- Permeability and drainage tests

TABLE 9. Summary of Testing Schedule

Tests			EMB1	EMB2	RAP1		RAP2		RAP3		RAP4		RAP5		Soil + RAP Mix
					<2 in.	<1.5 in.	<2 in.	<1.5 in.	<2 in.	<1.5 in.	<2 in.	<1.5 in.	<2 in.	<1.5 in.	
Gradation			x	x	x	-	x	-	x	-	x	-	x	-	-
Soil Characterization			x	x											
Asphalt content					x	-	x	-	x	-	x	-	x	-	-
Proctor (Standard)	32ºF				x	-	x	-	x	-	x	-	x	-	-
	40ºF				x	-	x	-	x	-	x	-	x	-	-
	Room		x	x	x	x	x	x	x	x	x	x	x	x	x
	100ºF				x	-	x	-	x	-	x	-	x	-	-
1-D	40ºF	14.5 psi/1d			x	-	x	-	x	-	x	-	x	-	x
	Room	14.5 psi/1d	x	x	x	-	x	-	x	-	x	-	x	-	-
		14.5 psi/7d	-	x	-	-	x	-	-	-	x	-	-	-	x
		5-stress/5d	OMC and saturated	OMC and saturated	x	x	x	x	x	x	x	x	x	x	OMC and saturated
		5-stress/5d (100% dens)	-	-	x	-	x	-	x	-	x	-	x	-	-
	100ºF	14.5 psi/1d			x	-	x	-	x	-	x	-	x	-	-
		5-Stress/5d			x	x	x	x	x	x	x	x	x	x	x
Direct Shear	Large	40ºF			-	-	-	-	-	-	-	-	-	-	-
		Room	x	x	x	-	x	-	x	-	x	-	x	-	x
		100ºF			-	-	-	-	-	-	-	-	-	-	-
Triaxial	40ºF				-	-	-	-	-	-	-	-	-	-	-
	Room	4.35 psi confined	x	x	x	x	x	x	x	x	x	x	x	x	x
	100ºF				x	-	-	-	-	-	-	-	x	-	x
Permeability			x	x			x								x
Drainage			PGE+RAP1+EMB1												x

Note: 'X' tested; '-' not tested; shaded cells mean not applicable.

CHAPTER 5: ANALYSIS AND RESULTS

After the laboratory tests were completed, the research team analyzed the results to determine the performance of the RAP samples and to compare the RAP performance to that of the soils as a benchmark.

5.1 Moisture-Density Relationship

The relationships between the moisture content and dry density for the RAP and soil samples and the soil + RAP mix were established based on standard Proctor tests. Also, the RAP samples were compacted at four different temperatures to investigate the effect of temperature on the MDD and OMC. As recommended in AASHTO T 224, corrections to the OMC and MDD were made, as more than 5% oversized particles were retained on the ¾-in. sieve. Figures 56 through 60 present the moisture-density relationship curves at 32ºF, 40ºF, 70ºF, and 100ºF for each of the five RAP samples, respectively. As expected, as the temperature drops, the MDD of the RAP decreases because the asphalt in RAP is harder at lower temperatures and does not deform under the impact of compaction as easily as at higher temperatures. The MDD is shown to decrease between 4 lb/cf and 10 lb/cf when the temperature drops from 100ºF to 32ºF.

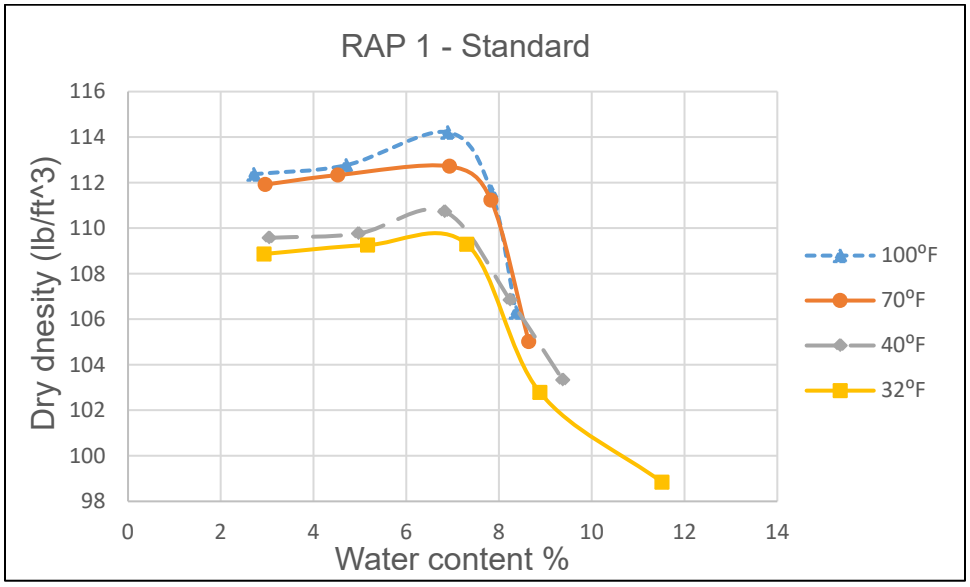

FIGURE 53. Dry density of RAP1 at different temperatures.

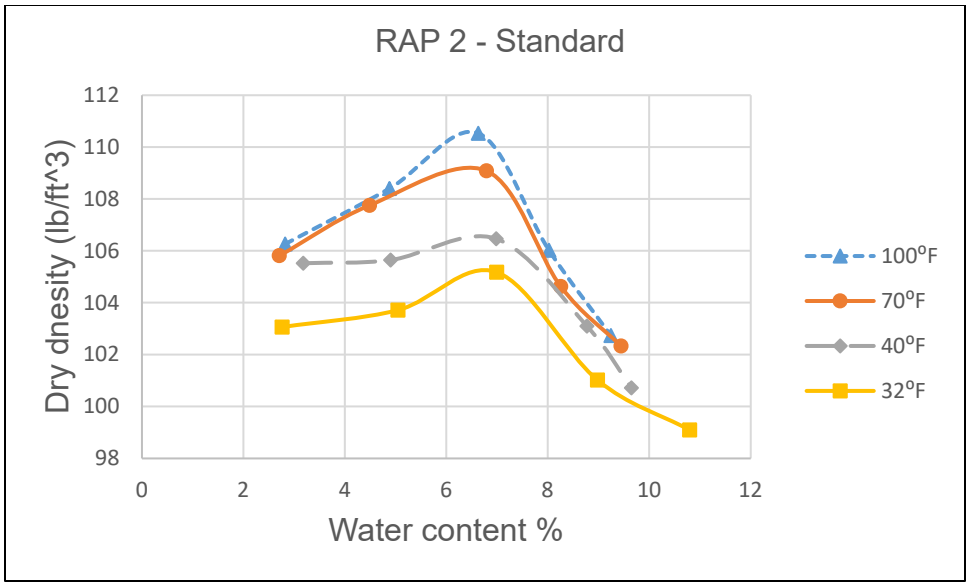

FIGURE 54. Dry density of RAP2 at different temperatures.

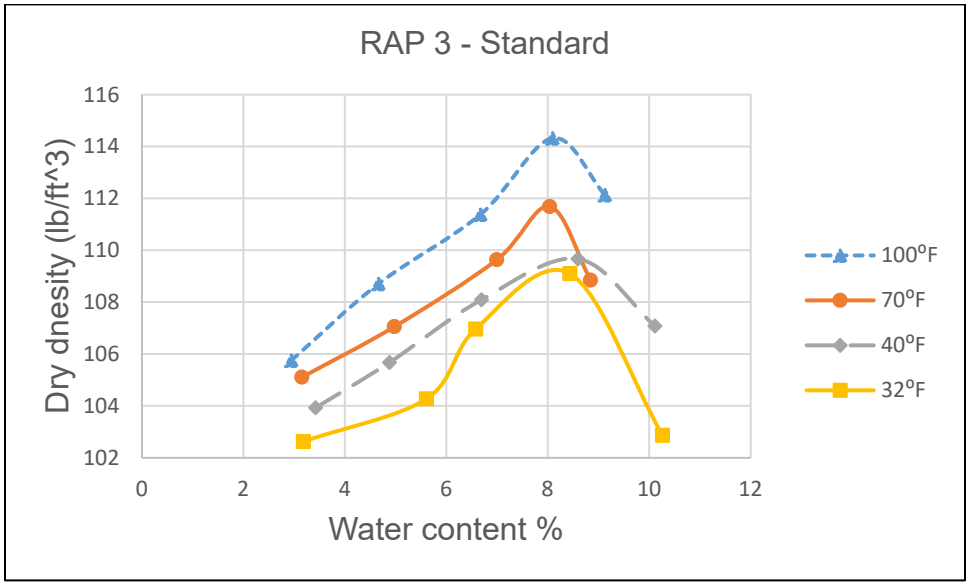

FIGURE 55. Dry density of RAP3 at different temperatures.

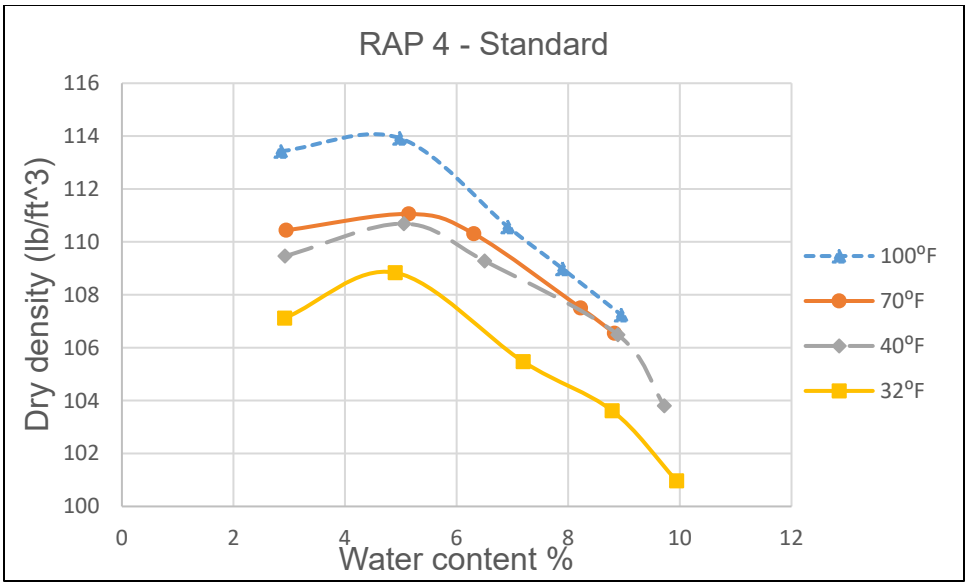

FIGURE 59. Dry density of RAP4 at different temperatures.

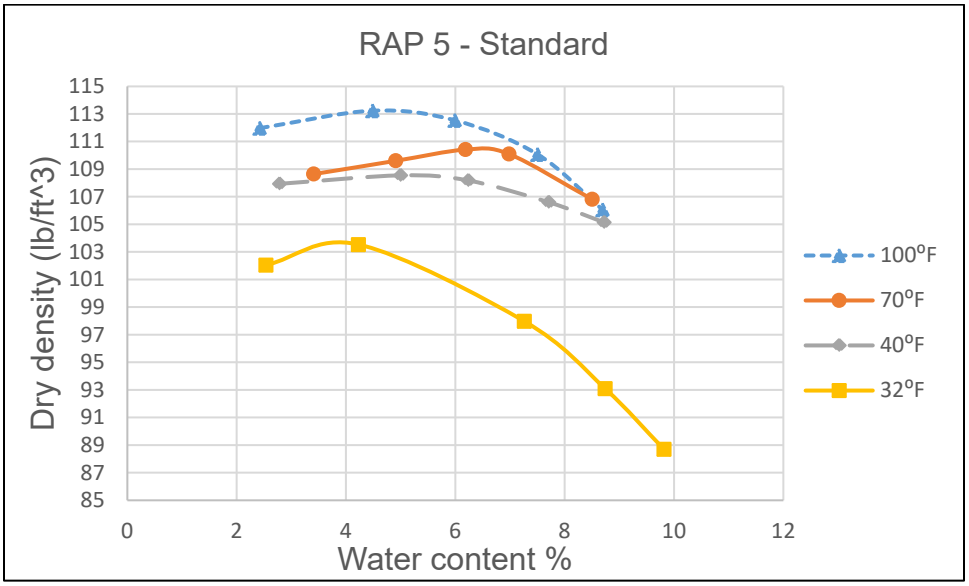

FIGURE 56. Dry density of RAP5 at different temperatures.

Figure 61 presents the moisture-density relationships for the soils, RAP samples, and the EMB1 + RAP2 (50:50) mix at room temperature (about 70ºF). The two soils and five RAP samples have about the same MDD, but the OMCs for the soils are much higher than for the RAP samples. The soil + RAP mix has significantly higher MDD values than the soils or RAP samples alone, but the OMC of the soil + RAP mix is between that of the soils and RAP samples. The reason for this outcome is believed to be that the fine soil particles fill the voids between the

RAP particles, which are much coarser than soil particles, thereby resulting in more efficient packing.

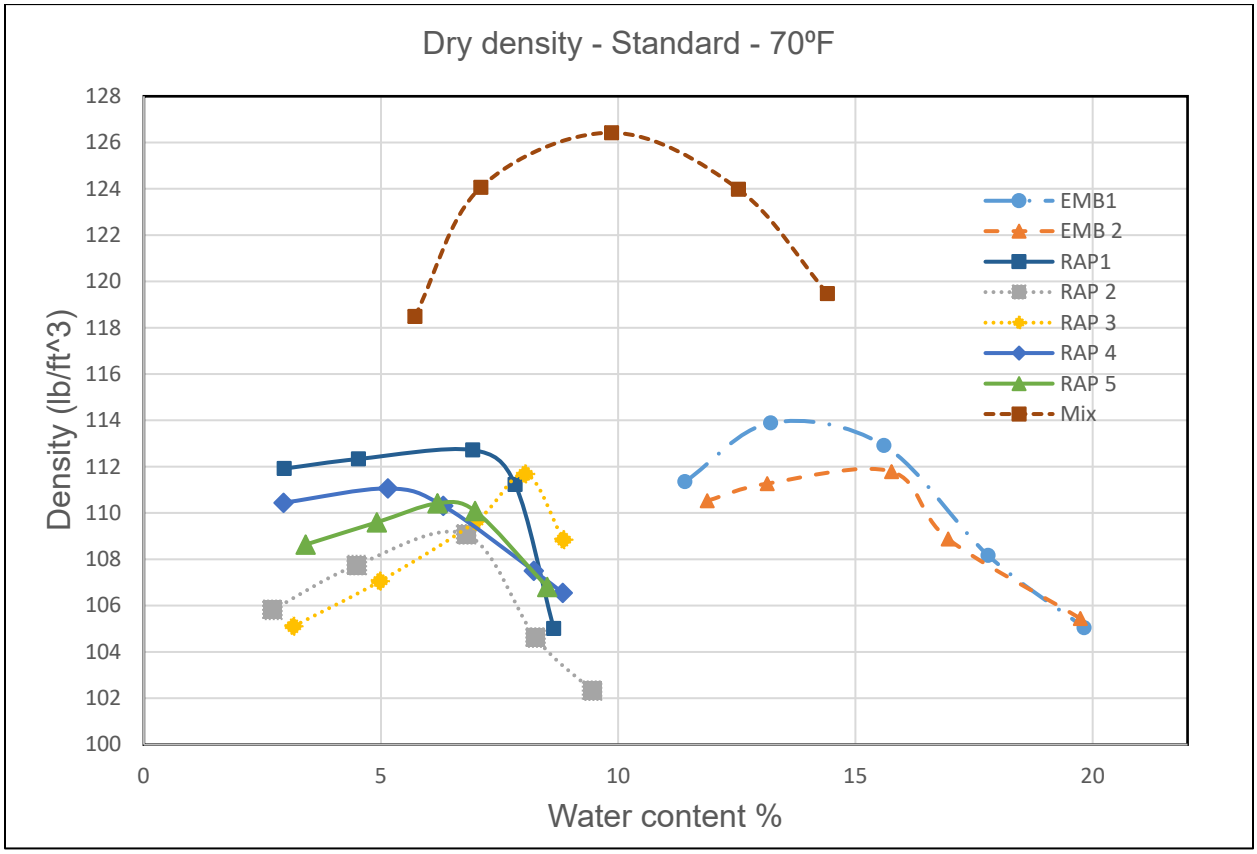

FIGURE 57. Dry density of soils, RAP samples, and EMB1 + RAP2 mix at 70ºF.

The modified Proctor test was conducted using RAP3 as a trial. A comparison between Figures 58 and 62 clearly illustrates the significant impact of the two different compaction methods (standard Proctor vs. modified Proctor) on the dry density outcomes. The MDD based on the modified Proctor test results has increased by 17.5%, 16.9%, and 15.3% at 70ºF, 40ºF, and 32ºF, respectively, in comparison to the standard Proctor test results.

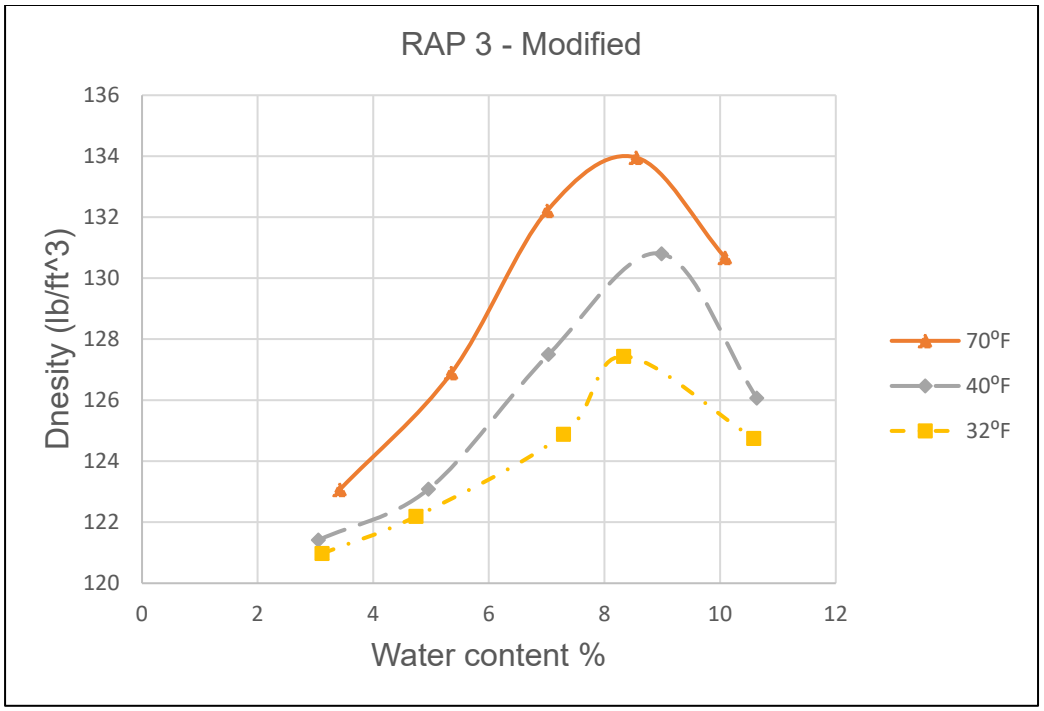

FIGURE 58. Dry density of RAP3 at different temperatures (modified Proctor test).

5.2 Permeability Test Results

5.2.1 Permeability Using Constant/Falling Head Test

Table 10 and Figure 63 present the permeability test results. As shown, both EMB1 and EMB2 have significantly lower permeability levels than RAP2, which is expected because the RAP samples have much coarser gradations than both soils. The soil + RAP mix also has much lower permeability than the RAP sample.

TABLE 10. Permeability of RAP2, Soils, and Soil + RAP Mix

Material	K (in./sec) No. 1	K (in./sec) No. 2	K (in./sec) No. 3	K (in./sec) No. 4	**Average** (in./sec)
RAP2	0.064	0.067	0.066	0.086	**0.07**
EMB1	2.16E-07	8.74E-08	2.51E-07	2.85E-07	**2.1E-07**
EMB2	8.79E-08	1.67E-07	1.3E-07	1.24E-07	**1.27E-07**
Soil + RAP mix	1.49E-05	1.6E-05	1.83E-05	1.33E-5	**1.56E-05**

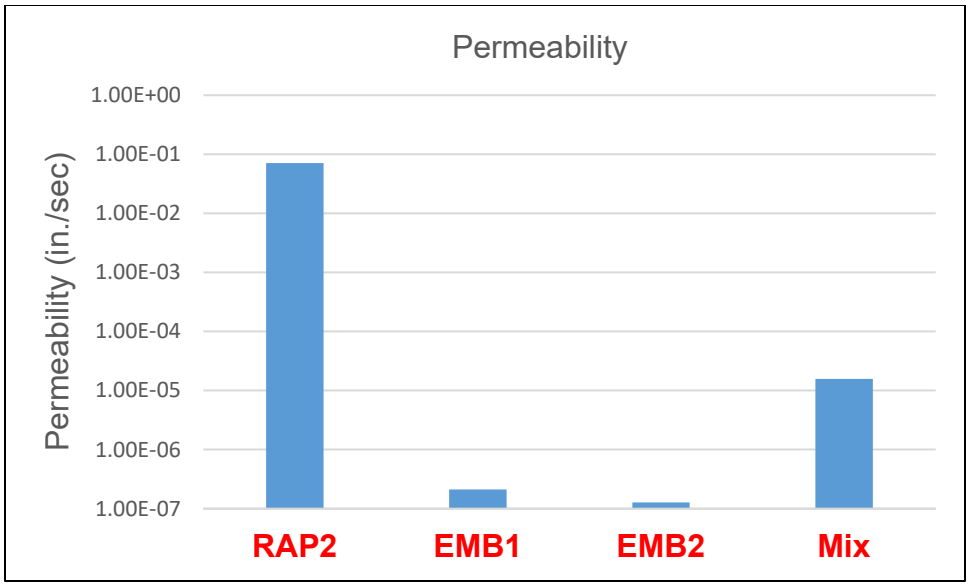

FIGURE 59. Average permeability of RAP2, soils, and soil + RAP mix.

5.2.2 Tube Permeability Test

The tube drainage system used in this study simulates the drainage system at the I-90 Jane Addams Memorial Tollway project and includes PGE, RAP (compacted to 95% density at the OMC), and EMB1 (compacted to 95% density at the OMC) placed respectively from top to bottom. Water was introduced to the PGE and the mass of the tube and materials together was measured periodically. Instead of draining from the weep-holes at the bottom of the PGE layer, as designed for the drainage layer to function, the water infiltrated the RAP layer. Figure 64 shows the increase in the mass of the tube and the materials. Within the first 30 minutes, the mass of the tube and materials increased, indicating that the water had drained into the RAP layer. After 30 minutes, the mass increased slowly, which was likely due to the slow infiltration of water from the RAP layer into the EMB1 layer. After more than 300 minutes, water started draining from the weep-holes at the bottom of the PGE layer.

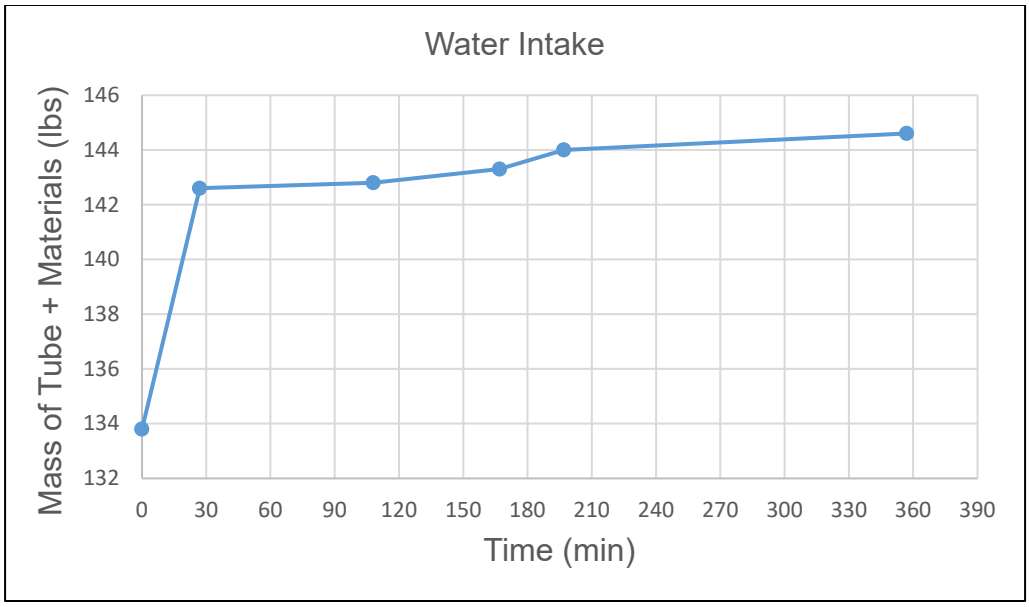

FIGURE 60. Weight of tube and specimen after water intake.

After the test, the PGE material was removed from the tube. Figure 65 shows the water that had collected in the RAP layer. Samples of the EMB1 soil under the RAP layer were collected to determine the moisture content. Table 11 shows that the moisture content of the soils had increased significantly from the OMC (about 16%). Figure 66 shows that the *in situ* forensic boring information for the I-90 Jane Addams Memorial Tollway also indicates that the moisture content in the clay underneath the RAP was very high, more than 20%, which verifies the findings from the tube tests. When a permeable RAP layer is located directly under a permeable PGE layer (which is designed to be the drainage layer), instead of draining from the PGE layer to the pipe underdrain, the collected water in the PGE layer drains into the RAP layer and is stored in the RAP layer to 'feed' the underlying soils, which eventually saturates the soil and renders the drainage system ineffective.

FIGURE 61. Water stored in RAP layer after PGE removal.

TABLE 11. Moisture Content of Soil in Tube after Adding Water

Soil Sampling Locations	EMB1 Moisture Contents
Top	37.3%
Middle	18.9%
Middle (close to the sides of the tube)	24.5%
Bottom (close to the sides of the tube)	20.8%
Bottom	19.5%

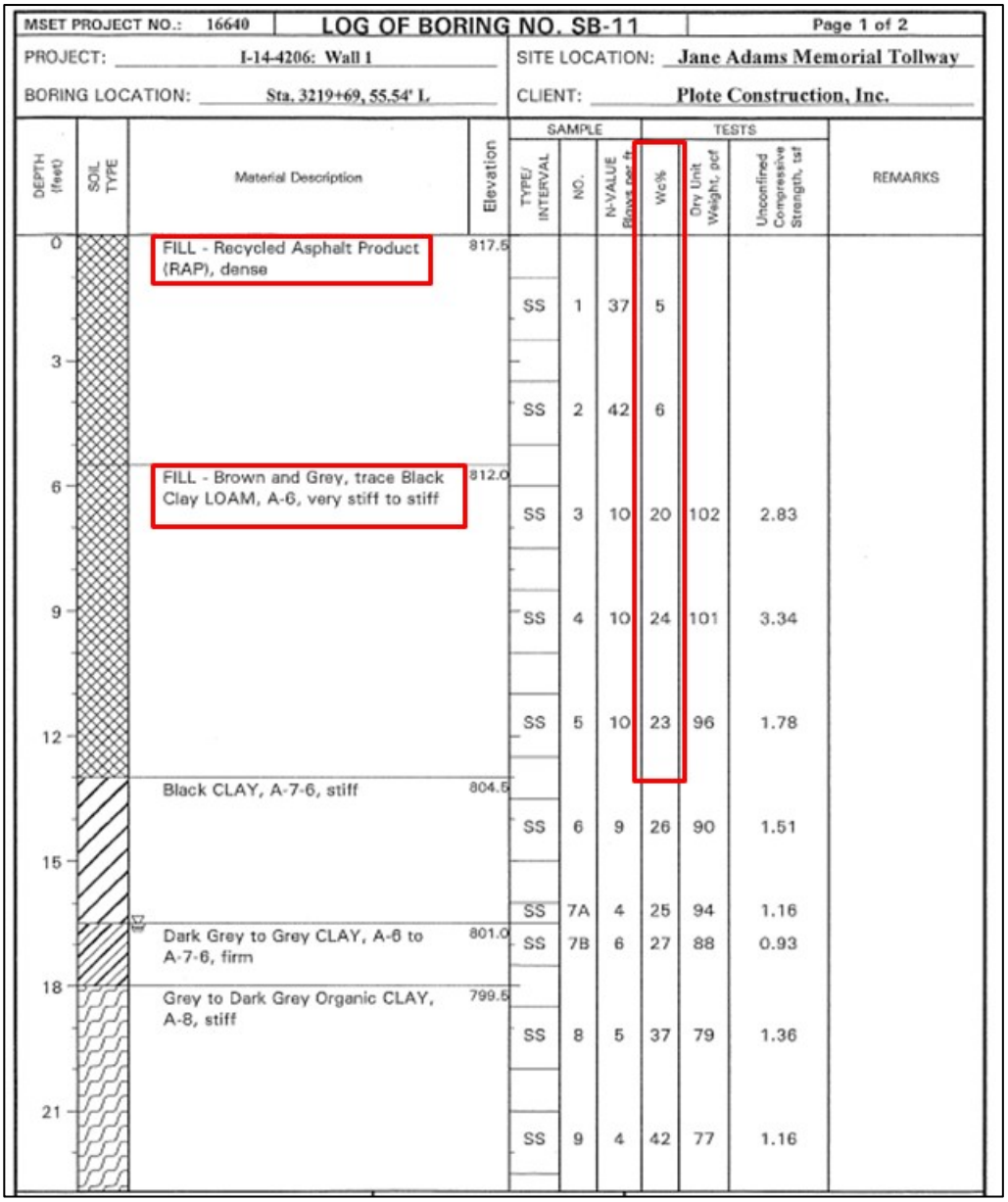

MSET PROJECT NO.: 16640 | LOG OF BORING NO. SB-11 | Page 1 of 2

PROJECT: I-14-4206: Wall 1 | SITE LOCATION: Jane Adams Memorial Tollway

BORING LOCATION: Sta. 3219+69, 55.54' L | CLIENT: Plote Construction, Inc.

DEPTH (feet)	SOIL TYPE	Material Description	Elevation	SAMPLE TYPE/ INTERVAL	SAMPLE NO.	SAMPLE N-VALUE Blows per ft	TESTS Wc%	TESTS Dry Unit Weight, pcf	TESTS Unconfined Compressive Strength, tsf	REMARKS
0		FILL - Recycled Asphalt Product (RAP), dense	817.5							
				SS	1	37	5			
3										
				SS	2	42	6			
6		FILL - Brown and Grey, trace Black Clay LOAM, A-6, very stiff to stiff	812.0							
				SS	3	10	20	102	2.83	
9				SS	4	10	24	101	3.34	
12				SS	5	10	23	96	1.78	
		Black CLAY, A-7-6, stiff	804.5							
				SS	6	9	26	90	1.51	
15				SS	7A	4	25	94	1.16	
		Dark Grey to Grey CLAY, A-6 to A-7-6, firm	801.0	SS	7B	6	27	88	0.93	
18		Grey to Dark Grey Organic CLAY, A-8, stiff	799.5							
				SS	8	5	37	79	1.36	
21										
				SS	9	4	42	77	1.16	

FIGURE 62. Actual moisture content of example from field boring.

Another test was conducted to introduce water to the top of the RAP layer directly. Figure 67 (left) shows that the water immediately entered the RAP layer, which was compacted in a bucket, and Figure 67 (right) shows that, during the RAP removal, the water had immediately drained into the RAP and collected in the RAP layer. However, Figure 68 shows that, when water was introduced to the top of the soil + RAP mix directly, no visible infiltration of water into the sample occurred, which verifies that the permeability of the soil + RAP mix is low, compared to that of the RAM sample.

FIGURE 63. Introduction of water to RAP directly (left) and water in RAP during removal (right).

FIGURE 64. No water infiltration into soil + RAP mix sample.

5.3 One-Dimensional Consolidation Test Results

5.3.1 One-Dimensional Consolidation Test (One Load Level)

Simple runs of the 1-D consolidation tests under one representative load level for 24 h were first conducted using the soil and RAP samples. The unprocessed RAP samples (< 2-in. sieve) were conditioned at different temperatures, 40ºF, 70ºF, and 100ºF, to simulate performance in different seasons. In addition, one soil (EMB2) and one RAP sample (RAP2) were tested for an extended period of seven days at room temperature (70ºF). Figure 69 presents the 1-D consolidation test results of the soils and unprocessed RAP samples. As shown, as the temperature increases, the RAP samples exhibit greater settlement than the soil samples due to the softer asphalt at higher temperatures. However, at room temperature, the soils and RAP samples have comparable settlement at 14.5 psi loading level.

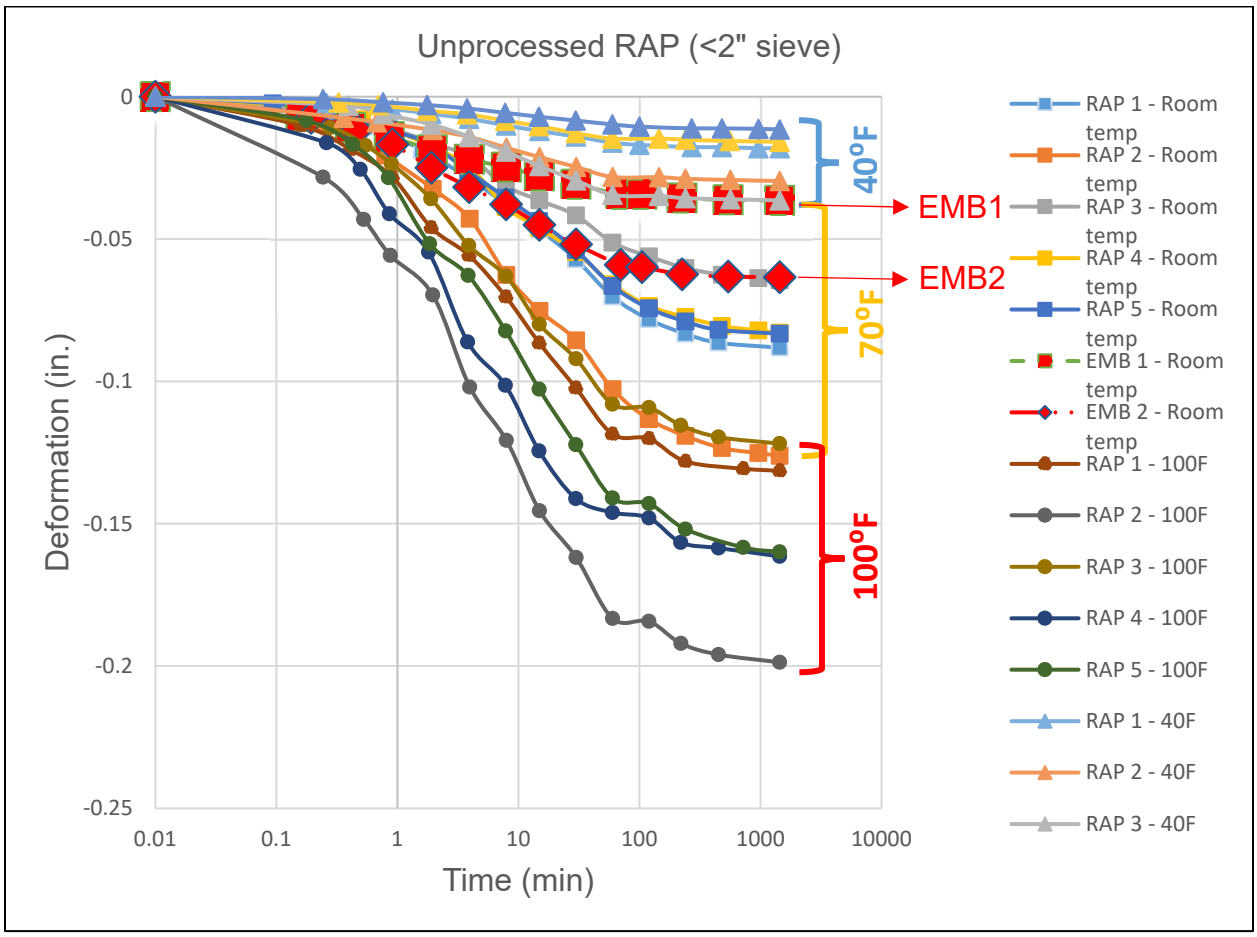

FIGURE 69. Unprocessed RAP and soil deformation under constant loading for 24 hours.

Figure 70 shows that RAP2 exhibited slightly less settlement than EMB2 at room temperature over an extended loading period of seven days. In addition, at the end of the seventh day, the settlement of both RAP2 and EMB2 nearly stabilized.

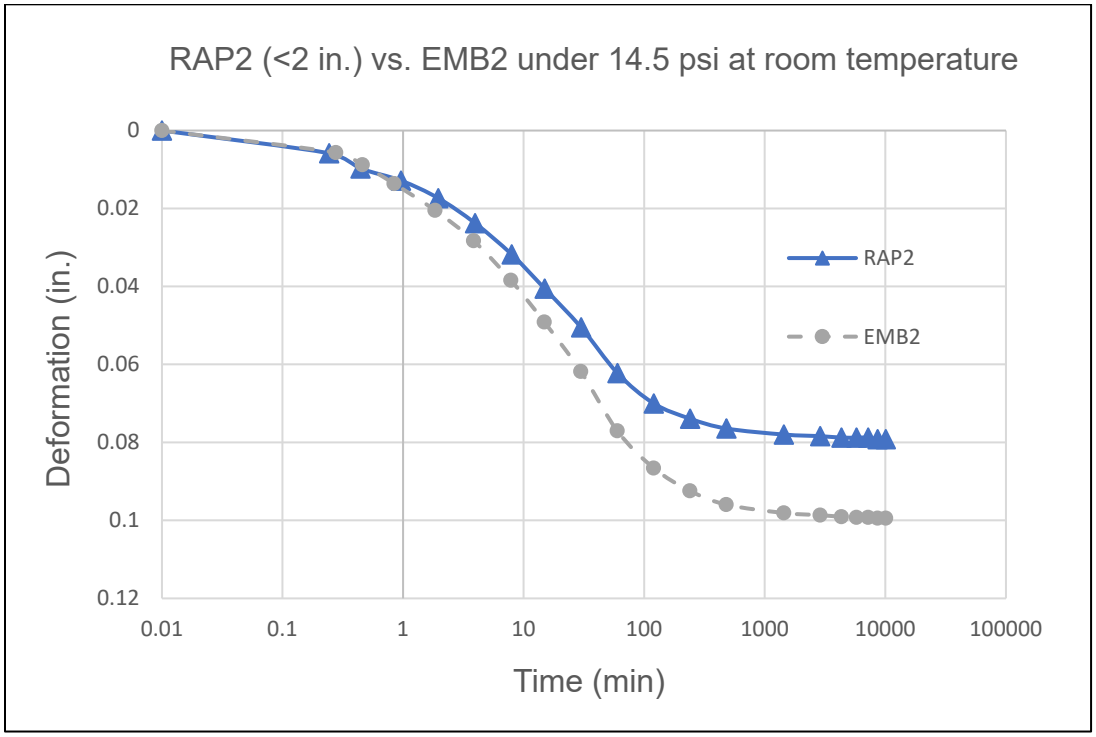

FIGURE 65. RAP2 vs. EMB2 under 14.5 psi for seven days.

5.3.2. One-Dimensional Consolidation Test Results (Multiple Load Increments)

Although the average pressure in the embankment layer was determined to be 14.5 psi, materials at different depths of the embankment may experience higher or lower stress levels. Therefore, RAP and soil behavior should be investigated under various load increments.

5.3.2.1 Unprocessed RAP vs. Soil Samples

The unprocessed RAP (< 2-in. sieve) samples and soils were compacted and tested at room temperature. The soil samples were tested at both the OMC and under saturated conditions. Figure 71 shows that the soils at the OMC and the RAP samples at the OMC exhibit comparable settlement. However, the soils at the OMC show less settlement at lower stress levels but greater settlement at higher stress levels compared to the RAP samples. The saturated soils exhibited significantly greater settlement, especially at high stress levels, than the RAP at OMC or soils at

OMC. The level of increase in the settlement strain from the as-compacted moisture condition to the saturated condition is in line with findings by Baktash (2021). Note that RAP, unlike soil, does not experience saturated conditions because RAP particles have a low percentage of fines.

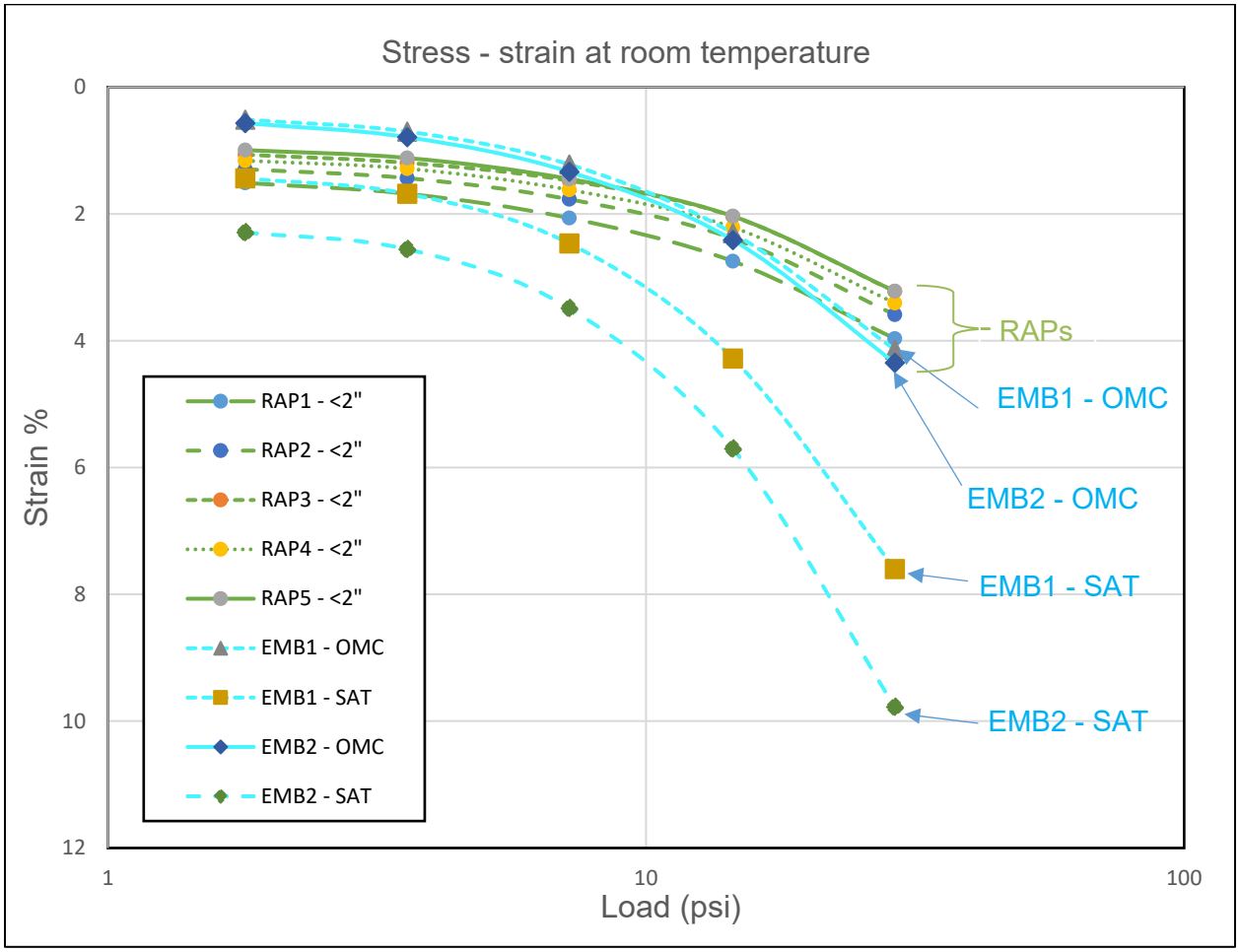

FIGURE 66. Unprocessed RAP (< 2-in. sieve) vs. soil under different load increments at room temperature.

5.3.2.2 Effects of Temperature on RAP Consolidation

Figure 72 shows that the RAP settlement at 100ºF is significantly greater (almost twice) than at 70ºF, except that the temperature effect on the < 2.0-in. sieve RAP settlement is almost negligible for the first load level of 1.8 psi, as that pressure is the minimum. This effect of temperature on RAP settlement is expected, because asphalt binder is significantly softer at 100ºF than at room temperature.

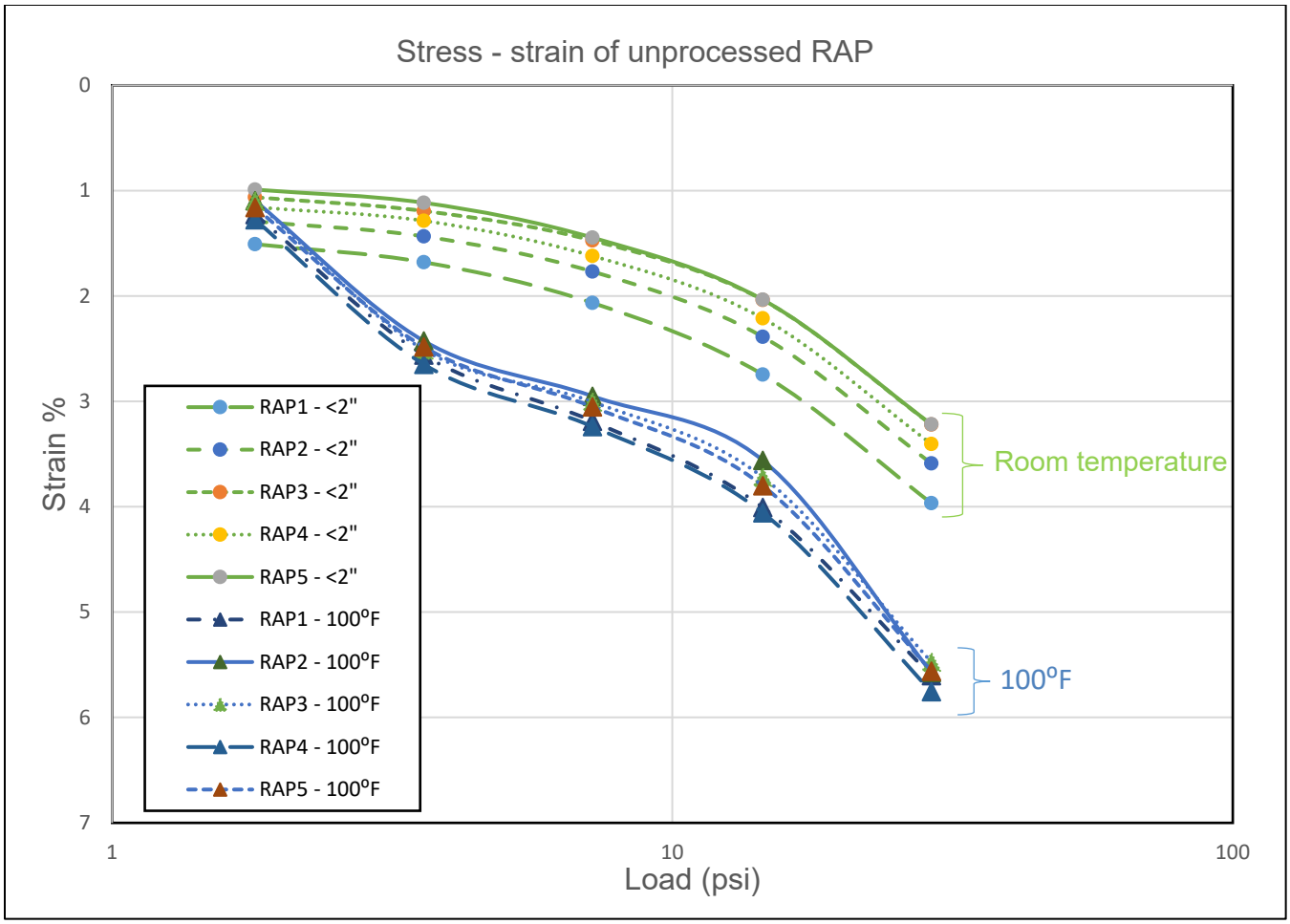

FIGURE 67. Unprocessed RAP at room temperature vs. 100ºF under different load increments.

5.3.2.3 Effect of Particle Size

The asphalt grindings were screened on a 1.5-in. sieve to be consistent with the Illinois Tollway's current special provision when RAP is used in an embankment. Figures 73 and 74 respectively show that the < 1.5-in RAP has significantly less settlement than the < 2.0-in. RAP at both room temperature and at 100ºF. Also, the < 1.5-in. RAP settlement is more consistent among the five processed RAP samples than the settlement of the < 2.0-in. RAP sample that has a more scattered range of data points. Therefore, it is recommended that RAP pass the 1.5-in. sieve for use in embankments.

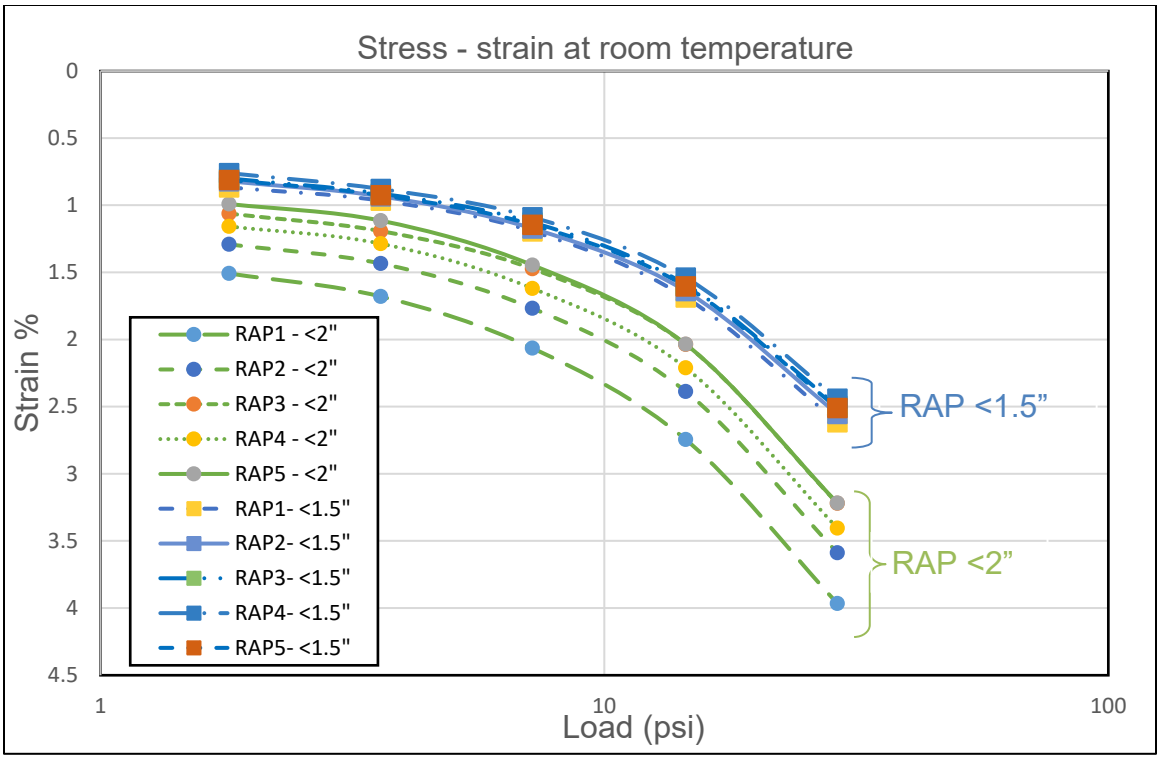

FIGURE 68. Unprocessed vs. processed RAP at room temperature under different load increments.

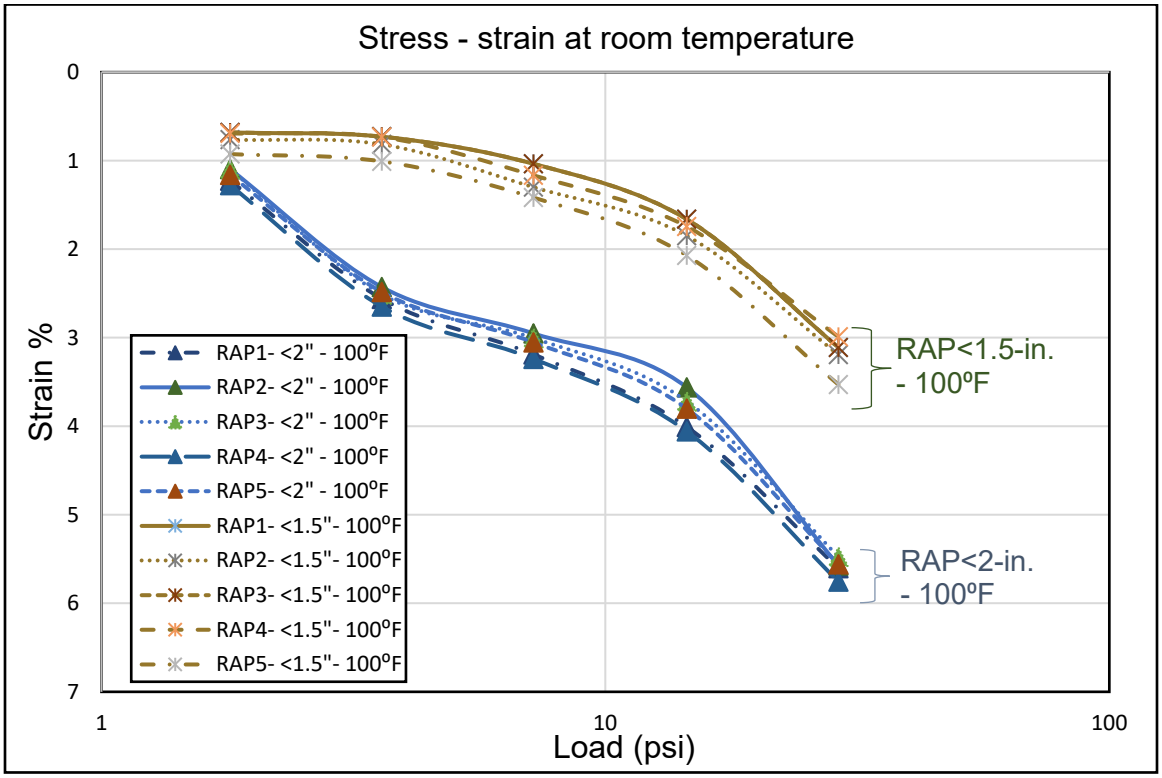

FIGURE 69. Unprocessed vs. processed RAP at 100°F under different load increments.

5.3.2.4 Effects of Density on RAP Settlement

Currently, the Illinois Tollway specifies the embankment soils or RAP (< 2-in. sieve) to be compacted to 95% MDD based on the standard Proctor test. Figure 70 indicates that the RAP samples experienced less settlement than the soils at high stress levels, but greater settlement at low stress levels. Therefore, the 1-D consolidation test was conducted using RAP compacted to 100% MDD to determine if a higher density level would improve the performance of the RAP significantly. Figure 75 shows that an increase in the compaction density from 95% to 100% significantly reduced the settlement in the RAP samples at all stress levels, especially at the higher stress levels. Therefore, it is recommended to compact RAP to 100% standard density. The standard Proctor tests should be conducted at room temperature (minimum 70ºF) in the laboratory.

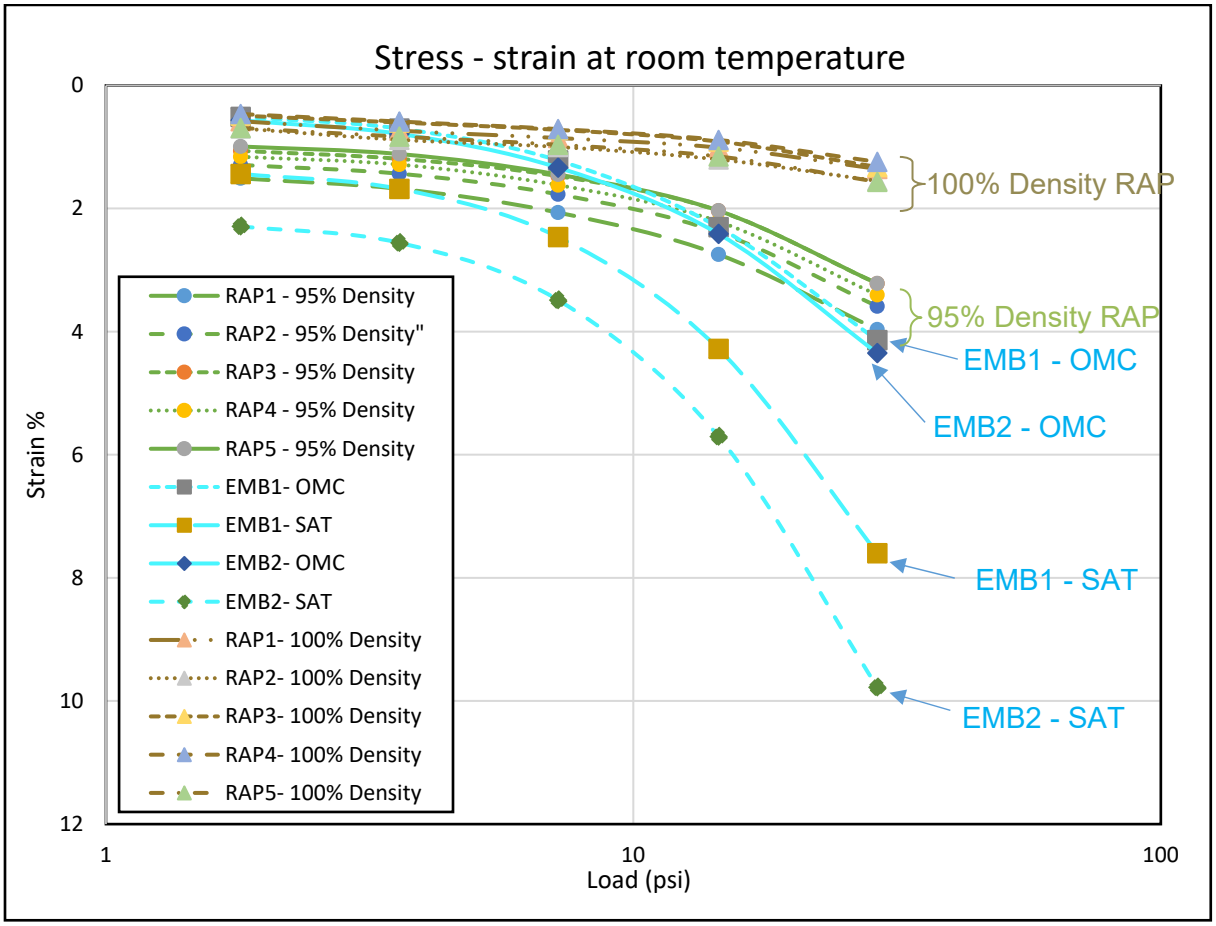

FIGURE 70. 95% maximum dry density vs. 100% maximum dry density of RAP (< 2-in. sieve) vs. soil at room temperature under different load increments.

5.3.2.5 Performance of Soil + Unprocessed RAP Mix

The soil + RAP mix has much higher MDD values than the soils or RAP samples alone, which shows promise for its use as good embankment material. As a trial, 1-D consolidation tests of the EMB1 + RAP2 (50:50) mix were run at the OMC and under saturated conditions at room temperature only, because this mix was not included in the original scope of work. The soil + RAP mix samples were compacted to 95% MDD. Figure 76 shows that the soil + RAP mix at the OMC has the least settlement of the tested samples. Even the saturated soil + RAP mix has settlement that is comparable to that of the RAP samples or soils at the OMC condition. The granular particles in RAP provide the skeleton and the fine soil particles fill the voids between the RAP particles. The soil and RAP seem to complement each other and provide good performance in terms of settlement as well as permeability, as previously reported.

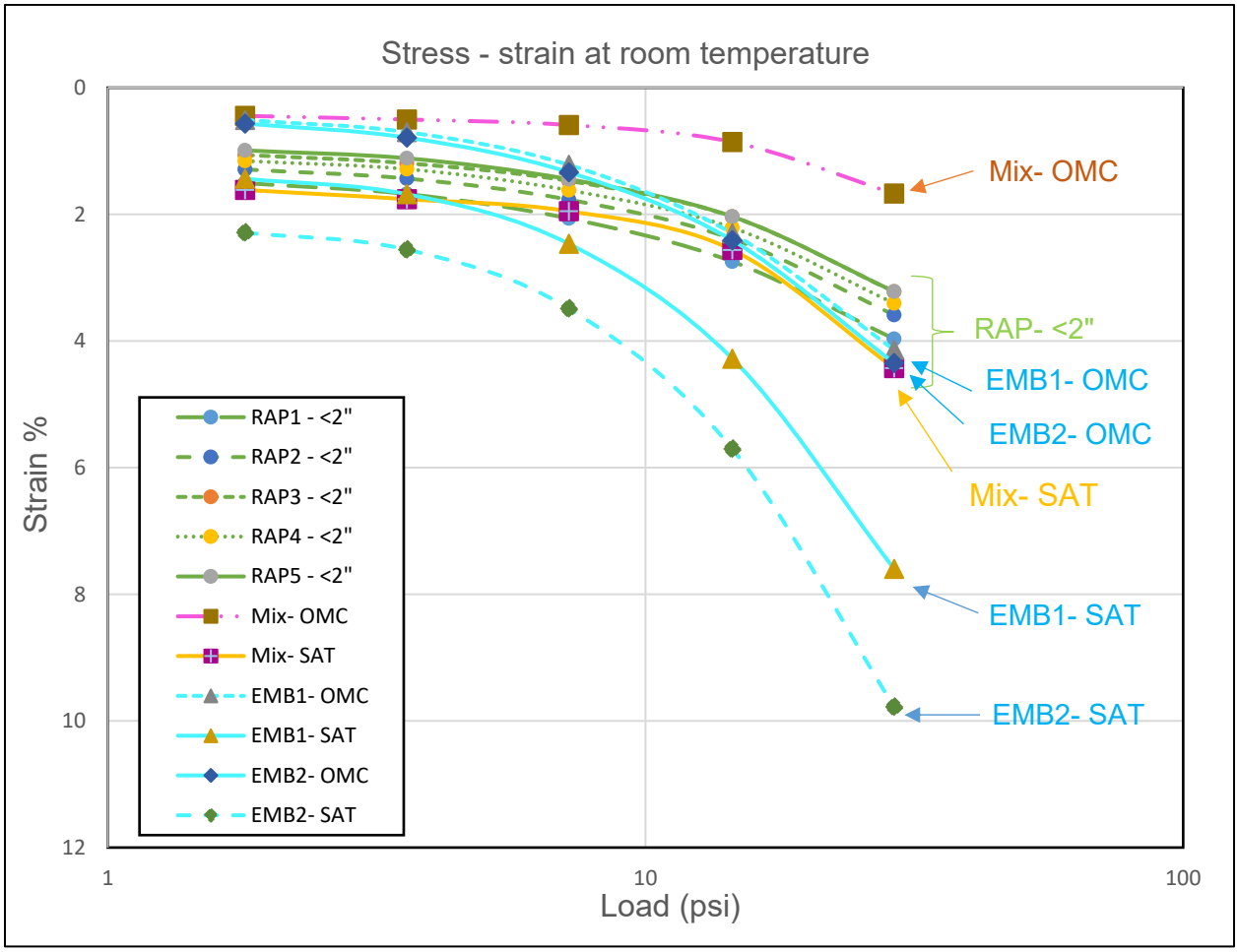

FIGURE 71. RAP < 2-in. vs. soil vs. soil + RAP mix at room temperature under different load increments.

5.3.2.6 Summary of 1-D Consolidation Test Results

Figure 77 presents a summary of the 1-D consolidation test results for the soils, RAP samples, and soil + RAP mix under various temperature and moisture conditions. All five RAP samples exhibited similar performance to that of the two soils; therefore, for the purpose of clarity and efficiency, only the averages of the soils and RAP are presented in Figure 77. The < 2.0-in. RAP samples with 95% density show less compression at high stress levels, but more compression at low stress levels, compared to the soils at the OMC and 95% density. The embankment fill that is located closest to the top of the embankment is subject to low overburden stress whereas the fill that is located deeper in the embankment is subject to high overburden stress. The soil + RAP mix and the RAP compacted to 100% density show the least amount of compression at any stress level. The < 1.5-in. RAP samples also performed better than the < 2.0-in. RAP samples and are not sensitive to temperature, in terms of compression. Therefore, it is recommended that RAP shall be processed to pass the 1.5-in. sieve and compacted to 100% standard density to achieve settlement that is comparable to that of soil at any stress level. A preliminary test of RAP using the modified Proctor method, which many agencies use to specify the compaction of RAP, indicates that the MDD of RAP can be more than 130 lb per cubic ft. Therefore, 100% standard density, which is about 110 lb per cubic ft, can be achieved during construction.

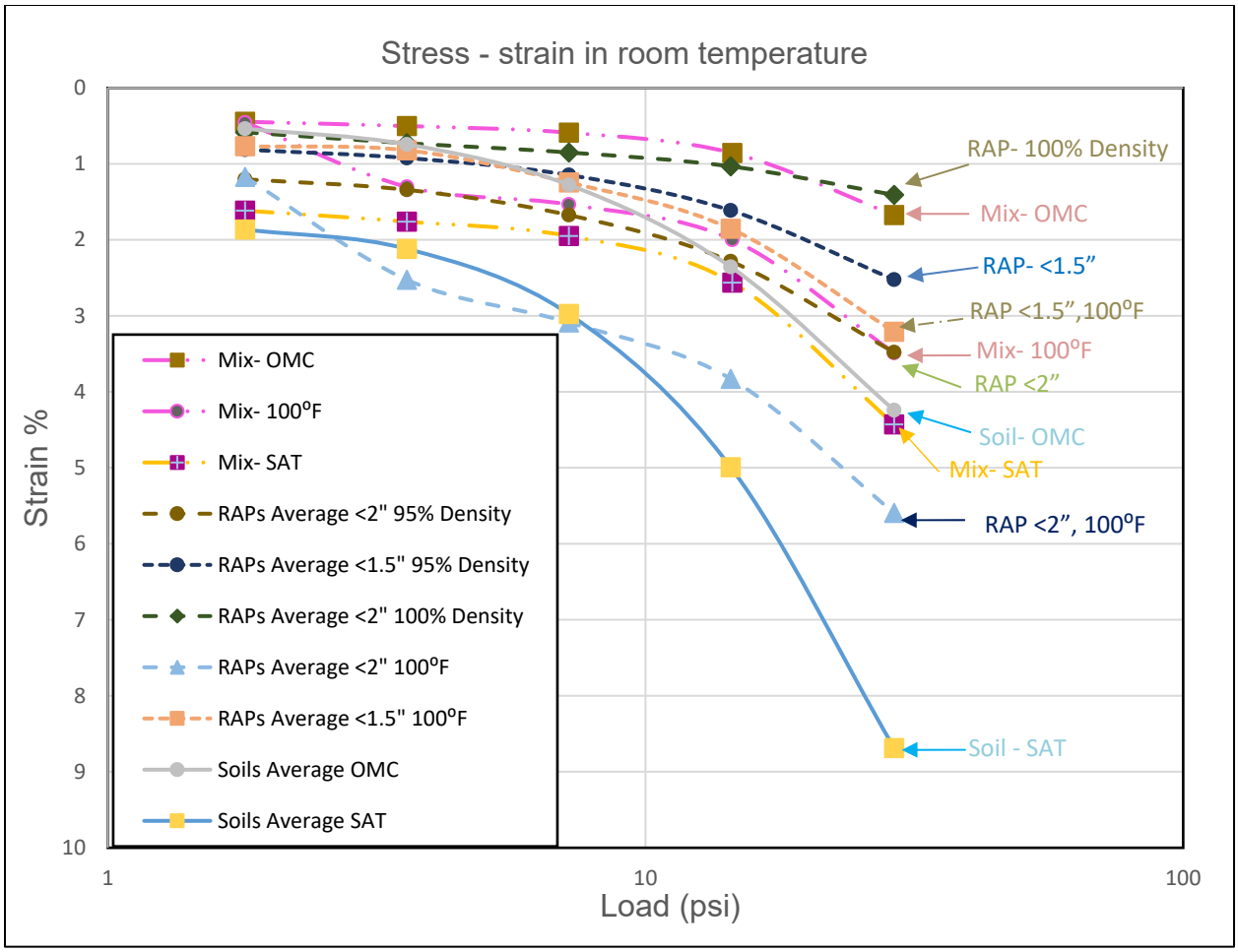

FIGURE 72. Summary of test results (cases of RAP1, EMB1, and soil + RAP mix).

Tables 12, 13, and 14 present the coefficient of compressibility (C_c) values of the tested materials under various conditions as a reference. For the purpose of estimating the settlement of RAP in an embankment, C_c at room temperature (70ºF) is recommended as the average temperature of different seasons. The current IDOT method that is used to determine C_c, shown in Equation (11), is based on the moisture content of soil and is not applicable to RAP because RAP is not sensitive to moisture content (the different settlement analysis approaches are discussed further in Section 5.6 of this report).

$$C_c = 0.009\ (LL - 10) \qquad (11)$$

where

LL = liquid limit (%) (moisture content of the sample is used for LL per IDOT).

TABLE 12. Summary of Coefficients of Compressibility (C_c) for Unprocessed RAP Samples

Materials	C_c	Material	C_c	Material	C_c
RAP1: < 2 in., 95% density	0.052	RAP1: < 2 in., 100% density	0.014	RAP1: < 2 in., 100ºF	0.067
RAP2: < 2 in., 95% density	0.056	RAP2: < 2 in., 100% density	0.016	RAP2: < 2 in., 100ºF	0.092
RAP3: < 2 in., 95% density	0.049	RAP3: < 2 in., 100% density	0.016	RAP3: < 2 in., 100ºF	0.071
RAP4: < 2 in., 95% density	0.050	RAP4: < 2 in., 100% density	0.014	RAP4: < 2 in., 100ºF	0.069
RAP5: < 2 in., 95% density	0.050	RAP5: < 2 in., 100% density	0.017	RAP5: < 2 in., 100ºF	0.073
Average RAP: < 2 in., 95% density	**0.051**	**Average RAP: < 2 in., 100% density**	**0.015**	**Average RAP: < 2 in., 100ºF**	**0.074**

TABLE 13. Summary of Coefficients of Compressibility (C_c) for < 1.5-in. RAP Samples

Material	C_c	Material	C_c
RAP1: < 1.5 in., 95% density	0.041	RAP1: < 1.5 in., 100ºF	0.056
RAP2: < 1.5 in., 95% density	0.043	RAP2: < 1.5 in., 100ºF	0.063
RAP3: < 1.5 in., 95% density	0.037	RAP3: < 1.5 in., 100ºF	0.060
RAP4: < 1.5 in., 95% density	0.038	RAP4: < 1.5 in., 100ºF	0.053
RAP5: < 1.5 in., 95% density	0.039	RAP5: < 1.5 in., 100ºF	0.062
Average RAP: < 1.5 in., 95% density	**0.039**	**Average RAP: < 1.5 in., 100ºF**	**0.058**

TABLE 14. Summary of Coefficients of Compressibility (C_c) for Soils and Soil + RAP Mix Samples

Materials	C_c	Materials	C_c
EMB1 – OMC	0.087	EMB1 – SAT	0.153
EMB2 – OMC	0.096	EMB2 - SAT	0.192
Mix – OMC	0.035	Mix - SAT	0.076
Mix - 100ºF	0.064		

5.4 Direct Shear

The two soils and RAP samples as well as the EMB1 + RAP2 mix were compacted to 95% MDD and OMC and were tested in the fabricated shear device with a 6-in. diameter mold at room temperature. Initially, the RAP samples were compacted with particles passing the 2.0-in. sieve. However, the results were scattered, likely due to the effects of the presence of large RAP particles at the shear failure plane. As a solution to this problem, the RAP particle size was reduced from 2 in. to 0.5 inch. Three replicates of each material were tested. Figures 78 through 85 present the results for all the materials tested. Table 15 and Figure 86 present the overall shear test results. The RAP samples have higher friction angles than the soils and the soil + RAP mix. This outcome is expected because RAP has coarser gradations than both the soils and the soil + RAP mix.

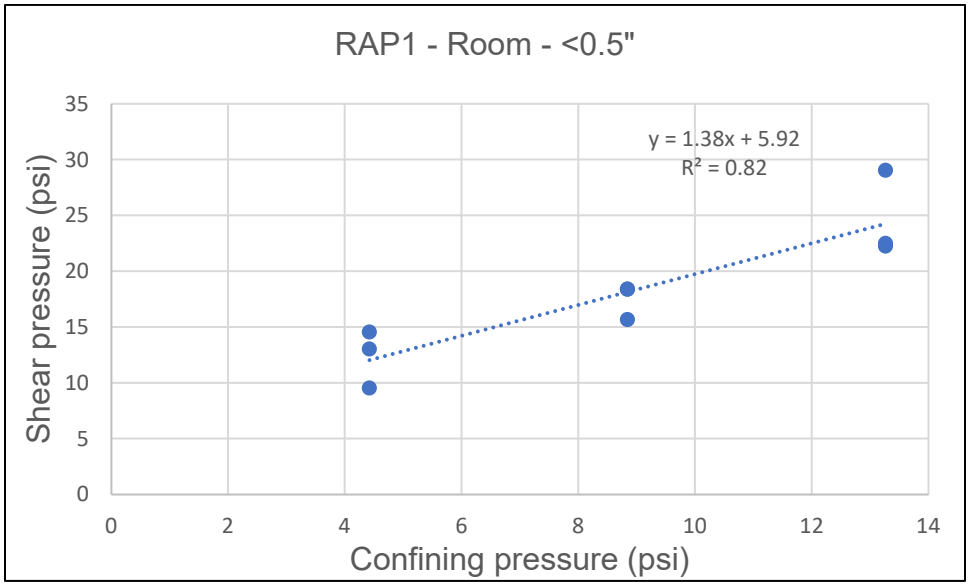

FIGURE 73. Direct shear test results for RAP1 particles smaller than 0.5 in.

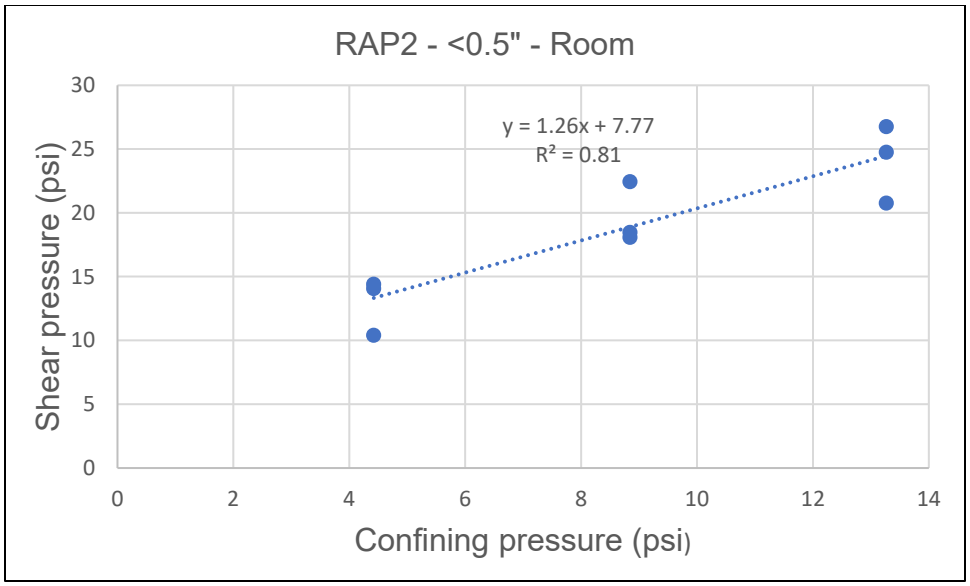

FIGURE 79. Direct shear test results for RAP2 particles smaller than 0.5 in.

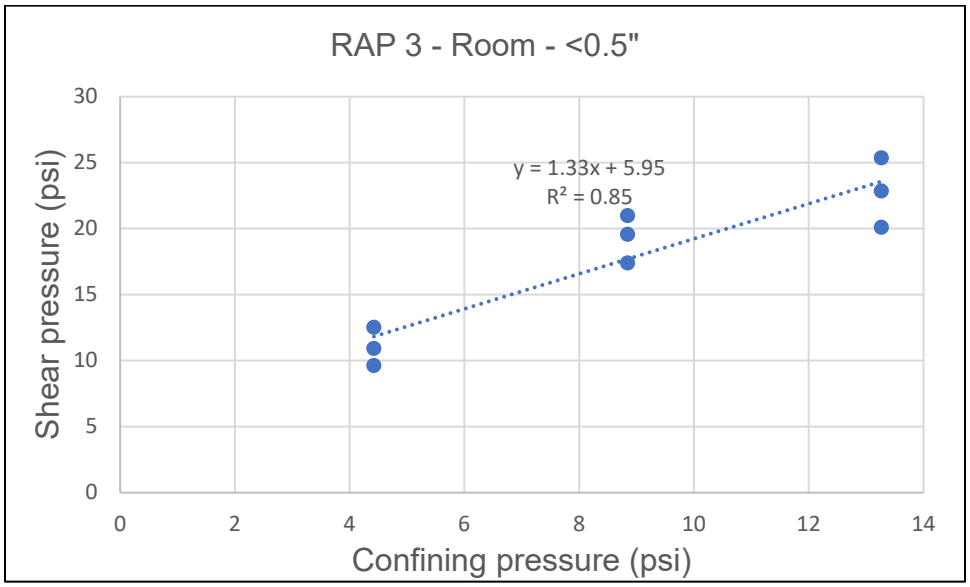

FIGURE 74. Direct shear test results for RAP3 particles smaller than 0.5 in.

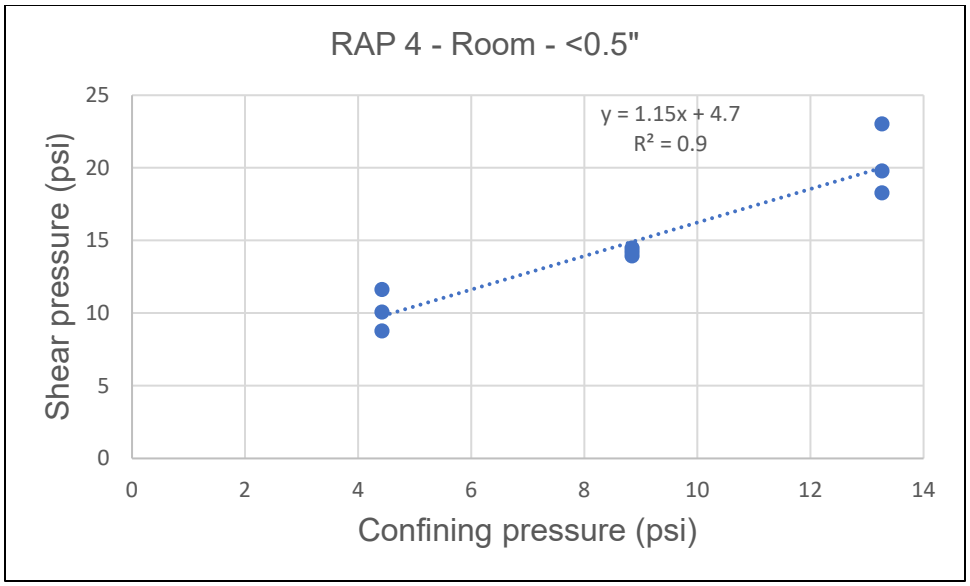

FIGURE 75. Direct shear test results for RAP4 particles smaller than 0.5 in.

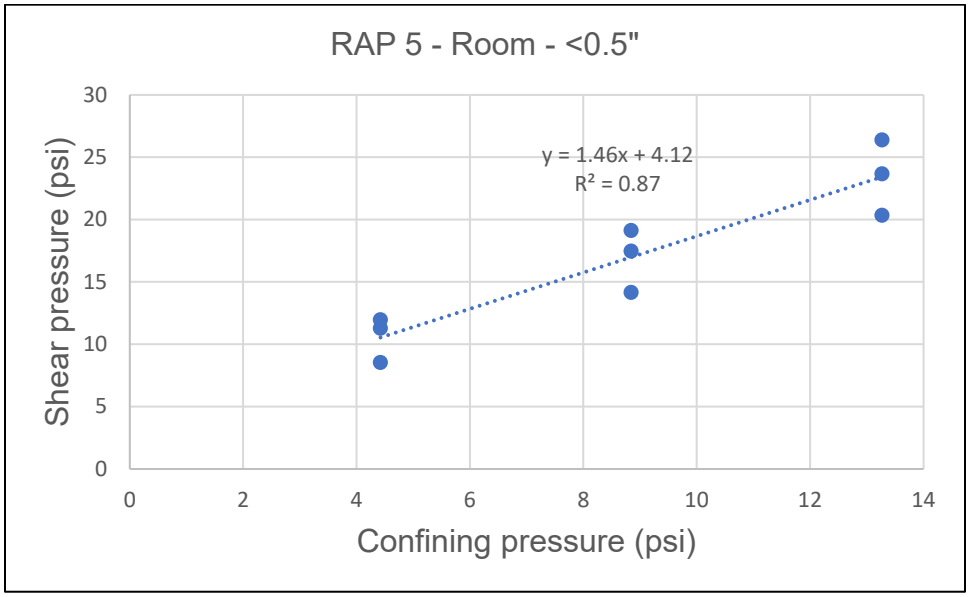

FIGURE 76. Direct shear test results for RAP5 particles smaller than 0.5 in.

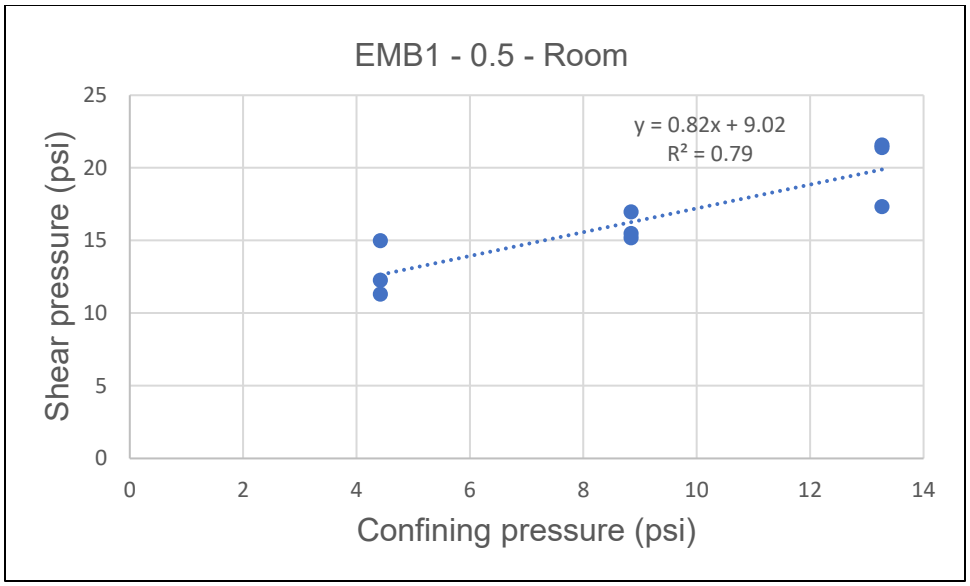

FIGURE 77. Direct shear test results for EMB1 particles smaller than 0.5 in.

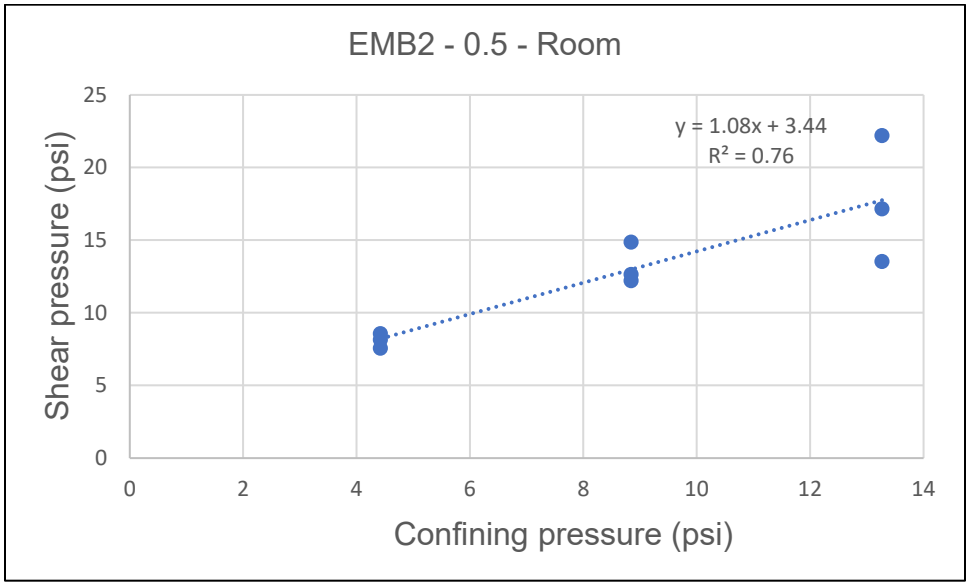

FIGURE 78. Direct shear test results for EMB2 particles smaller than 0.5 in.

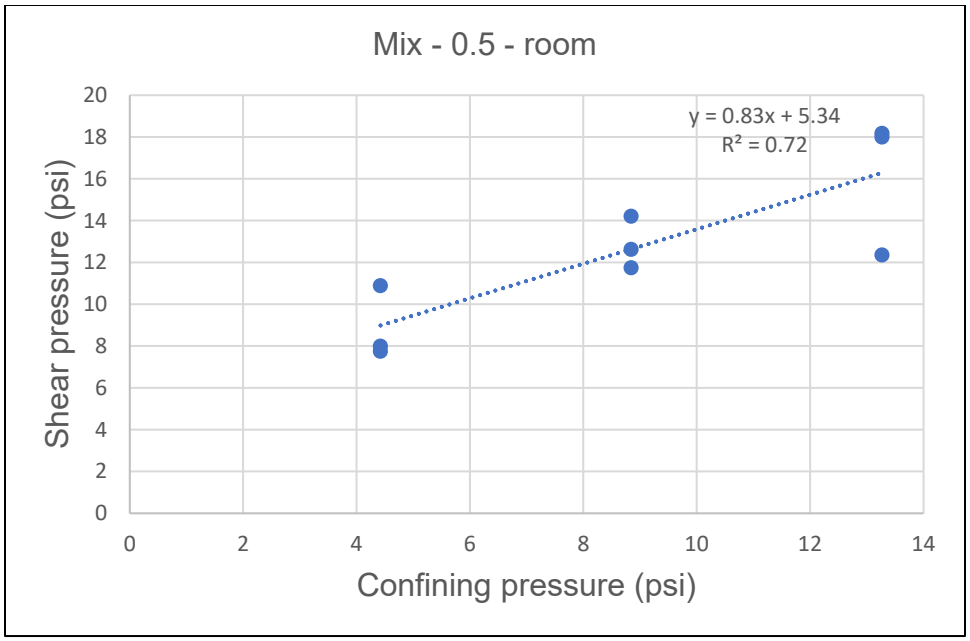

FIGURE 79. Direct shear test results for soil + RAP mix particles smaller than 0.5 in.

TABLE 15. Shear Properties of RAP Samples, Soils, and Soil + RAP Mix

Material	Cohesion (psi)	Friction angle, º	Material	Cohesion (psi)	Friction angle, º
RAP1	5.92	54.13	**RAP5**	4.11	55.52
RAP2	7.76	51.55	**EMB1**	9.02	39.3
RAP3	5.94	53.04	**EMB2**	3.43	47.18
RAP4	4.69	49.11	**Soil + RAP mix**	5.33	39.54

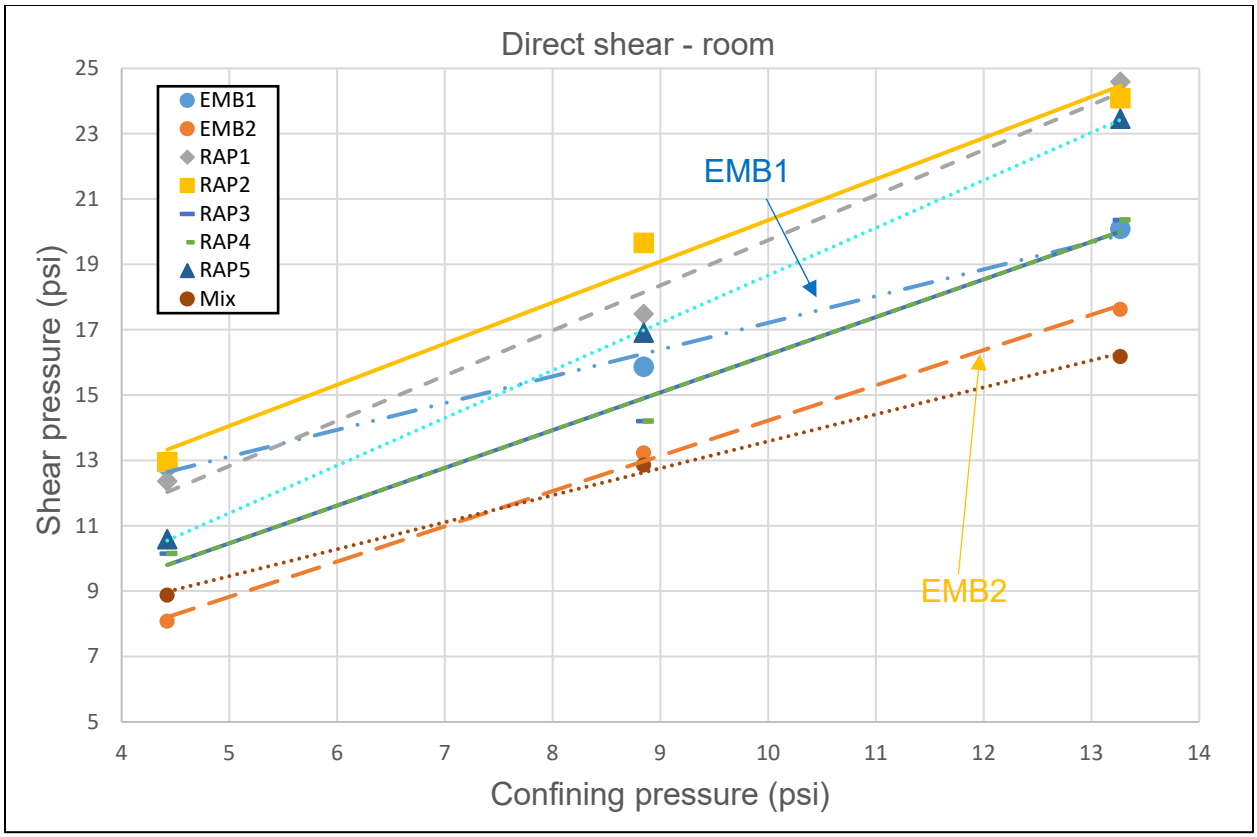

FIGURE 80. Summary of direct shear test results for sample particles smaller than 0.5 in.

5.5 Dynamic Triaxial Test Results

Dynamic triaxial tests were conducted at 4.35 psi confining pressure, 2.9 psi seating load, and 2.9 psi cyclic load to simulate the stress state in an embankment immediately under the pavement structure. During the tests, the drainage valve was kept open and the tests were conducted at room temperature. The samples were compacted to 95% MDD at the OMC.

Figure 87 shows that, under dynamic loading, EMB1 and EMB2 exhibited much less permanent deformation than the RAP samples (< 2.0-in. sieve), except RAP5. The soil + RAP mix also had comparable permanent deformation to that of the soils. These results indicate that RAP (< 2.0-in. sieve) does not perform well under dynamic traffic loading at room temperature. However, when the RAP particle size is smaller than the 1.5-in. sieve, the permanent deformation under dynamic loading is closer to that of the soils and the soil + RAP mix. However, Figure 88 shows that, at the end of the tests, the permanent deformation of the RAP samples continued to increase and did not stabilize, whereas the permanent deformation of

EMB1, EMB2, and the soil + RAP mix did stabilize. Again, even when the particle size of the RAP samples is less than 1.5 in., the permanent deformation under dynamic traffic loading is still a concern. The soil + RAP mix (EMB1 + RAP2), however, performed as well as EMB1.

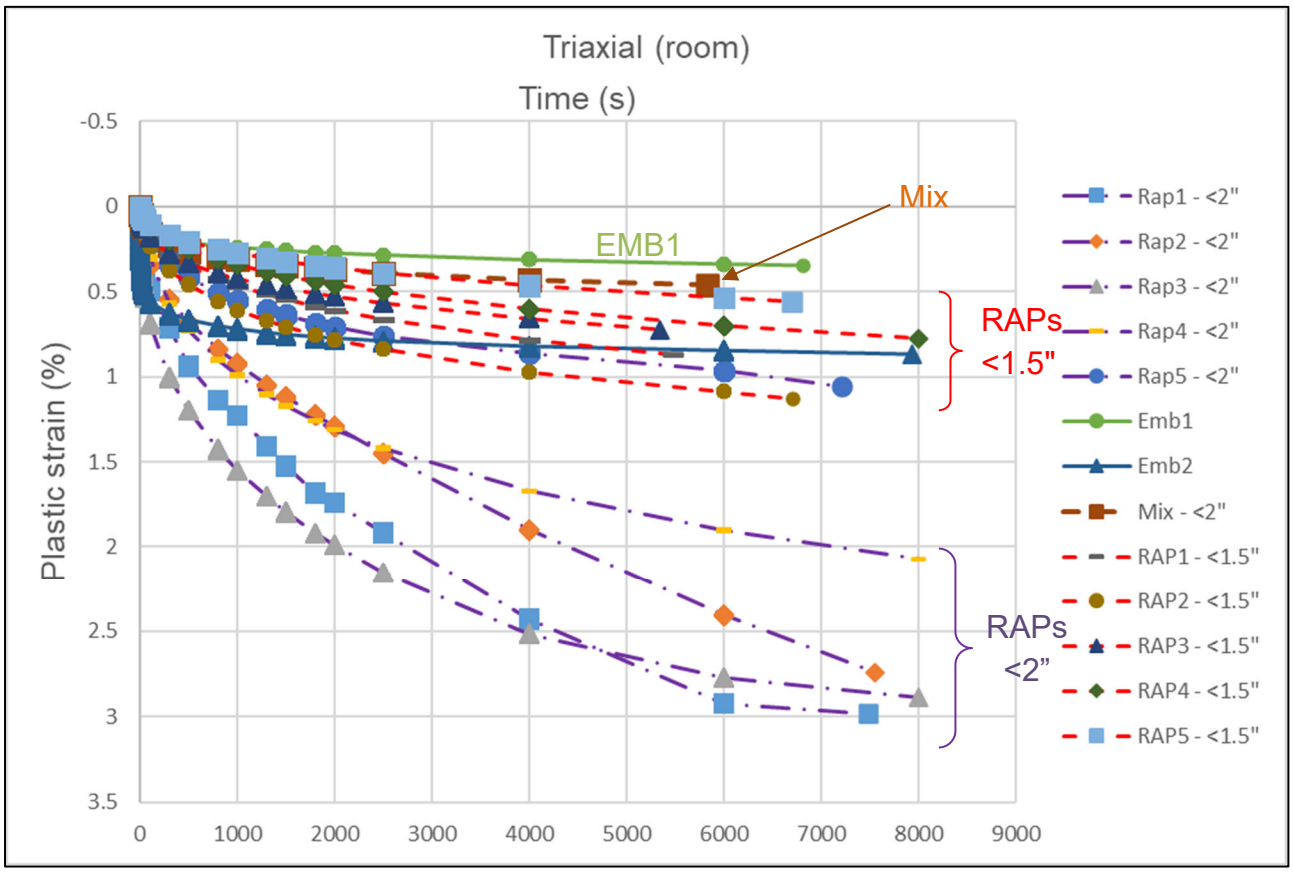

FIGURE 81. Summary of all triaxial test samples at room temperature.

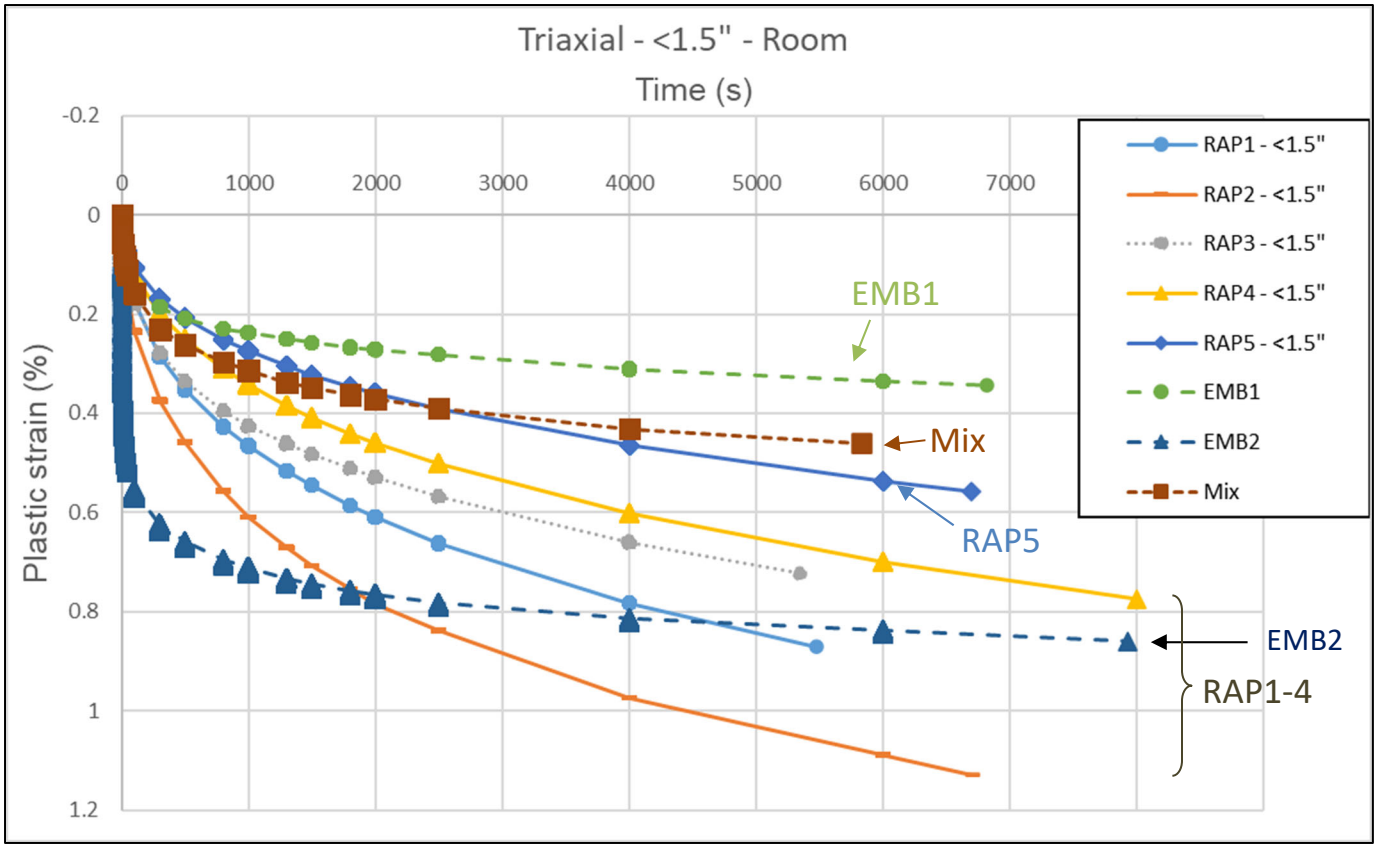

FIGURE 82. Summary of triaxial test results for RAP samples smaller than 1.5 in., soils, and soil + RAP mix.

One solution to mitigate the above concerns when RAP is used in embankments is to keep the RAP out of the stress influence zone of traffic loading, for instance, the traffic load-induced stress at a depth that is less than 1% of the truck load tire contact pressure, e.g., 100 psi. WESLEA, a linear elastic layer analysis program, was used to analyze four typical pavement structures (presented here as cases) used by Illinois Tollway to determine the influence zone of traffic loading in those various pavement structures. The composition of each of the four pavement structure cases is as follows.

Case 1: (1) 13-in. concrete + 3-in. WMA + 9-in. subgrade aggregate special (pavement structure used for the I-90 Jane Addams Memorial Tollway) and (2) 10.5-in. concrete + 3-in. WMA + 9-in. subgrade aggregate special (ramp pavement structure of the I-390 Elgin Expressway)

Case 2: 15-in. stone matrix asphalt (SMA) + 12-in. aggregate base

Case 3: 13-in. concrete + 3-in. WMA + subgrade aggregate special + pile-supported box concrete culvert

Case 4: 15-in. SMA + 12-in. aggregate base + subgrade aggregate special + pile-supported box concrete culvert

Typical material modulus values were input to WESLEA: 4×10^6 psi for concrete, 350,000 psi for WMA, and 10,000 psi for the subgrade or aggregate special. A modulus value of 1 million psi was assumed for the pile-supported box concrete culvert. For Case 1 (concrete pavement structure without culvert), the vertical stress induced by the traffic load decreased from 100 psi at the surface to about 1 psi at a depth of 6 ft. from the 13-in. concrete pavement surface or 7 ft from the 10.5-in. concrete pavement surface, shown in Figure 89. Because the pavement structure is about 2-ft thick, RAP should be avoided in the top 5 ft of the embankment in such a rigid pavement. For Case 2, shown in Figure 90, RAP must be deeper than 10 ft from the pavement surface to stay out of the influence zone of traffic loading. Because the pavement structure is about 2-ft thick, no RAP should be used within the top 8 ft of the embankment. For Case 3 (concrete pavement structure with culvert), shown in Figure 91, RAP must be deeper than 9 ft from the pavement surface to stay out of the influence zone of traffic and 13 ft for Case 4 (asphalt pavement structure with culvert), shown in Figure 92. The traffic-induced stress in an embankment appears to be greater in a sandwiched pavement structure (unbound soils or RAP between concrete/asphalt surface and a rigid subsurface structure). Therefore, RAP should not be used in such a pavement structure due to poor performance concerns and the relatively small quantity of embankment materials above the structure. The same recommendation applies to other rigid, buried metal or concrete structures as well as bedrock, because they all have very high stiffness values, similar to the box concrete culvert.

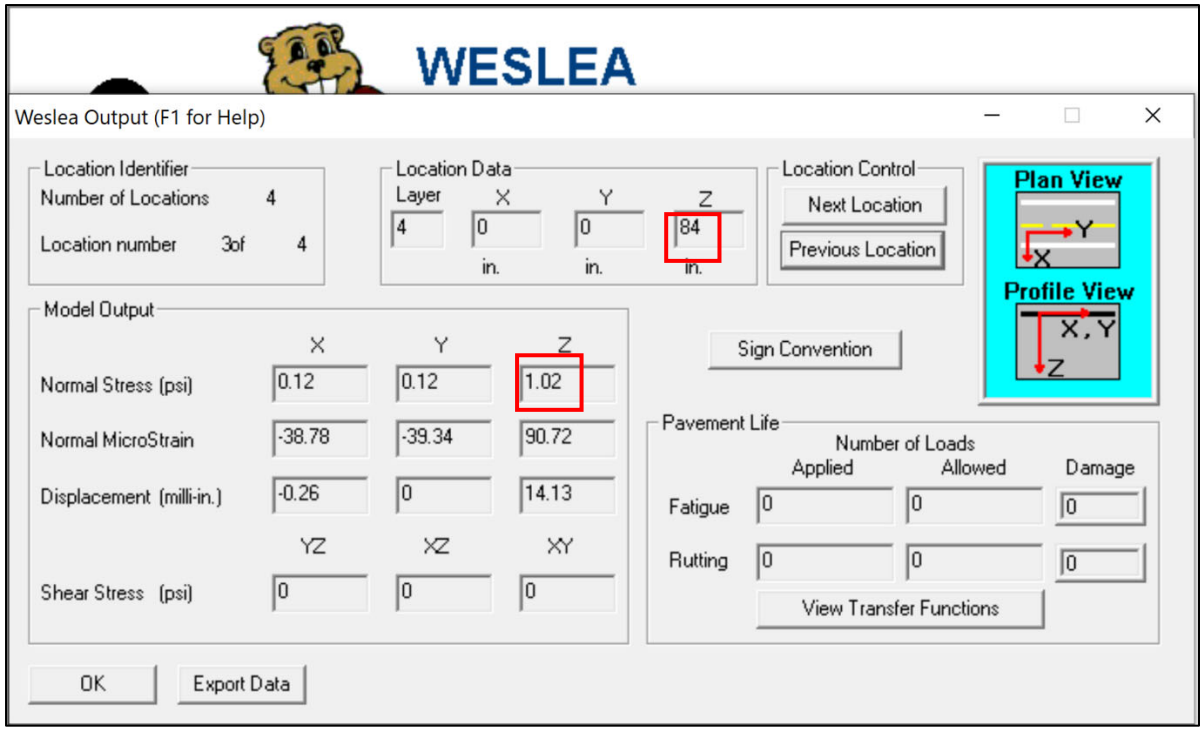

FIGURE 89. Case 1: Stress level 7 ft from surface (11-in. concrete + 3-in. WMA + 9-in. subgrade aggregate special).

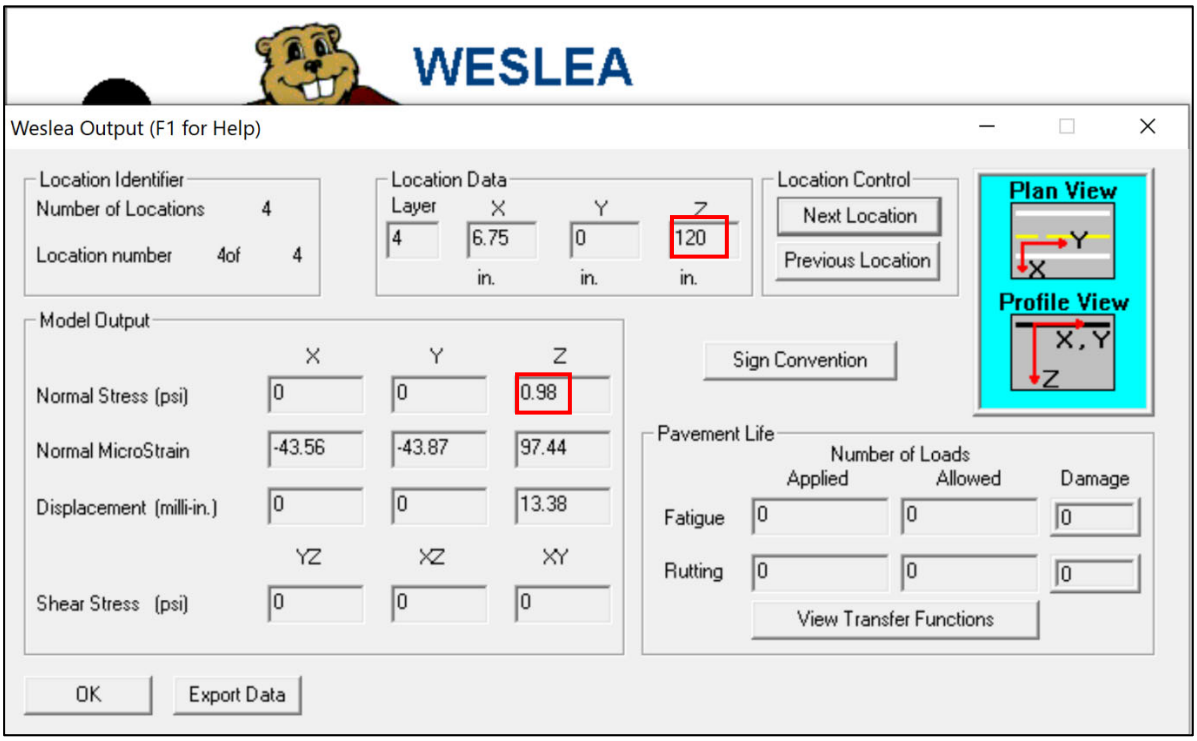

FIGURE 83. Case 2: Stress level 10 ft from surface (15-in. SMA + 12-in. aggregate base).

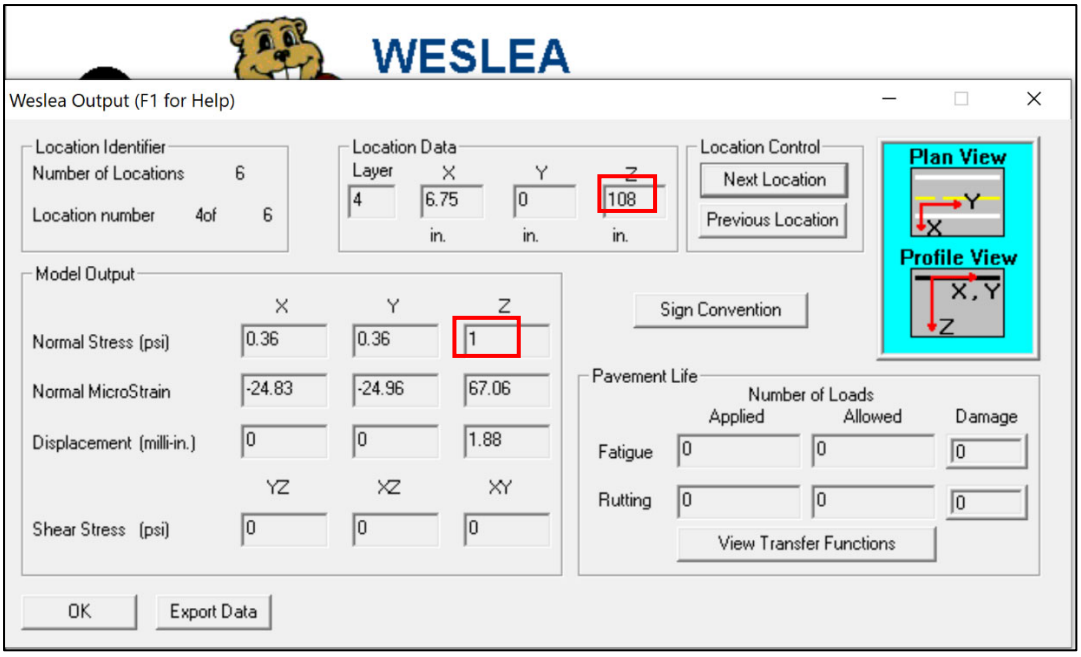

FIGURE 84. Case 3: Stress level 9 ft from surface (13-in. concrete + 3-in. WMA + subgrade + pile-supported box concrete culvert).

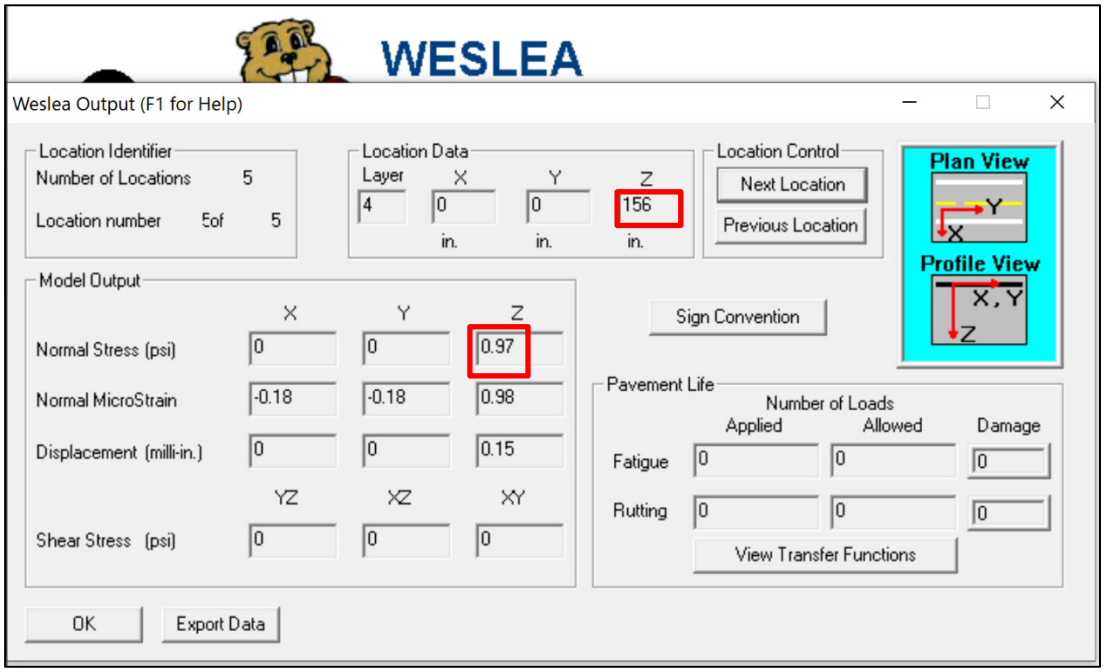

FIGURE 85. Case 4: Stress level 12 ft from surface (15-in. SMA + 12-in. aggregate base + subgrade aggregate special + pile-supported box concrete culvert).

5.6 Field Settlement Analysis

The soil settlement analysis conducted by the designer and contractor of the I-90 Jane Addams Memorial Tollway project during both the design stage and the forensic stage indicated that minimal settlement was expected. However, severe settlement and subsequent pavement cracks occurred within a few months after completion of the construction. Therefore, based on the laboratory test results, the research team used different scenarios for settlement analysis in an attempt to determine the reasons for the excessive settlement.

5.6.1 Scenario 1: IDOT Analysis from Design/Forensic Reports

Current IDOT soil settlement analysis is limited to the natural soil below the embankment, as indicated by the red box in Figure 93. The embankment settlement was excluded from IDOT's analysis, assuming that self-weight settlement occurred during construction prior to the placement of the pavement structure. The coefficients of compressibility (C_c) of the natural soils in the IDOT settlement analysis were based on the moisture content, as expressed in Equation (11). The research team then retrieved the calculated settlement values at different boring locations for the I-90 Jane Addams Memorial Tollway project from forensic reports by the contractor. Figure 94 shows that the expected long-term settlements for these locations are less than one inch, even though on average 3 in. ~ 4 in. of settlement were reported at these locations within a few months after the construction.

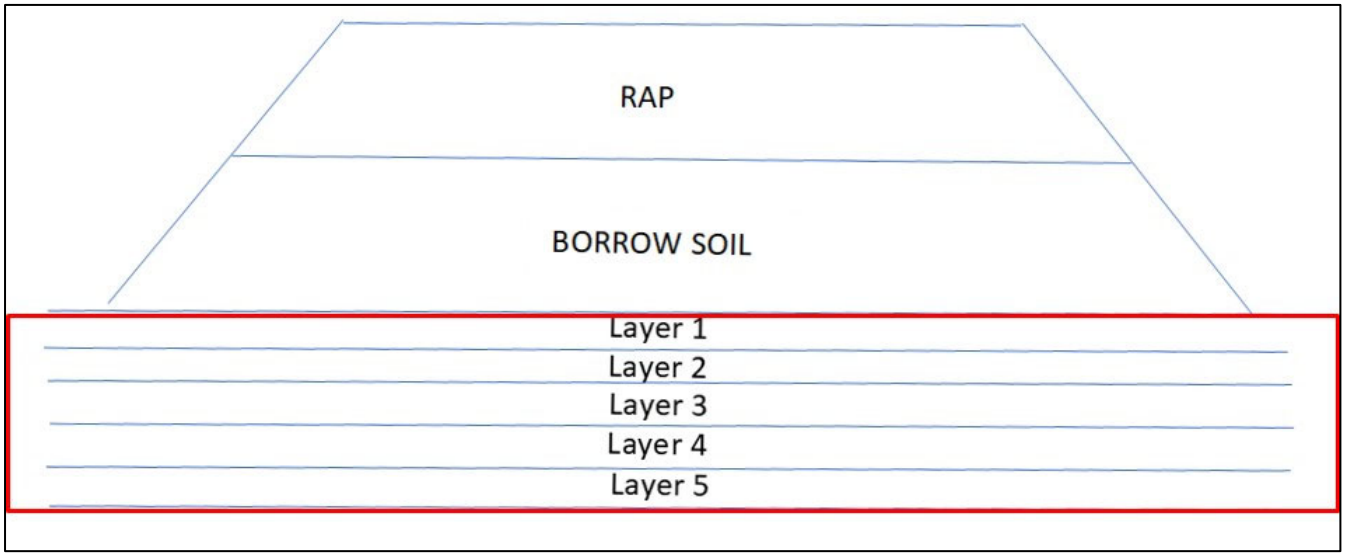

FIGURE 86. Basis for IDOT's settlement analysis.

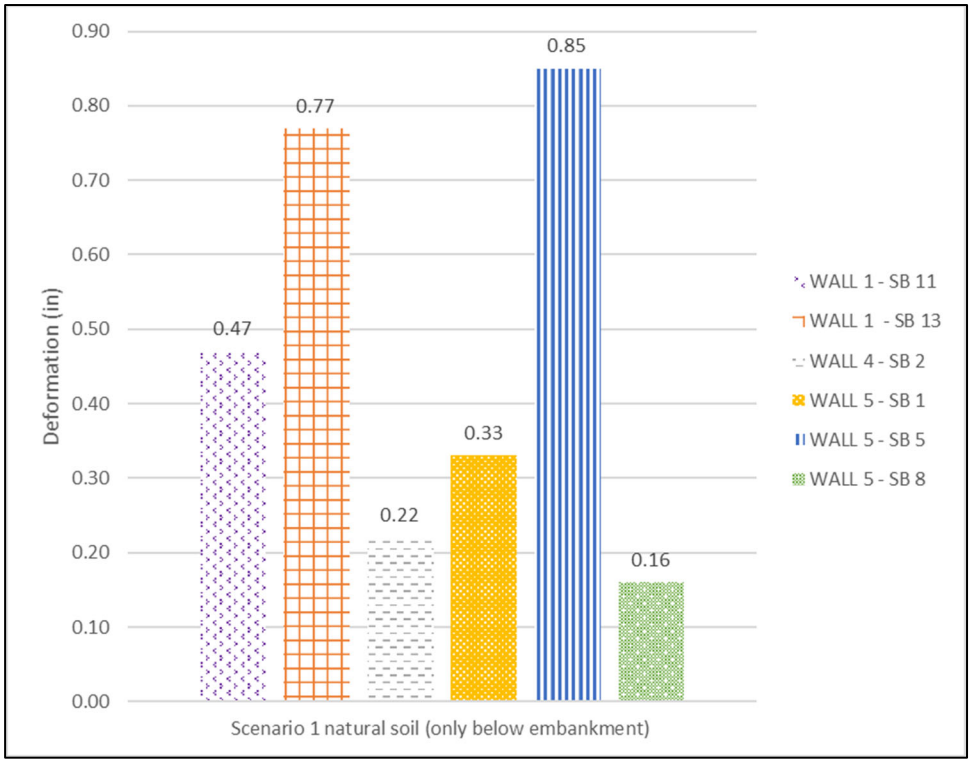

FIGURE 87. Scenario 1: Natural soil only below embankment consolidation.

5.6.2 Scenario 2: Settlement of Natural Soil below Embankment and Soil Section of Embankment Layer

In Scenario 2, illustrated in Figure 95, in addition to the natural soil, the embankment (borrow) soil also was included in the analysis. The research team employed three approaches for the analysis of this scenario. Approach A follows the current IDOT settlement analysis (Equations 12) to determine the settlement of the soil at the OMC and saturated conditions, referred to as Scenarios 2-1-A and 2-2-A and shown in Figures 96 and 97, respectively. The settlement of the embankment soil was found to be minimal; for instance, the settlement was 0.04 in. and 0.1 in. for the OMC and the saturated soils for Wall 1 – SB 11. This outcome may be because Equation (12) is applicable only to normally- or over-consolidated soils whereas embankment soils typically are under-consolidated.

$$S = \frac{C_c H_L}{(1+e_0)} Log\left(\frac{P_0^{'} + \Delta P^{'}}{P_0^{'}}\right) \quad (12)$$

where

S = estimated primary settlement;

H_L = thickness of compressible soil layer;

e_0 = initial void ratio;

P_0' = effective overburden pressure at the center of compressible soil layer;

$\Delta P'$ = increase in stress at the center of compressible soil layer resulting from embankment or foundation loads; and

C_c = compression index (dimensionless); see Equation (11).

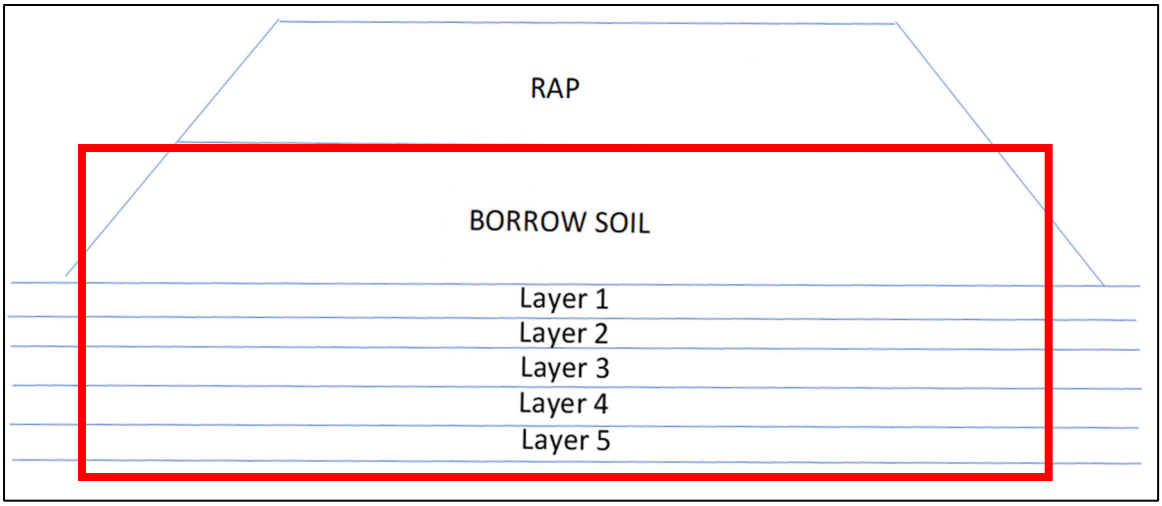

FIGURE 88. Scenario 2: Below embankment (natural ground) and soil in embankment layer settlement.

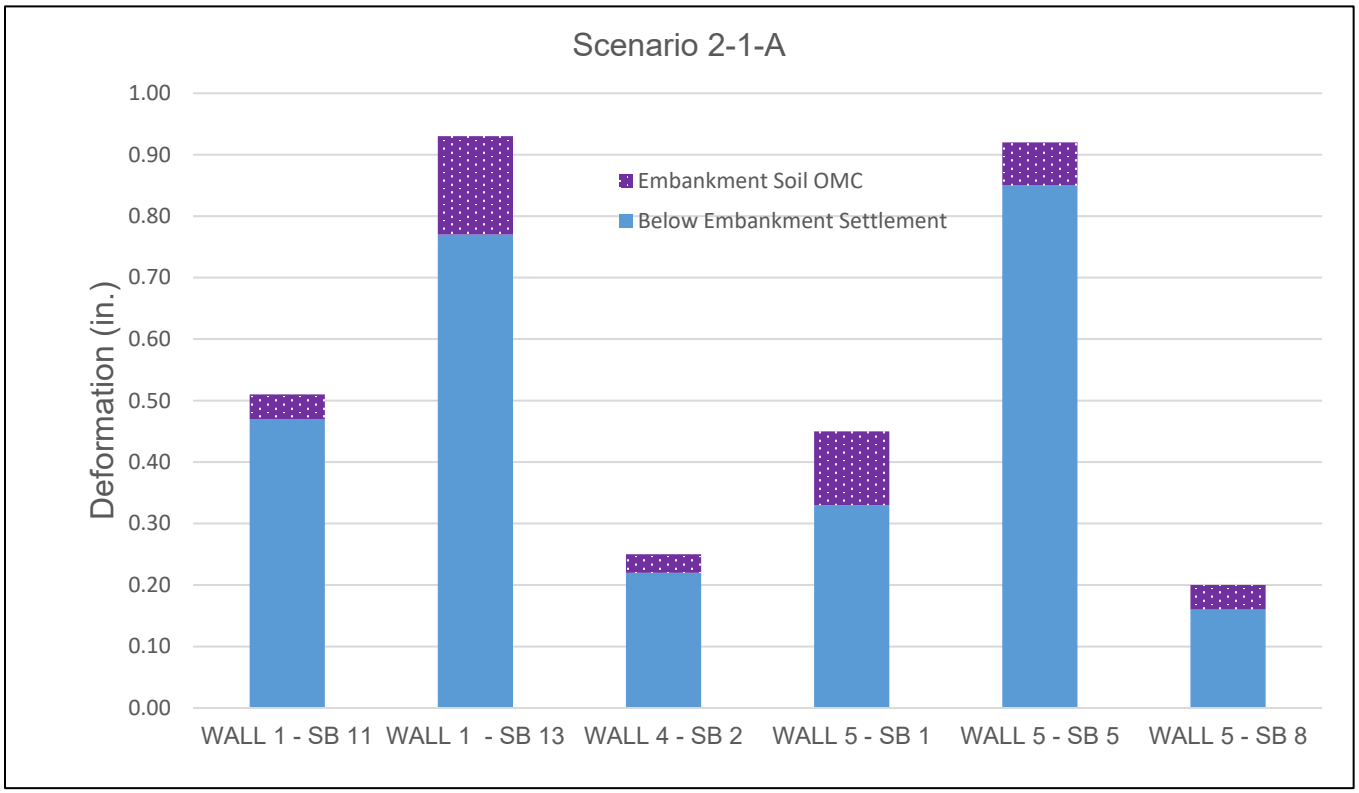

FIGURE 96. Scenario 2-1-A: Settlement of soil below embankment and OMC soil of embankment layer (Approach A).

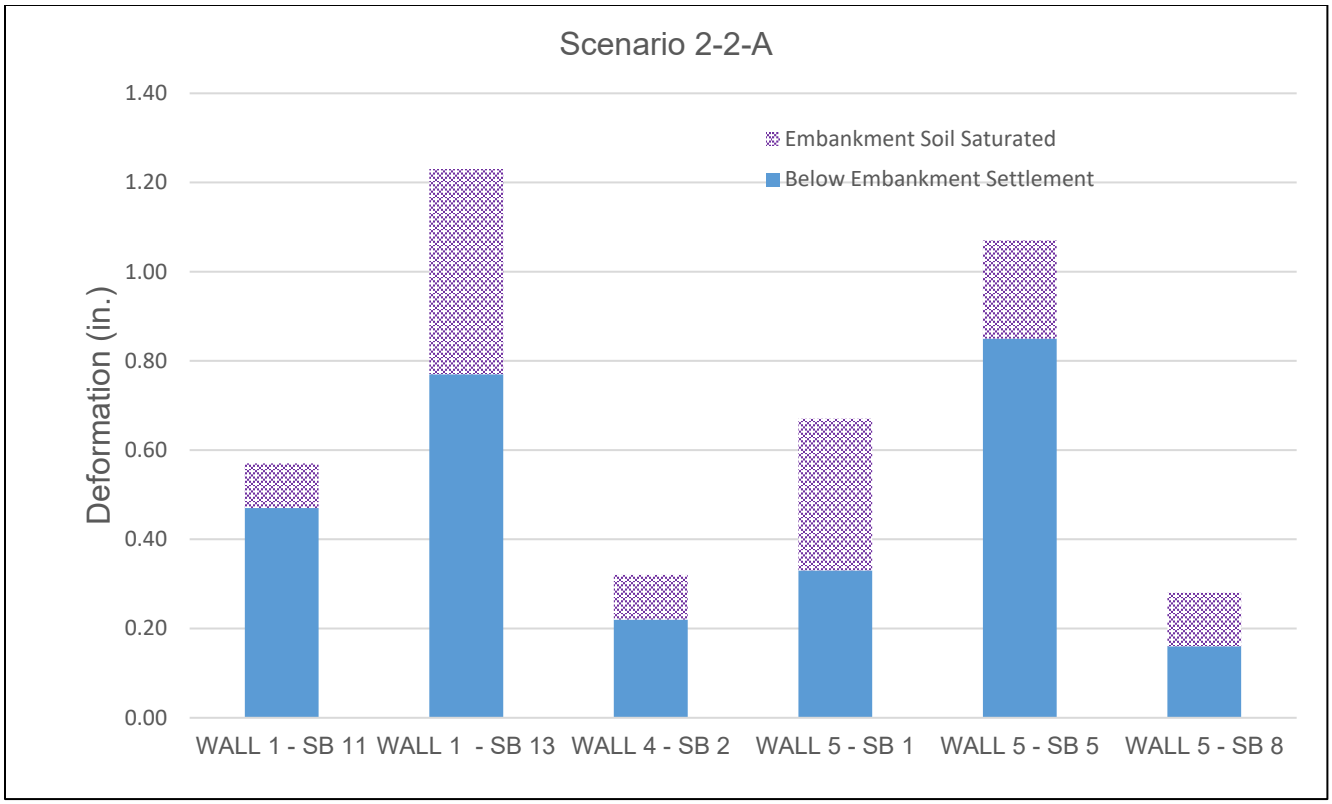

FIGURE 89. Scenario 2-2-A: Settlement of soil below embankment and saturated soil of embankment layer (Approach A).

Approach B uses the measured strain of the soils obtained from the 1-D consolidation tests to estimate the settlement by multiplying the strain at the corresponding overburden pressure in a sublayer by the sublayer thickness. Both OMC and saturated conditions were included in the analysis. Figures 98 and 99 respectively show the estimated settlements when the embankment soils are in their OMC and saturated conditions, referred to as Scenarios 2-1-B and 2-2-B, respectively. When the embankment soil is at the OMC, total settlement varies from 0.96 in. to 3.72 in. which includes that of the natural ground and embankment soil, depending on the location, as different locations have different embankment soil thicknesses. When the embankment soil is in saturated conditions, the total settlement increases significantly up to 6.40 inches. Assuming the settlement of the soils at the OMC has occurred during construction prior to the placement of the pavement structure, the subsequent saturation of the embankment soil could lead to additional settlement of the pavement surface, e.g., another 3 inches. In the case of the I-90 tollway, according to the permeability and tube drainage test results, water infiltrated the

RAP layer from the drainage layer. Because the slopes of embankments are capped with vegetation soil, water that collects in the RAP layer may slowly saturate the embankment soil, which could lead to excessive settlement.

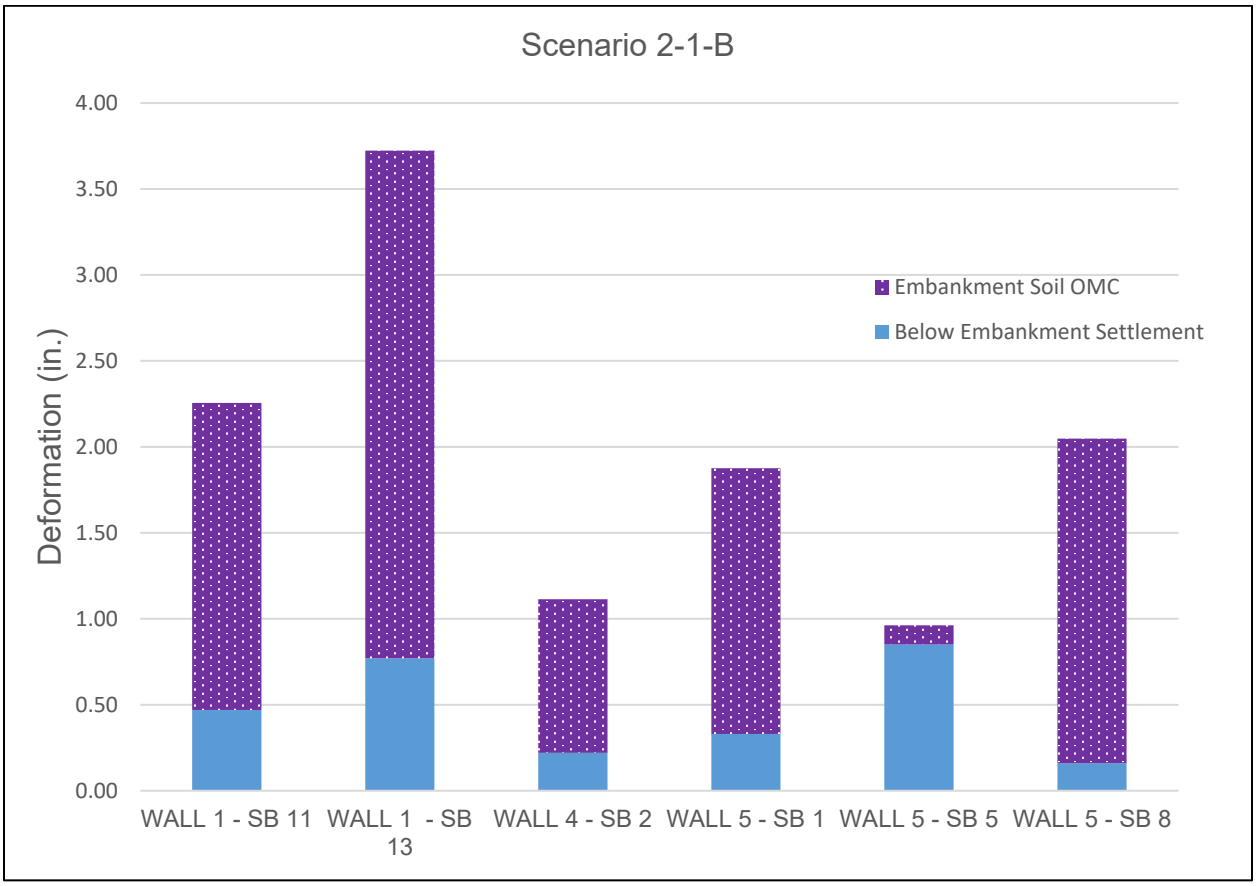

FIGURE 90. Scenario 2-1-B: Settlement of soil below embankment and OMC soil of embankment layer (Approach B).

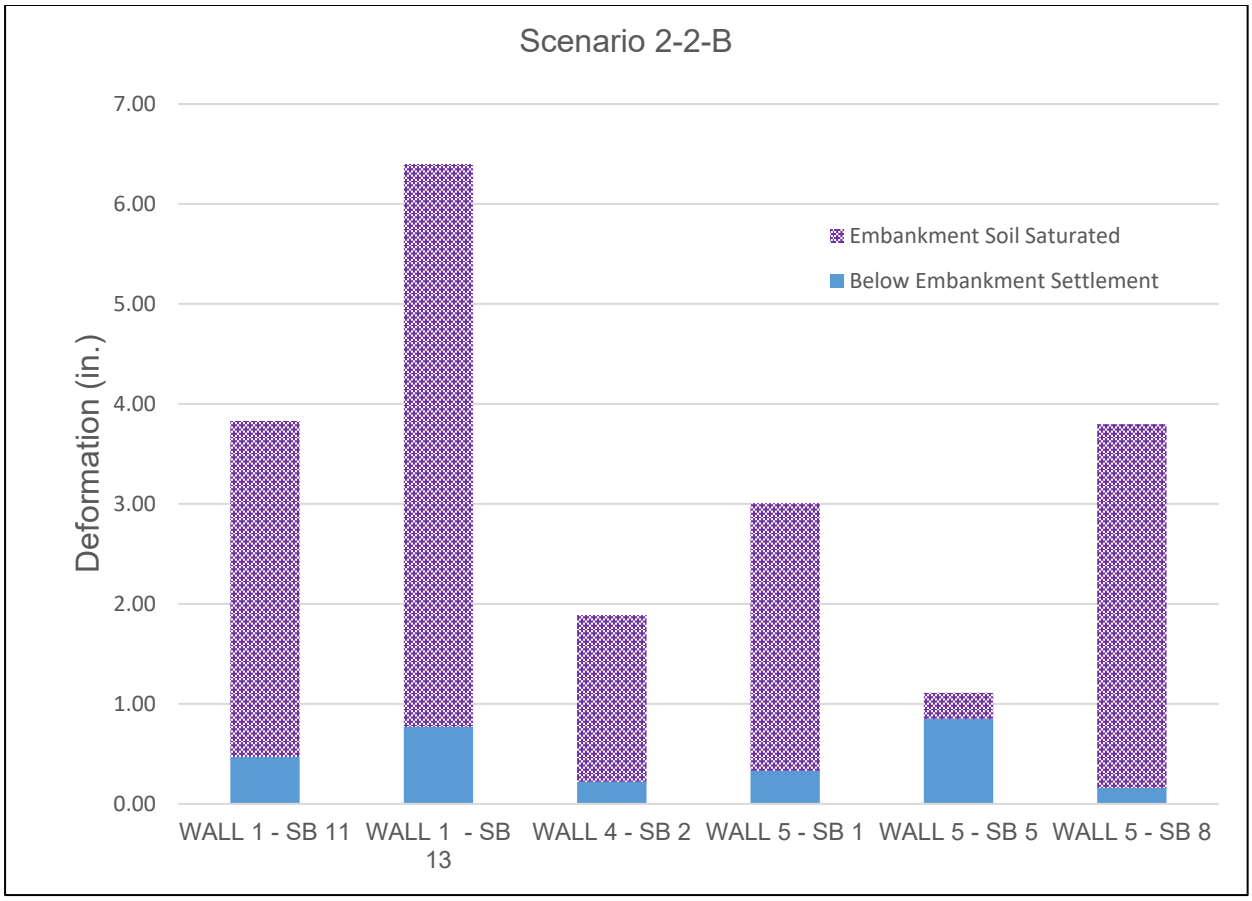

FIGURE 99. Scenario 2-2-B: Settlement of soil below embankment and saturated soil of embankment layer (Approach B).

Approach C uses the alternative method suggested by the IDOT's Geotechnical Manual (Section D.9.2.1.1), as shown in Equation (13), which is applicable to soils at any state.

$$S = H_L \frac{\Delta e}{1+e_0} \tag{13}$$

where

S = estimated primary settlement;

H_L = thickness of compressible soil layer;

e_0 = initial void ratio;

$\Delta e = e_0 - e_f$; and

e_f = final void ratio.

The settlement analyses for the soil under OMC and saturated conditions are referred to Scenarios 2-1-C and 2-2-C, respectively. Figures 100 and 101 present the Approach C results for

the two scenarios, respectively. Total settlement, which includes that of the natural ground and embankment soil at the OMC, varies from 0.8 in. to 2.77 in. at various locations. The maximum deformation for the saturated soil was found to be 6.43 inches. The results for Approach C are close to those for Approach B.

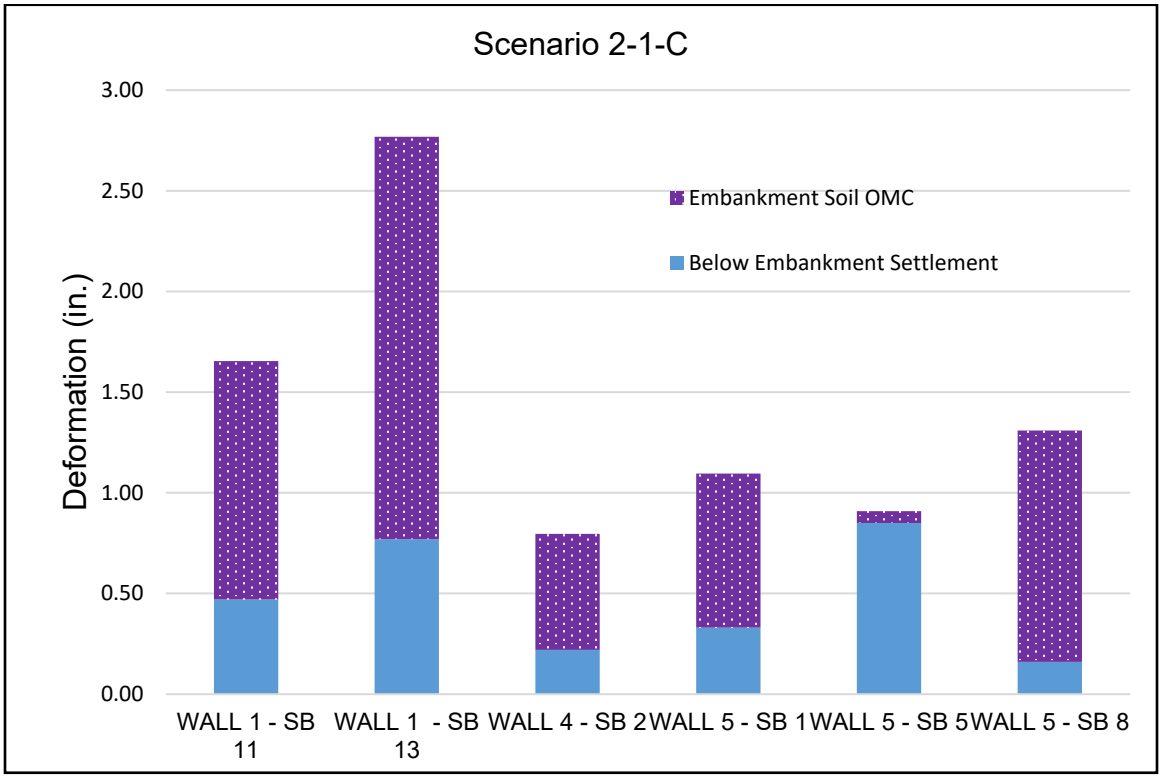

FIGURE 91. Scenario 2-1-C: Settlement of soil below embankment and OMC soil of embankment layer (Approach C).

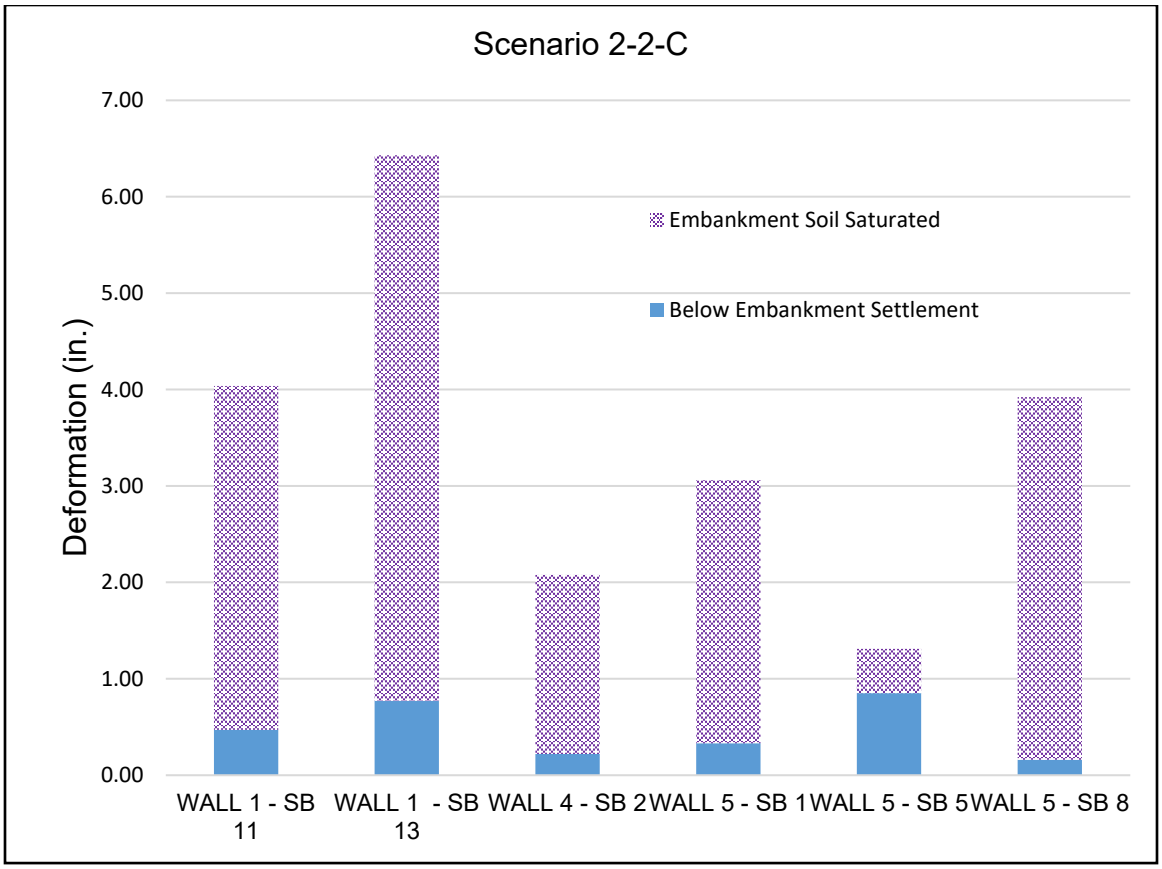

FIGURE 92. Scenario 2-2-C: Settlement of soil below embankment and saturated soil of embankment layer (Approach C).

5.6.3 Scenario 3: Settlement of Natural Soil below Embankment and Embankment Layer (Soil and RAP)

Figure 102 presents Scenario 3 where the RAP embankment layer is included in the settlement analysis. Again, settlement analyses based on Approach B and Approach C were conducted based on laboratory test results. Approach A was not used because it is not applicable to RAP.

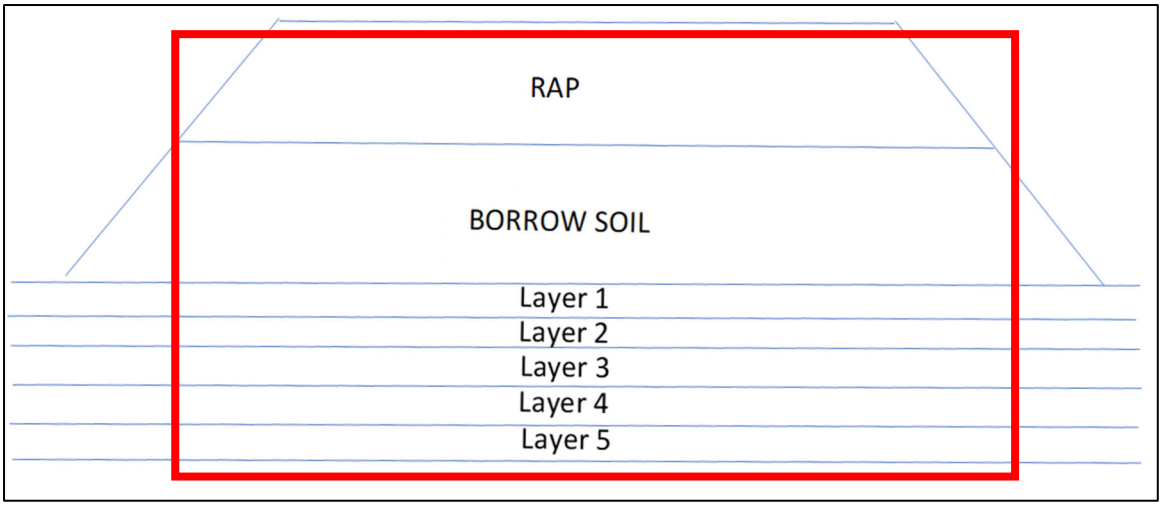

FIGURE 93. Scenario 3: Settlement of natural soil below embankment and embankment layer (soil and RAP).

The settlement of RAP is sensitive to the RAP temperature, as shown by the laboratory test results. Therefore, the settlement of the RAP samples at both room temperature and at 100°F is included in the analysis. The 100°F temperature represents an extreme case that is unlikely to occur inside the embankment but nonetheless reflects the worst-case settlement conditions. In addition, the cases of embankment soils under OMC and saturated conditions are included herein. These conditions result in four combinations: two RAP temperatures and two embankment soil moisture conditions.

Figures 103 through 106 respectively present the four scenarios, referred to as Scenarios 3-1-B to 3-4-B, based on Approach B, for (1) RAP at room temperature (70°F) and embankment soil at the OMC, (2) RAP at room temperature (70°F) and embankment soil in the saturated condition, (3) RAP at 100°F and embankment soil at the OMC, and (4) RAP at 100°F and embankment soil in the saturated condition. As shown, the settlement in the RAP layer at room temperature is typically less than 1 in., depending on the thickness of the RAP layer, and the primary settlement is still within the embankment soil layer. When the RAP temperature is increased to 100°F, the RAP settlement slightly increases by half an inch or less. Overall, the primary settlement comes from the embankment soil layer. Again, assuming that self-weight embankment soil settlement has occurred during the construction of the embankment prior to the placement of the pavement structure, which would not affect the pavement structure, the subsequent saturation of the embankment soil would lead to another 3 in. of settlement of the

pavement surface, which matches the field measurements of the settlement at the I-90 Jane Addams Memorial Tollway.

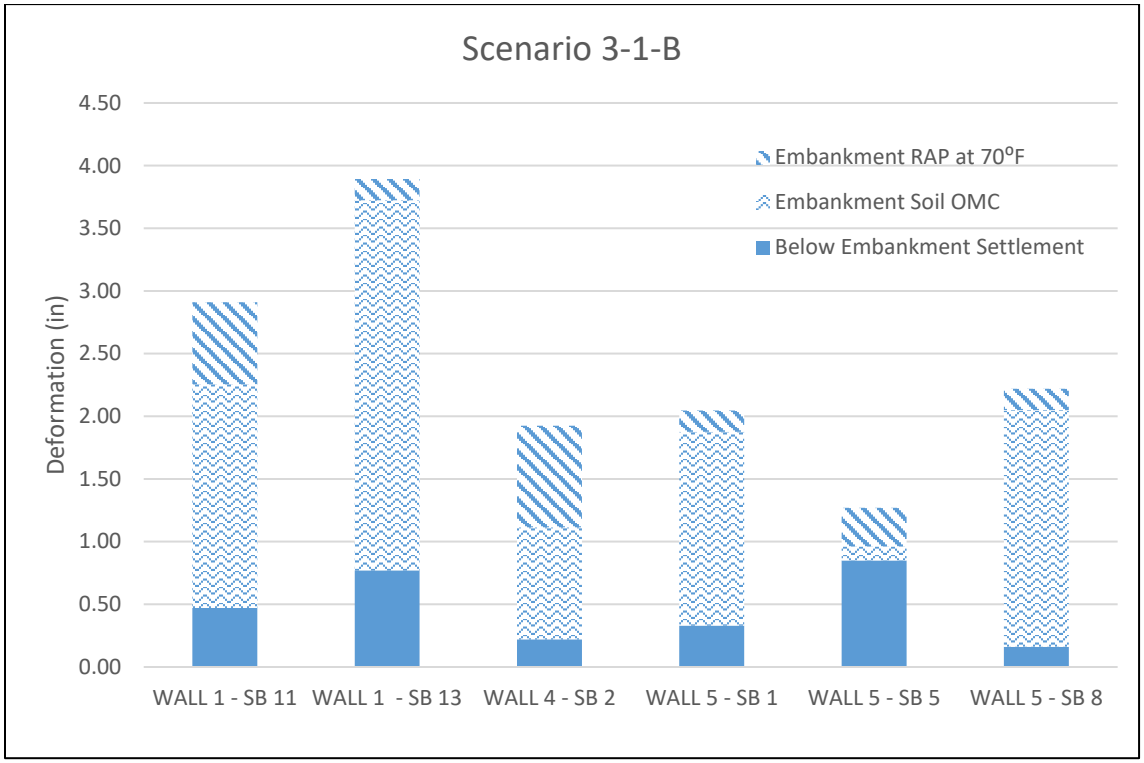

FIGURE 94. Scenario 3-1-B: Settlement of soil below embankment and OMC soil of embankment layer and RAP at 70ºF (Approach B).

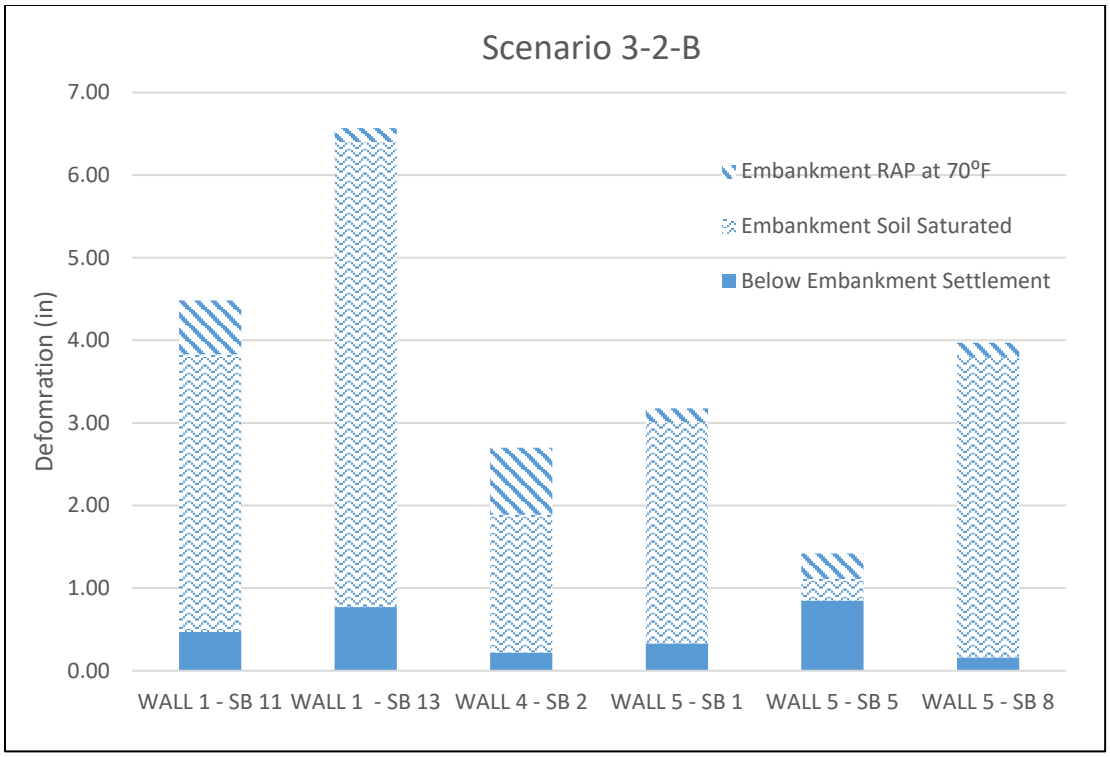

FIGURE 95. Scenario 3-2-B: Settlement of soil below embankment and saturated soil of embankment layer and RAP at 70ºF (Approach B).

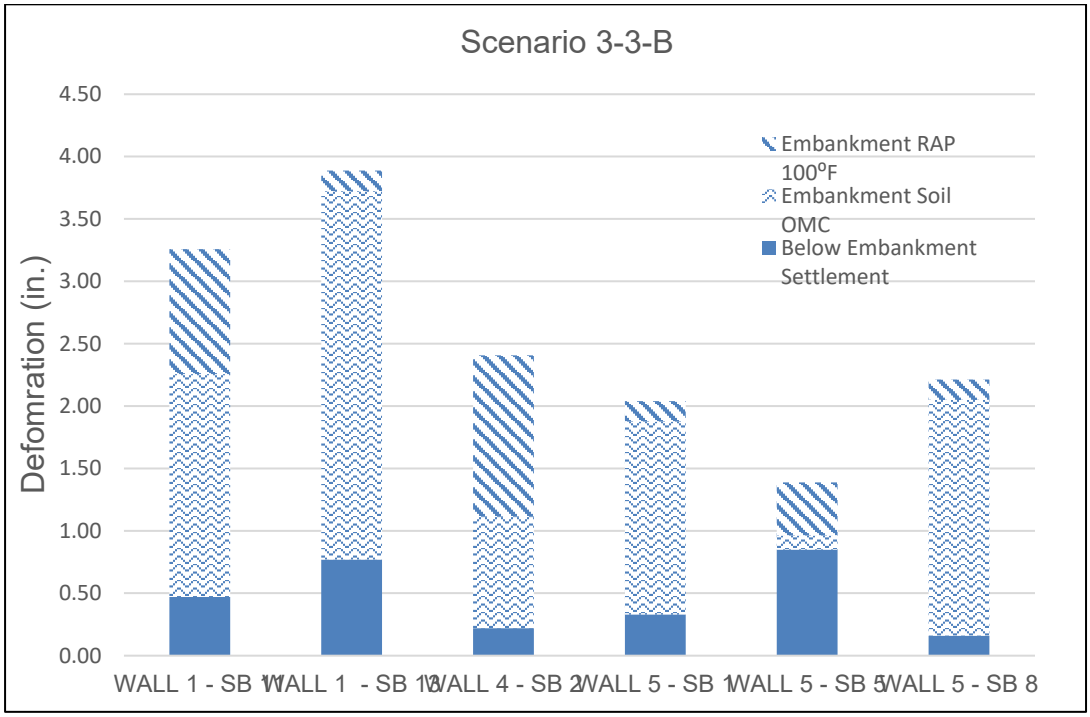

FIGURE 96. Scenario 3-3-B: Settlement of soil below embankment and OMC soil of embankment layer and RAP at 100ºF (Approach B).

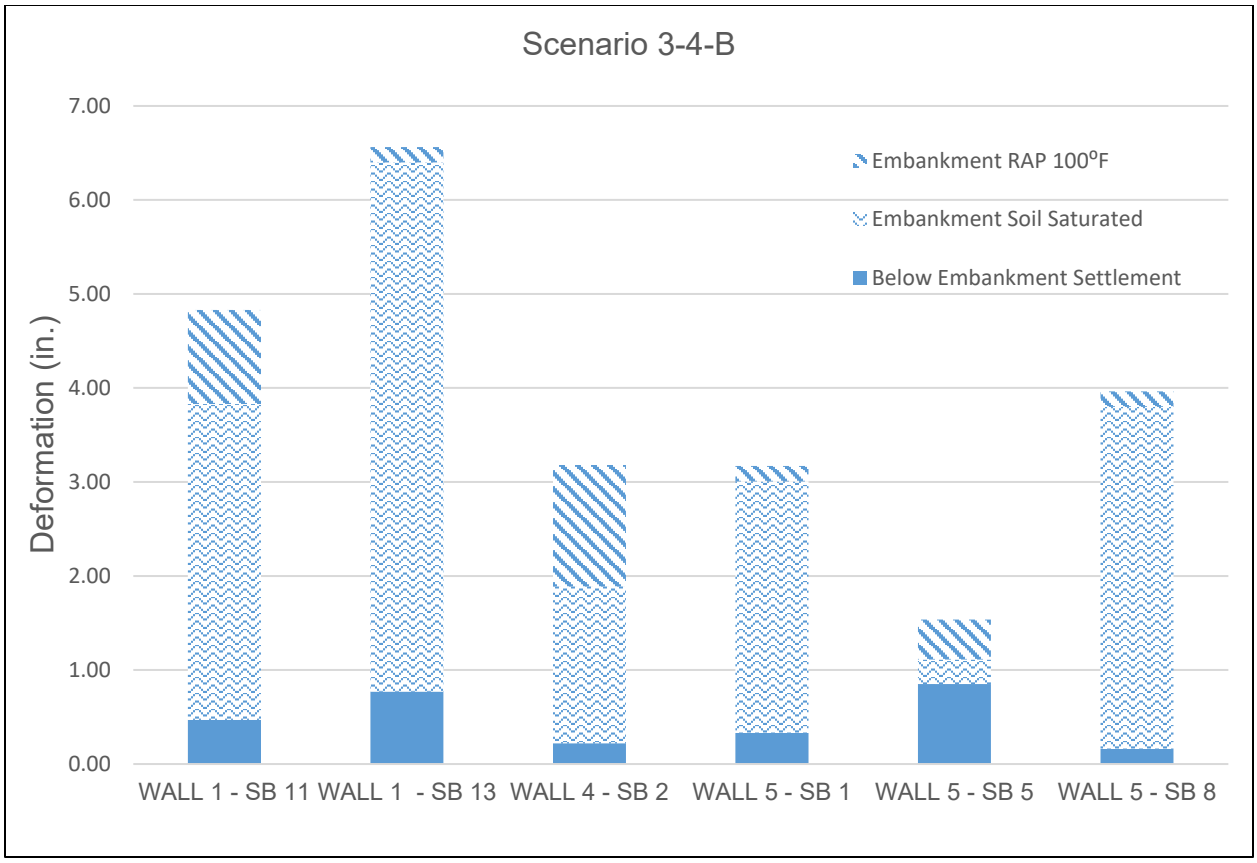

FIGURE 97. Scenario 3-4-B: Settlement of soil below embankment and saturated soil of embankment layer and RAP at 100ºF (Approach B).

Figures 107 through 110 show the analysis results based on Approach C. Figures 107 and 109 show the expected settlement when the embankment soil is at the OMC and the RAP is at room temperature (70°F) and 100°F, respectively. As shown, the settlement in the RAP layer at room temperature is typically less than one inch. When the RAP temperature is increased to 100°F, the RAP settlement increases to a value just under 1.5 inches. Overall, the primary settlement comes from the embankment soil layer. Figures 108 and 110 show the settlement analysis results when the embankment soil is in saturated conditions. Again, the primary settlement is in the embankment soil layer.

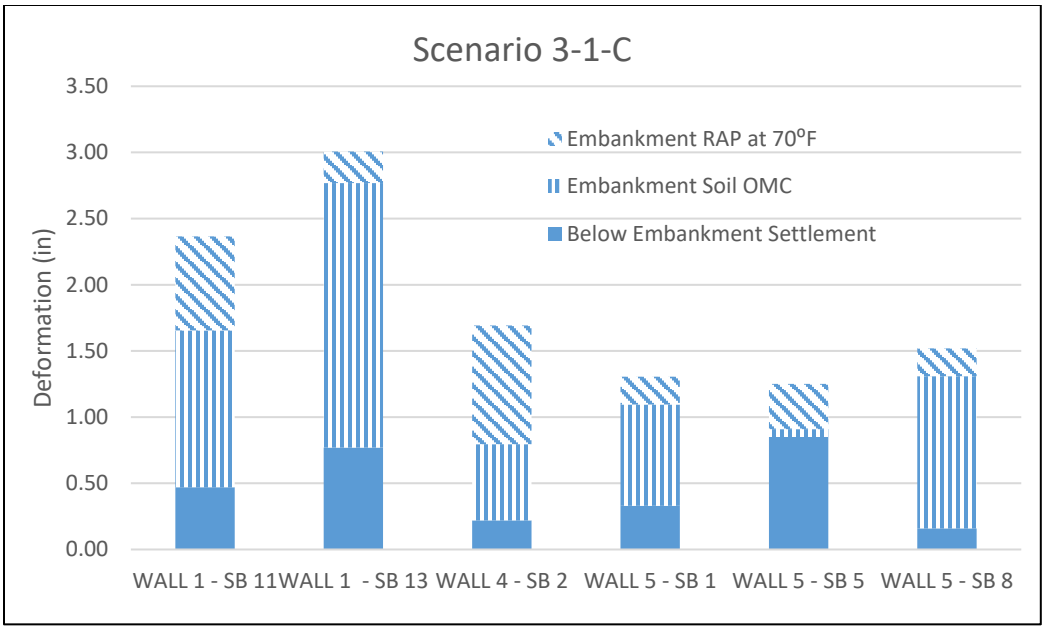

FIGURE 98. Scenario 3-1-C: Settlement of soil below embankment and OMC soil of embankment layer and RAP at 70ºF (Approach C).

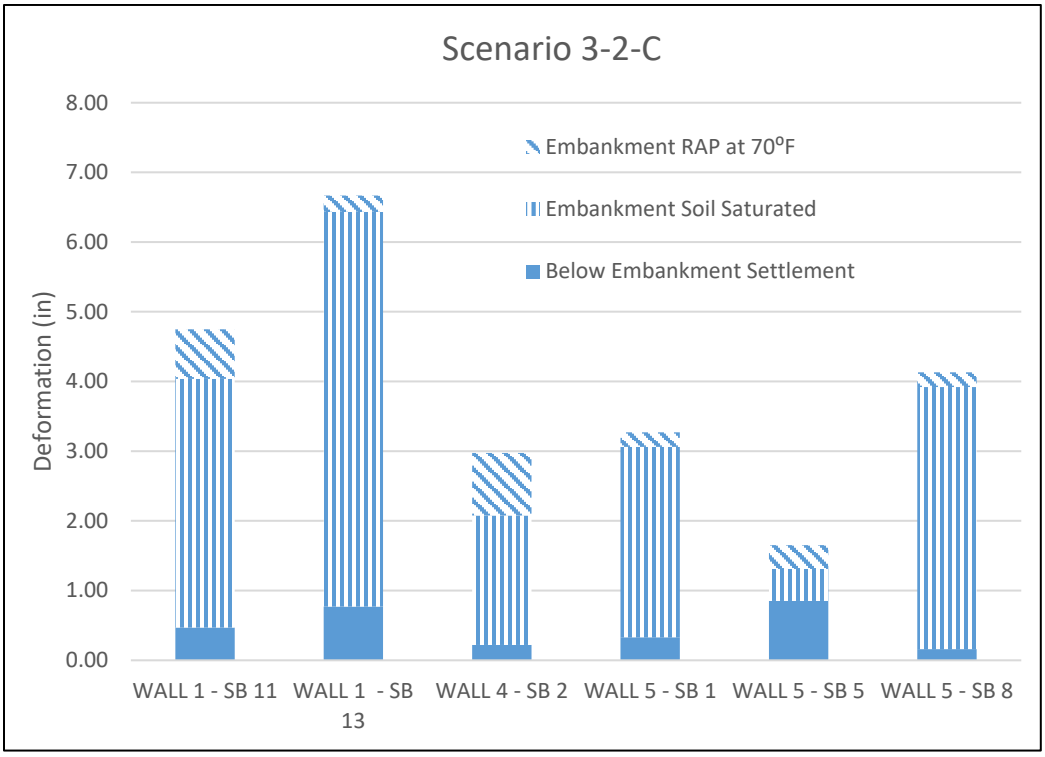

FIGURE 99. Scenario 3-2-C: Settlement of soil below embankment and saturated soil of embankment layer and RAP at 70ºF (Approach C).

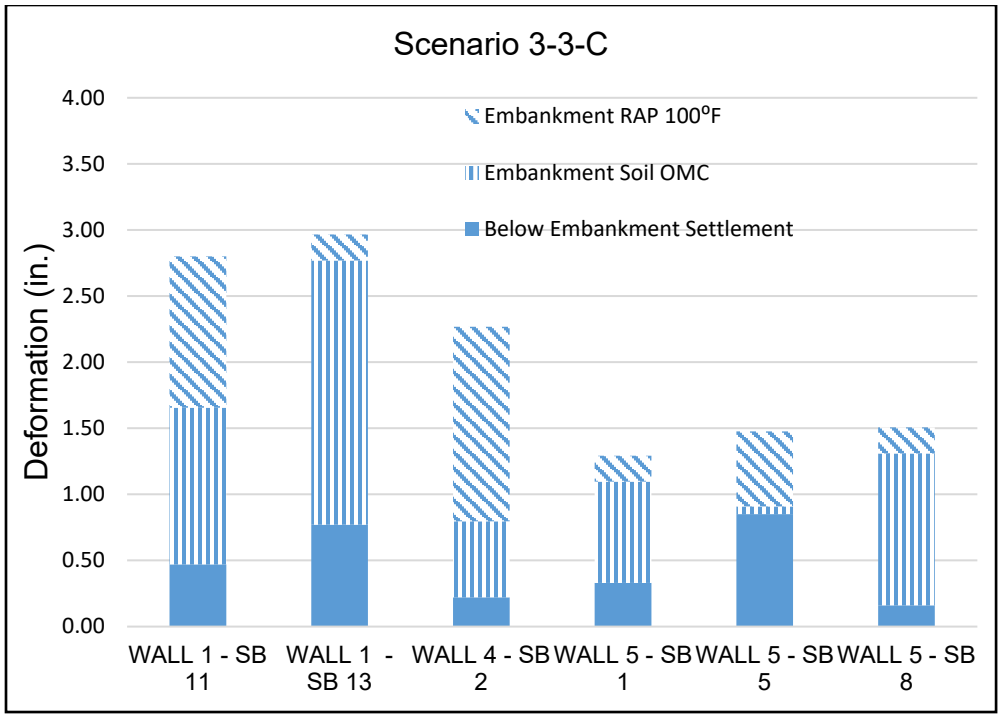

FIGURE 100. Scenario 3-3-C: Settlement of soil below embankment and OMC soil of embankment layer and RAP at 100°F (Approach C).

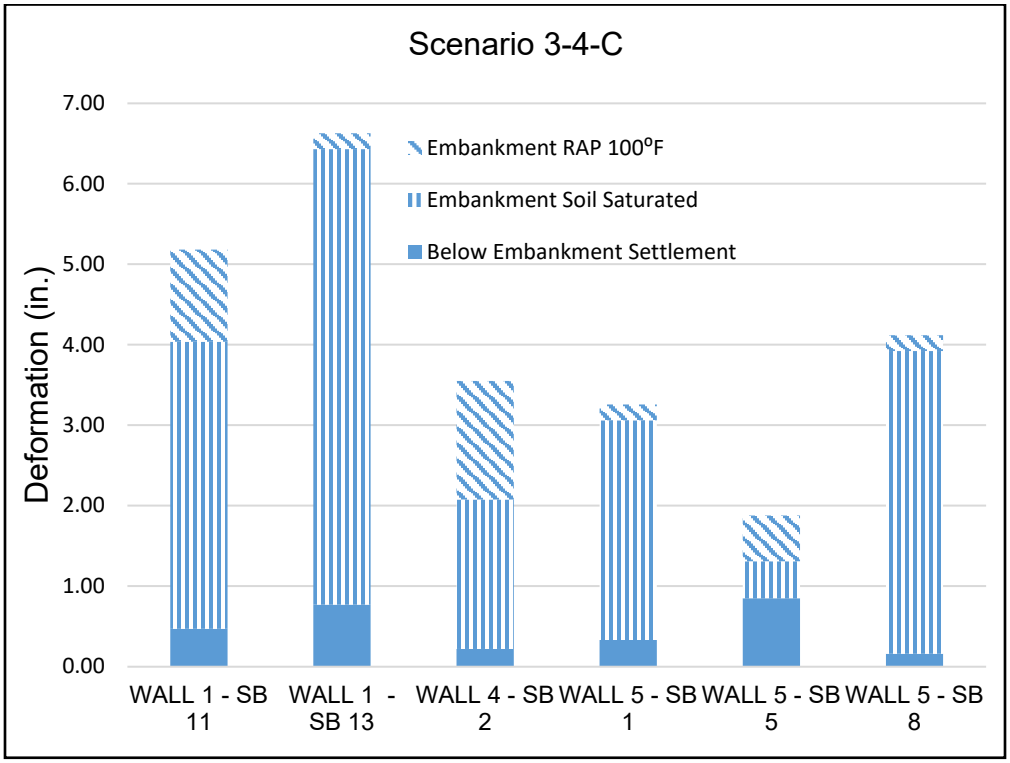

FIGURE 101. Scenario 3-4-C: Settlement of soil below embankment and saturated soil of embankment layer and RAP at 100°F (Approach C).

Illinois Tollway's Special Provision specifies a 3-ft soil cap when the embankment material is permeable or frost-susceptible. The purpose of the soil cap is to prevent the infiltration of water into the embankment. Therefore, another scenario, Scenario 3-5, includes a 3-ft soil cap on top of the RAP layer. Figures 111 and 112 show the settlement analysis results when the embankment soil is in OMC conditions, based on Approaches B and C, respectively. This scenario is based on the assumption that the soil cap effectively prevents water from infiltrating the RAP layer and saturating the embankment soil under the RAP layer. Figures 113 and 114 present Scenario 3-6 and show the settlement analysis results when the embankment soil is under saturated conditions when the soil cap cannot completely prevent the infiltration of water, based on Approaches B and C, respectively. If the soil cap is effective in the long run, then the estimated settlement based on Approach B can be 3 in. or less, or 2.2 in. based on Approach C. However, if the soil cap is not effective in the long run, then settlement up to 4.5 in. or more is possible because the RAP in the embankment can still store the infiltrated water, which in turn saturates the underlying embankment soil. The use of a soil + RAP mix instead of RAP may be effective in reducing the risk of excessive settlement associated with water infiltration into RAP.

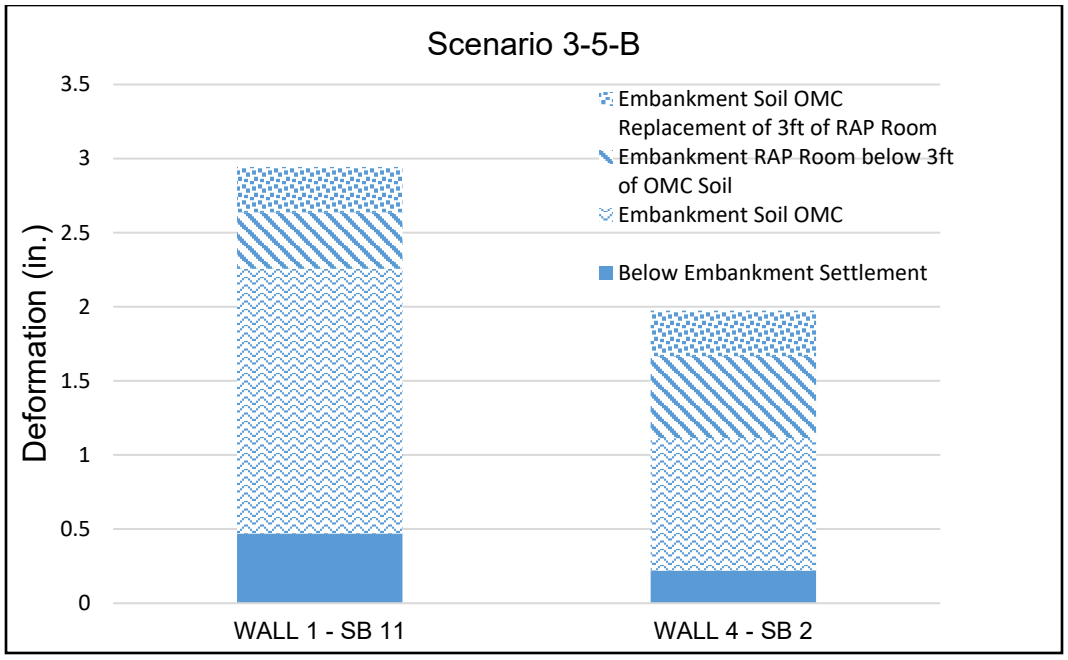

FIGURE 102. Scenario 3-5-B: Settlement of soil below embankment (natural ground) and OMC embankment soil beneath RAP layer and RAP at room temperature and soil on top of RAP at OMC (Approach B).

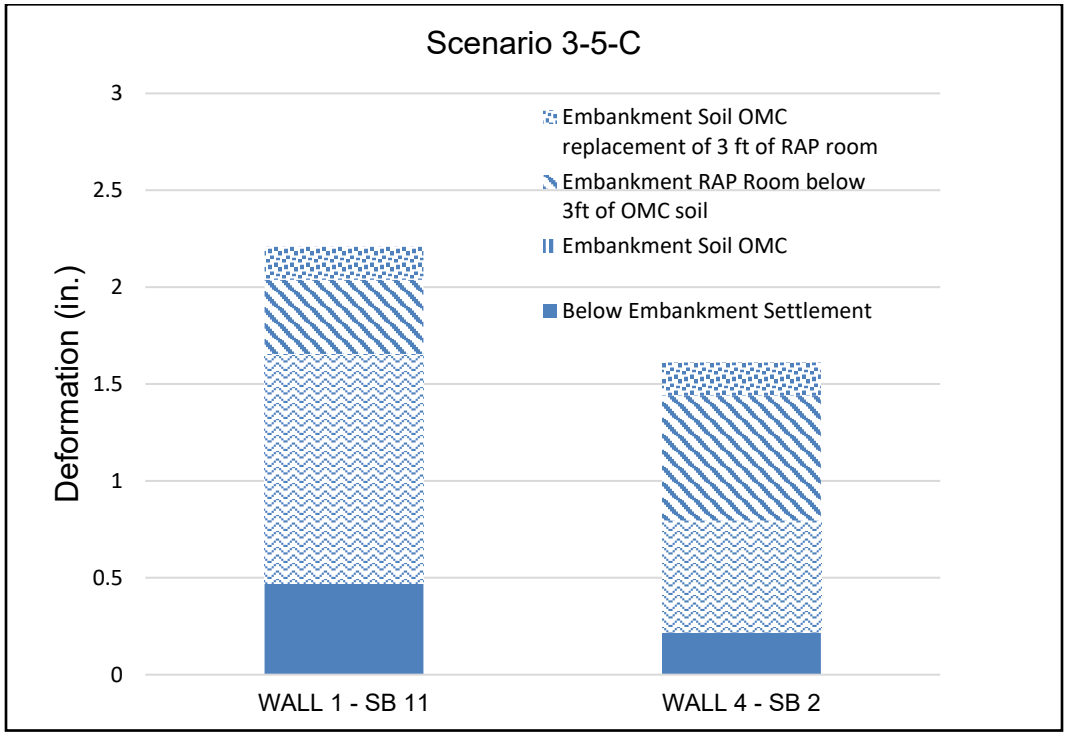

FIGURE 103. Scenario 3-5-C: Settlement of soil below embankment (natural ground) and OMC embankment soil beneath RAP layer and RAP at room temperature and soil on top of RAP at OMC (Approach C).

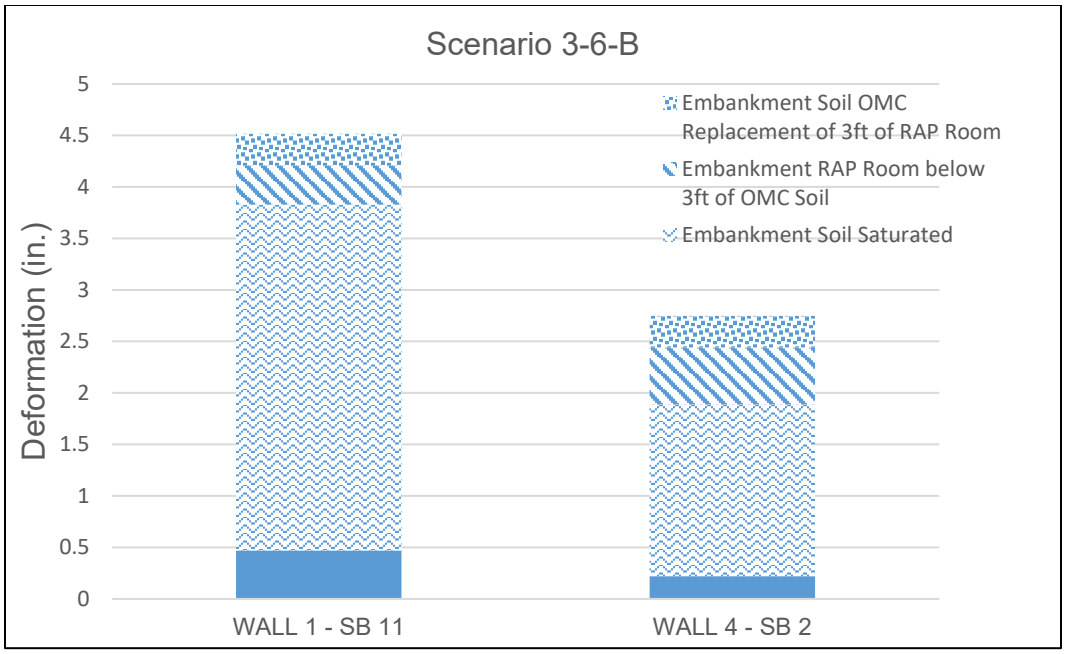

FIGURE 104. Scenario 3-6-B: Settlement of soil below embankment (natural ground) and saturated embankment soil beneath RAP layer and RAP at room temperature and soil on top of RAP at OMC (Approach B).

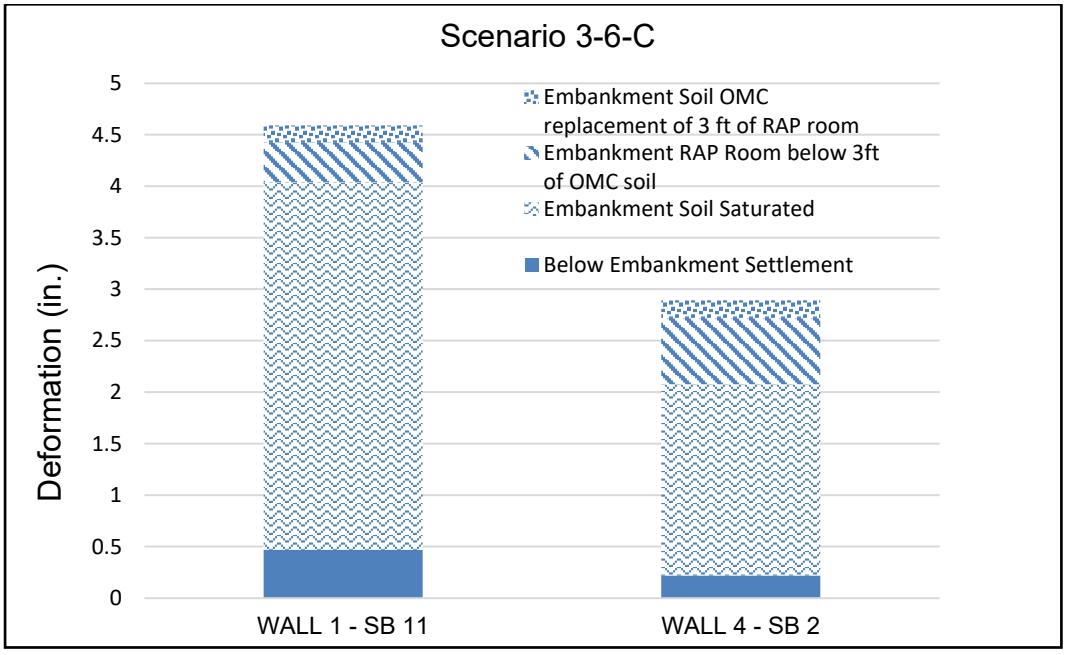

FIGURE 105. Scenario 3-6-C: Settlement of soil below embankment (natural ground) and saturated embankment soil beneath RAP layer and RAP at room temperature and soil on top of RAP at OMC (Approach C).

5.6.4 Recommendations

Based on the settlement analysis results, RAP used in an embankment is recommended to be separated from the drainage system, which includes the PGE, underdrain pipe, and backfill, by using an impermeable (or low permeability) material, such as a soil cap as described in Illinois Tollway's special provision. Another recommendation is to include embankment materials in the settlment analysis during the design stage, considering the possible saturation of the embankment soil. When RAP (processed or unprocessed) is used in an embankment, a strain-based method (Approach B) or Equation (13) (Approach C) should be used. This method accounts for using *in situ* RAP grindings for fast-track embankment construction, such as the case of the I-90 Jane Addams Memorial Tollway (Contract 4206). Figures 115 and 116 respectively present the relationship between total stress and accumulative strain that is based on the average 1-D consolidation test results for the five processed and unprocessed RAP samples at room temperature (70ºF). A linear relationship exists between the overburden stress and settlement strain, as expressed in Equations (14) and (15) for < 1.5-in. RAP and < 2.0-in. RAP, respectively. The settlement in each RAP sublayer can be calculated by multiplying the strain in each RAP sublayer by the sublayer thickness.

$$\varepsilon_p = 0.063\sigma+0.6972 \quad \text{(RAP particle size < 1.5 in.)} \tag{14}$$

$$\varepsilon_p = 0.0839\sigma+1.06 \quad \text{(RAP particle size < 2.0 in.)} \tag{15}$$

where

ε_p = settlement strain, %; and

σ = overburden stress, psi.

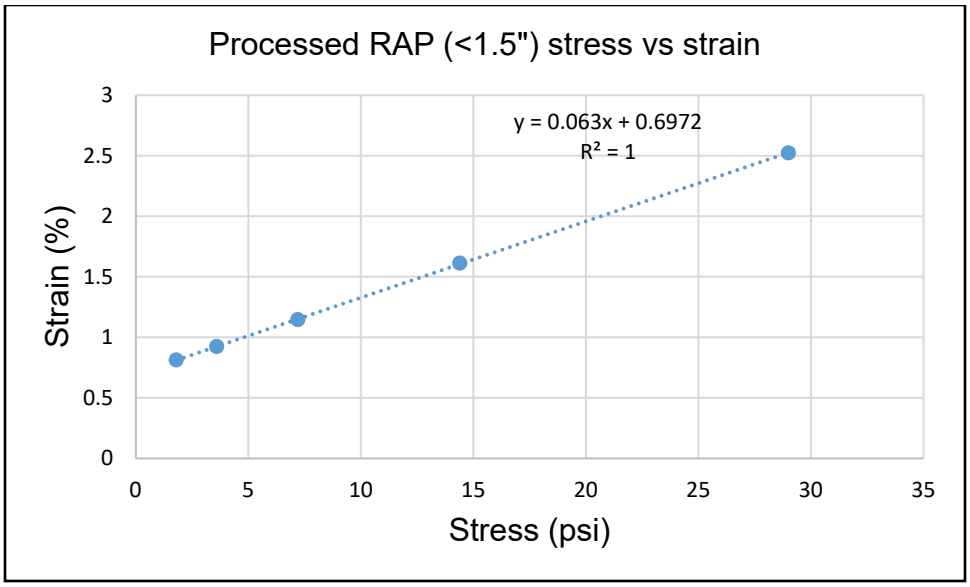

FIGURE 106. Stress vs. strain for average of processed RAP samples (< 1.5 in.).

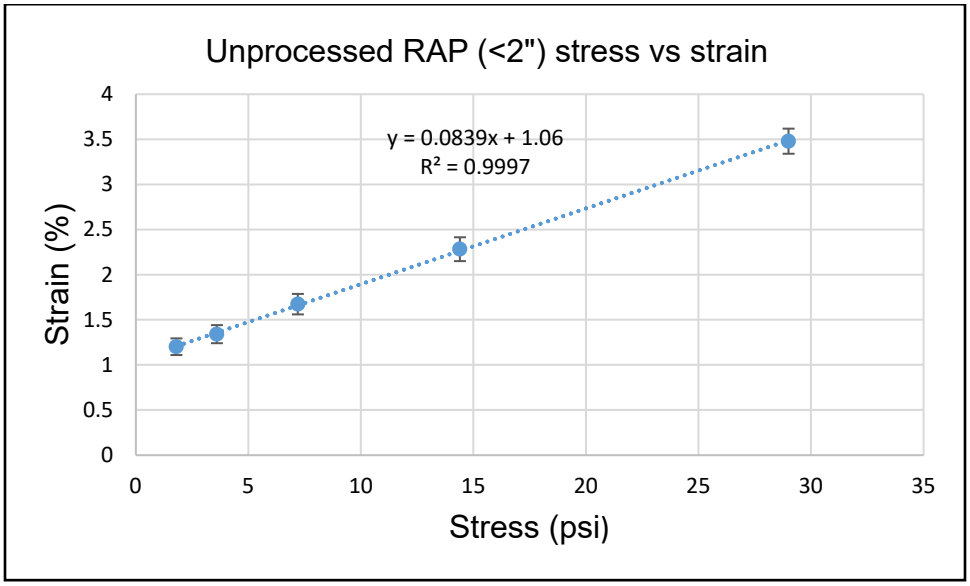

FIGURE 107. Stress vs. strain for average of unprocessed RAP samples (< 2 in.).

Unlike RAP, which exhibits fairly consistent behavior among different sources, soils may exhibit very different consolidation behavior. Thus, laboratory 1-D consolidation tests of the embankment soils are recommended. For the purpose of demonstration, Figure 117 and Equations (16) and (17) present the relationship between stress and strain based on the average 1-D consolidation test results of two soils under saturated and OMC conditions, respectively.

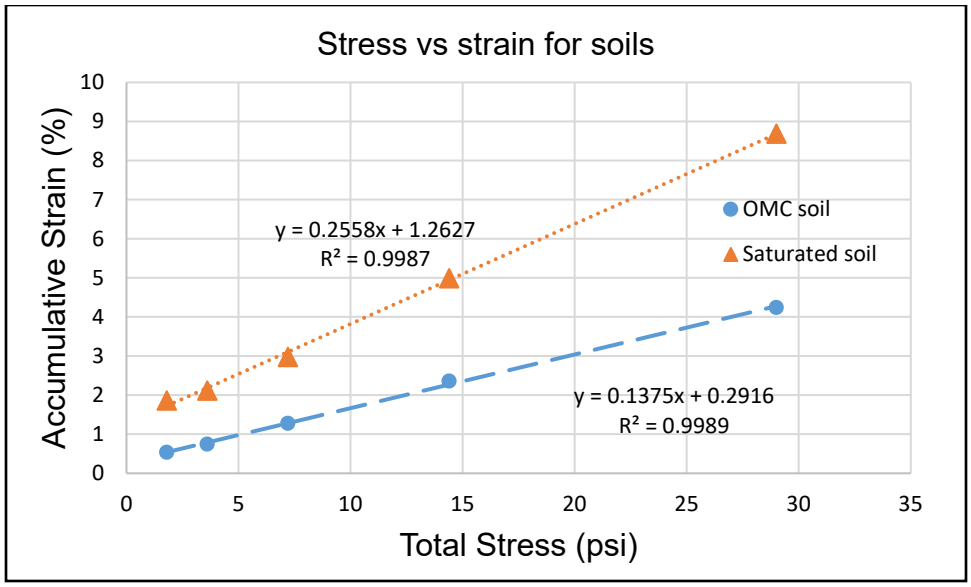

FIGURE 108. Stress vs. strain for average of soils.

$$\varepsilon_p = 0.2558\sigma+1.27 \quad \text{(saturated soil)} \tag{16}$$

$$\varepsilon_p = 0.1375\sigma+0.29 \quad \text{(soil at OMC)} \tag{17}$$

where

ε_p = settlement strain, %; and

σ = overburden stress, psi.

CHAPTER 6: CONCLUSIONS AND RECOMMENDATIONS

In this study, the research team investigated the use of RAP as embankment material. Based on a literature review, survey results, forensic study, laboratory experiments, and settlement analyses, the following conclusions and recommendations can be made.

6.1 Conclusions

1. The MDD of the five RAP samples investigated in this study increased as the temperature was increased, indicating the effect of placement temperature on the compaction of RAP. The MDD values of the RAP samples were almost the same as those of the two soils investigated in this study. The mixture of soil and RAP (soil + RAP mix) had significantly higher MDD values than the soils or RAP samples alone. The reason for this outcome is that the fine particles of the soil filled the voids between the coarse RAP particles.
2. The RAP samples exhibited significantly greater permeability than the two soils or soil + RAP mix. When RAP was located immediately below the drainage layer, the water in the drainage layer drained into the RAP layer, which in turn collected the water and saturated the embankment soil under the RAP layer.
3. An increase in the 1-D consolidation test temperature significantly increased the settlement of the RAP samples. The saturated soils exhibited much greater settlement than at the OMC, as expected. At room temperature, the settlement of the RAP samples was similar to that of the soils. However, the RAP samples at room temperature showed greater settlement at low stress levels than the soils. In order to achieve settlement at low stress levels that is comparable to settlement of natural soils, RAP needs to be compacted to 100% standard density determined at room temperature (minimum 70ºF).
4. The RAP samples that passed the 1.5-in. sieve experienced significantly less settlement than the RAP samples that passed the 2.0-in. sieve. In order to achieve good performance, RAP needs to be processed and be able to pass the 1.5-in. sieve.
5. Preliminary 1-D consolidation test results for the soil + RAP (50/50) mix indicate that a soil + RAP mix will experience less settlement than soil or RAP alone and

has great potential to serve as embankment material in terms of its resistance to settlement and water infiltration.

6. Under dynamic triaxial testing, which mimics traffic loads, most of the RAP samples (< 2.0-in. sieve) had significantly higher permanent deformation levels than the two soils or soil + RAP mix. The other RAP samples (< 1.5-in. sieve) had lower permanent deformation levels, but did not stabilize as soil or the soil/RAP mix did under dynamic loading. Therefore, RAP should not be used within the influence zone of traffic loading.
7. Based on the stress analysis results, RAP should not be used within the top 5 ft of an embankment in a rigid pavement structure or within the top 8 ft of an embankment in a flexible pavement structure. Also, RAP should not be used in an embankment above a buried rigid structure or bedrock.
8. The RAP samples exhibited relatively minor settlement, e.g., less than 1 in. at room temperature (70^{o}F), depending on the RAP layer thickness. However, the presence of RAP introduces the possibility that water will infiltrate and collect in the RAP layer and then saturate the underlying embankment soil, especially when the RAP layer is not capped with soil.
9. Even though RAP settlement typically is relatively minor, the RAP layer should be included in settlement analysis for the case of possible fast-track RAP embankment construction by contractors, such as the case of I-90 Jane Addams Memorial Tollway project (Contract 4206). A relationship between stress and plastic strain for unprocessed RAP (< 1.5-in.) and RAP (< 2.0-in.) at room temperature (70^{o}F) is recommended to be used by the designer to account for the strain-based settlement of the RAP layer, as expressed in Equations (14) and (15).
10. The current IDOT soil settlement analysis method does not include embankment settlement. However, the 1-D consolidation test results indicate that significant settlement can occur in embankment soil when it is saturated in an embankment after the placement of the pavement structure, which would cause severe surface settlement. A strain-based method or void-ratio-based method (i.e., Equation (13)) that is based on laboratory 1-D consolidation tests is recommended for all future projects.

6.2 Recommendations for Further Study

Based on this study, the following considerations and topics are reommended for further study.

1) The long-term effectiveness of soil capping is unknown. The effectiveness of soil capping should be studied by instrumenting and monitoring the moisture content in embankment soil.
2) The use of RAP in embankments, even when capped with soil, can pose the risk of water infiltration and water storage in the RAP layer, which will saturate the underlying embankment soil. A soil + RAP mix seems to be excellent alternative material in terms of resistance to settlement and permeability and providing good performance under dynamic traffic loading compared to soils or RAP alone. Thus, soil + RAP mixtures should be studied in terms of the soil-to-RAP ratio, placement method, and quality control for their possible use in embankments.
3) The effectiveness of a permeable base layer should be evaluated. Although a permeable base layer may remove moisture from the pavement, it presents risks to the embankment settlement.

6.3 Proposed Revisions to Illinois Tollway's Special Provision for Embankment Materials

The proposed revisions (highlighted in red below) to Illinois Tollway's Special Provision for embankments are as follows.

1. Embankment Source Submittal Requirements

Unless otherwise specified in the contract plans, any proposed earth excavation, borrow excavation, and furnished excavation locations are to be designated by the Contractor and approved by the Engineer prior to their use. The Contractor shall submit the following information to the Engineer for approval no later than 30 days prior to the planned start of work at each area:

(a) Location map for the proposed excavation:

i. Property boundaries

ii. Planned excavation extents

iii. Access locations

iv. Planned depths and quantity of excavation

v. Contractor's proposed sampling locations for geotechnical and environmental testing

(b) Narrative that describes the planned use, schedule, and quantities planned for the excavation.

(c) Written permission for the Illinois Tollway and Engineer to enter the non-job site property to collect earth excavation and furnished excavation soil samples for geotechnical and environmental testing.

2. Zone A Embankment Material

Zone A embankment material shall be as required in Sections 202, 204, and 205 of the Standard Specifications, except as follows.

All on-site material used for Zone A embankments must be approved by the Engineer prior to placement. Where furnished excavation is used, the excavation source location, excavation plan, and material must be approved by the Engineer in writing prior to any off-site work.

(a) The laboratory Standard Dry Density shall be a minimum of 98 lb/cu ft when determined according to AASHTO T 99 (Method C).

b) The organic content shall be less than 10% determined according to AASHTO T-194 (Wet Combustion).

c) ~~Soils~~ Fill materials (including mineral soils, reclaimed asphalt, broken concrete, and other embankment materials) that demonstrate the following properties shall be restricted to the interior of the embankment and shall be covered on both the sides and top of the embankment by a minimum of 3 ft of soil not considered detrimental in terms of erosion potential or excess volume change.

1. A grain size distribution with less than 35% passing the No. 75 um (#200) sieve as tested per AASHTO T 88.

2. A plasticity index value of less than 12 as tested per AASHTO T 90.

3. A liquid limit value in excess of 50 as tested per AASHTO T 89.

d) For each test method listed in Items (a) through (c) above, one test will be performed for every 5000 cubic yards of embankment, or as required by the Engineer.

e) RAP shall not be used within the ground water table or as fill if ground water is present.

f) In areas that support roadway pavement and structures, the placement of RAP shall be allowed only when the ambient air temperature is 40°F and rising.

g) RAP used shall be used according to the current IDOT Bureau of Materials and Physical Research Policy Memorandum, 'Reclaimed Asphalt Pavement (RAP) for Aggregate Applications', and the 'Illinois Tollway Special Provision for Reclaimed Asphalt Materials (RAM)'. Gradation deleterious count shall not exceed 10% of total RAP and 5% of other by total weight. In addition, the material shall have 100% passing the 1.5-in. sieve and be well graded down through fines. The resulting gradation shall vary by no more than 25%Cumulative Retained when screened across the 1 ½ in., 1 in., ¾ in., 5/8 in., ½ in., 3/8 in., ¼ in., #4, #8, and #16 sieves. Gradations may be performed dry, without the need for washing per ASTM C136. RAP shall not be used within the top five feet of an embankment in a rigid pavement or within the top eight feet of an embankment in a flexible pavement. RAP shall not be used in an embankment above any rigid underground structure or bedrock.

Zone A embankment material shall be sampled, tested, and approved before use. The contractor shall identify embankment sources and provide equipment as the Engineer requires for the collection of samples from those sources. Samples will be furnished to the Engineer a minimum of 14 days prior to use in order that laboratory tests for approval and compaction can be performed. Embankment material placement cannot begin until tests are completed and approval given. The Engineer may collect independent soil samples and perform confirmatory tests prior to approval.

3. Zone B Embankment Material

Zone B embankment material shall be free from stumps, large roots, frozen materials, and chemical contaminants that inhibit the growth of vegetation. Excess topsoil and material not suitable for placement in Zone A embankments may be used in Zone B embankments.

Construction Requirements

1. Placing Zone A Embankment Material

Zone A embankment material shall be placed in accordance with Article 205.04 of the Standard Specifications, with the following additional requirements.

In addition to Article 202.03 of the Standard Specifications, broken concrete, reclaimed asphalt with no expansive aggregate, or uncontaminated dirt and sand generated from construction or demolition activities shall be placed in 6-inch lifts and disked with the underlying lift until a uniform homogenous material is formed. This process also applies to the overlaying lifts. The disk must have a minimum blade diameter of 24 inches.

When embankments are to be constructed on hillsides or existing slopes that are steeper than 3H:1V, steps shall be keyed into the existing slope by stepping and benching as shown in the plans or as directed by the engineer.

2. Placing Zone B Embankment Material

Zone B embankment material shall be deposited in uniform layers not to exceed 8 in. in loose depth for the full width of the zones, except that wet material shall be placed in layers not exceeding 6 in. in depth and successive layers of wet material shall not be placed. Each lift shall be thoroughly compacted before the next lift is started.

Layers of drier material shall be alternated with layers of wetter material. The level of the Zone B embankment shall be kept lower than the elevation level of a Zone A embankment. Each layer of Zone B embankment shall be stepped or benched a minimum distance of 2 ft into an adjacent Zone A embankment to prevent the formation of slippage planes between the two zones. When topsoil is used in a Zone B embankment, it shall be mixed prior to or during placement with other Zone B materials to prevent the formation of slippage planes or zones of significantly different density.

Rigid control of the moisture content of the material placed in a Zone B embankment will not be required. However, if, in the opinion of the Engineer, material placed for a Zone B embankment is excessively wet, then the material shall be allowed to dry before being compacted or a layer of drier material may be placed over the loose layer of wet material. The two layers shall then be mixed by disking, harrowing, or other means until a moisture content that is satisfactory to the Engineer is attained before compaction of the layer commences. If, in the opinion of the Engineer, material placed for a Zone B embankment is excessively dry, then water shall be added and mixed into the layer by disking before compaction of the layer commences.

No embankment material that does not meet the requirements of a Zone A embankment shall be imported to the project for use as Zone B embankment material, unless approved by the Engineer.

3. Compaction of Zone A Embankment Material

Zone A embankment material shall be compacted in accordance with Article 205.06 of the Standard Specifications, except as follows.

RAP shall be compacted to no less than 100% of the standard laboratory density (AASHTO T 99 (Method C)) determined at room temperature (minimum 70ºF). The soil classification for moisture content control will be determined by the Soils Inspector using visual field examination techniques and the IDH Textural Classification Chart.

When tested for density in place, each lift shall have a maximum moisture content as follows.

a) A maximum of 110% of the optimum moisture for all forms of clay soils.

b) A maximum of 105% of the optimum moisture for all forms of clay loam soils.

c) A maximum of 90% of the optimum moisture for silt and silt loam soils.

Each lift of embankment material shall be disked sufficiently to break down oversized clods, mix the different materials, secure uniform moisture content, effectively drying as necessary, and ensure uniform density and compaction.

The Contractor shall disk and dry the embankment material to achieve proper moisture content and density. The Contractor will be permitted to use an approved additive to provide a quicker drying time. As soon as acceptable moisture contents are achieved, the Contractor must complete the compaction of the layer as specified herein and to the satisfaction of the Engineer. No separate payment will be made for this work.

If the Engineer approves the Contractor to place the embankment with an excessively high moisture content (greater than 120% of the OMC at the time of placement), then the Contractor will be compensated in accordance with the Illinois Tollway Special Provision for Embankment Modification.

Compacting equipment, compacting operations, and modification procedures shall be coordinated with the rate of placing the embankment so that the required density is obtained.

Density and moisture content tests shall be performed at a minimum frequency indicated in the Contractor Quality Program Manual. Each test location shall be verified for stability as well. Embankment stability will be measured using a dynamic cone penetrometer according to the test method in the IDOT Geotechnical Manual. The penetration rate must be equal to or less than 1.5 in. per blow.

4. Compaction of Zone B Embankment Material

Zone B embankment material shall be compacted to no less than 80% of the standard laboratory density (AASHTO T 99) for the full width of the zone.

REFERENCES

AASHTO. (2011). *Guide Specifications for LRFD Seismic Bridge Design*, 2nd edition. American Association of State Highway and Transportation Officials, Washington, DC.

Abdelrahman, M., Alam, T., & Zollars, J. (2010). Performance of high recycled asphalt pavement (RAP) content as base layer in flexible pavement. *The Journal of Solid Waste Technology and Management, 36*(3), 131-142.

Alam, T. B., Abdelrahman, M., & Schram, S. A. (2010). Laboratory characterisation of recycled asphalt pavement as a base layer. *International Journal of Pavement Engineering, 11*(2), 123-131. https://doi.org/10.1080/10298430902731362

Arm, M. (2000). Self-cementing properties of crushed demolishing concrete in unbound layers results from triaxial tests and field tests. *Waste Management Series, 1*, 579-587. https://doi.org/10.1016/S0956-053X(00)00095-7

Attia, M., & Abdelrahman, M. (2010). Sensitivity of untreated reclaimed asphalt pavement to moisture, density, and freeze thaw. *Journal of Materials in Civil Engineering, 22*(12), 1260-1269. https://doi.org/10.1061/(ASCE)MT.1943-5533.0000135

Augustesen, A., Liingaard, M., & Lade, P. V. (2004). Characterization of models for time-dependent behavior of soils. *International Journal of Geomechanics, 4*(3), 157-177. https://doi.org/10.1061/(ASCE)1532-3641(2004)4:3(157)

Bandara, N., & Rowe, G. M. (2003). *Design subgrade resilient modulus for Florida subgrade soils*. (STP12524S). ASTM International. https://www.astm.org/

Baktash, N. (2021). *Experimental Investigation of Creep in Unsaturated Soils*. [Ph.D. Thesis, The University of New South Wales]. http://unsworks.unsw.edu.au/fapi/datastream/unsworks:76398/SOURCE02?view=true

Bejarano, M. O. (2001). *Evaluation of recycled asphalt concrete materials as aggregate base.* (Technical Memorandum TM-UCB-PRC-2001-4). Prepared for California Dept. of Transportation.

Bennert, T., Papp, W. J., Maher, A., & Gucunski, N. (2000). Utilization of construction and demolition debris under traffic-type loading in base and subbase applications. *Transportation research record, 1714*(1), 33-39. https://doi.org/10.3141/1714-05

Bennert, T., & Maher, A. (2005). T*he development of a performance specification for granular base and subbase material.* (No. FHWA-NJ-2005-003). Prepared for New Jersey. Dept. of Transportation.

Berg, R. R., Samtani, N. C., & Christopher, B. R. (2009). *Design of mechanically stabilized earth walls and reinforced soil slopes–Volume II.* (No. FHWA-NHI-10-025). Prepared for U.S. Dept. of Transportation, Washington, DC.

Bergaya, F., Lagaly, G., & Vayer, M. (2013). Cation and anion exchange. *Developments in clay science, 5,* 333-359. https://doi.org/10.1016/B978-0-08-098259-5.00013-5

Camargo, F. F., Wen, H., Edil, T., & Son, Y. H. (2013). Comparative assessment of crushed aggregates and bound/unbound recycled asphalt pavement as base materials. *International Journal of Pavement Engineering, 14*(3), 223-230. https://doi.org/10.1080/10298436.2012.655737

Campanella, R. G., & Vaid, Y. P. (1974). Triaxial and plane strain creep rupture of an undisturbed clay. *Canadian Geotechnical Journal, 11*(1), 1-10. https://doi.org/10.1139/t74-

001
Chesner, W. H., Collins, R. J., MacKay, M. H., & Emery, J. (2002). *User guidelines for waste and by-product materials in pavement construction* (No. FHWA-RD-97-148). Prepared for Recycled Materials Resource Center, US Department of Transportation, Federal Highway Administration.
Christopher, B. R., Schwartz, C. W., & Boudreau, R. L. (2010). *Geotechnical aspects of pavements: Reference manual.* Prepared for US Department of Transportation, Federal Highway Administration.
Cleary, E. D. (2005). *Long-term Behavior of RAP-soil Mixtures for Use as Backfill behind MSE Walls.* [Doctoral Dissertation, Florida Institute of Technology].
Copeland, A. (2011). *Reclaimed asphalt pavement in asphalt mixtures: State of the practice* (No. FHWA-HRT-11-021). Prepared for Office of Research, Development, and Technology, Federal Highway Administration.
Cosentino, P. J., Kalajian, E. H., Shieh, C. S., Mathurin, W. J. K., Gomez, F. A., Cleary, E. D., & Treeratrakoon, A. (2003). *Developing specifications for using recycled asphalt pavement as base, subbase or general fill materials, phase II* (No. FL/DOT/RMC/06650-7754). Prepared for Florida Department of Transportation.
Cosentino, P. J., Kalajian, E. H., Bleakley, A. M., Diouf, B. S., Krajcik, R. E., Misilo, T. J., Petersen, A.J. & Sajjadi, A. M. (2012). *Improving the properties of reclaimed asphalt pavement for roadway base applications* (No. FL/DOT/BDK81 97702). Prepared for Florida Department of Transportation.
Cosentino, P. J., Kalajian, E. H., Dikova, D., Patel, M., & Sandin, C. (2008). In*vestigating the Statewide Variability and Long Term Strength Deformation Characteristics of RAP and RAP-Soil Mixtures* (No. FL/DOT/RMC/06650-7754). Prepared for Florida Department of Transportation.
Dikova, D. (2006). *Creep Behavior of RAP-Soil Mixtures in Earthwork Applications*. [Master of Science thesis, Florida Institute of Technology].
Doig, B. (2000). *Influence of Storage Time and Temperature on the Triaxial Characterization of RAP*. [Master of Science Thesis, Florida Institute of Technology].
Edil, T. B., Tinjum, J. A., & Benson, C. H. (2012). *Recycled unbound materials.* (Report No. MN/RC, 35). Prepared for Minnesota Department of Transportation.
El, M. I., & Attia, S. (2010). *Characterization of the structural behavior of reclaimed asphalt pavement as pavement base layer.* North Dakota State University.
Elias, V., Christopher, B. R., Berg, R. R., & Berg, R. R. (2001). *Mechanically stabilized earth walls and reinforced soil slopes: design and construction guidelines (updated version)* (No. FHWA-NHI-00-043). Prepared for Federal Highway Administration. United States.
Garg, N., & Thompson, M. R. (1996). Lincoln Avenue reclaimed asphalt pavement base project. *Transportation Research Record, 1547*(1), 89-95. https://doi.org/10.3141/1547-13
Guthrie, W. S., Brown, A. V., & Eggett, D. L. (2007). Cement stabilization of aggregate base material blended with reclaimed asphalt pavement. *Transportation Research Record, 2026*(1), 47-53. https://doi.org/10.3141/2005-06
Hoppe, E. J., Lane, D. S., Fitch, G. M., & Shetty, S. (2015). *Feasibility of Reclaimed Asphalt Pavement (RAP) Use As Road Base and Subbase Material*. (VCTIR 15-R6, 1–42). Prepared for Virginia Department of Transportation.
Kazmee, H., Tutumluer, E., & Beshears, S. (2016). Pavement working platforms constructed with large-size unconventional aggregates. *Transportation Research Record, 2578*(1), 1-11.

https://doi.org/10.3141/2578-01
Kim, W., & Labuz, J. F. (2007). *Resilient Modulus and Strength of Base Course with Recycled Bituminous Material.* (Report Mn/DOT 2007-05). Prepared for Minnesota Department of Transportation.
Kim, W., Labuz, J. F., & Dai, S. (2007). Resilient modulus of base course containing recycled asphalt pavement. *Transportation research record, 2005*(1), 27-35. https://doi.org/10.3141/2005-04
Kong, X. (2016). *Prediction of Subgrade Settlement Based Fuzzy Self Adaptable Method of Artificial Intelligence.* 2016 9th International Symposium on Computational Intelligence and Design (ISCID), Hangzhou, China. https://doi.org/10.1109/ISCID.2016.1041
Lacasse, S., & Berre, T. (2005). *Undrained creep susceptibility of clays*. Proceedings of the 16th International Conference on Soil Mechanics and Geotechnical Engineering, Amsterdam, Netherlands.
Lade, P. V., & Liu, C. T. (1998). Experimental study of drained creep behavior of sand. *Journal of engineering mechanics, 124*(8), 912-920. https://doi.org/10.1061/(ASCE)0733-9399(1998)124:8(912)
Lafleur, J., Mlynarek, J., & Rollin, A. L. (1989). Filtration of broadly graded cohesionless soils. *Journal of Geotechnical Engineering, 115*(12), 1747-1768. https://doi.org/10.1061/(ASCE)0733-9410(1989)115:12(1747)
MacGregor, J. A., Highter, W. H., & DeGroot, D. J. (1999). Structural numbers for reclaimed asphalt pavement base and subbase course mixes. *Transportation research record, 1687*(1), 22-28. https://doi.org/10.3141/1687-03
McDaniel, R. S., & Anderson, R. M. (2001). *Recommended use of reclaimed asphalt pavement in the Superpave mix design method: technician's manual* (No. Project D9-12 FY'97). Prepared for National Cooperative Highway Research Program.
Mesri, G., & Castro, A. (1987). Cα/Cc concept and K_0 during secondary compression. *Journal of Geotechnical Engineering,113*(3), 230-247. https://doi.org/10.1061/(ASCE)0733-9410(1987)113:3(230)
Mesri, G., Feng, T. W., & Benak, J. M. (1992). Postdensification penetration resistance of clean sands. *Journal of Geotechnical Engineering, 118*(3), 511-513. https://doi.org/10.1061/(ASCE)0733-9410(1990)116:7(1095)
Mitchell, J. K., & Soga, K. (2005). *Fundamentals of Soil Behavior* (Vol. 3). New York: John Wiley & Sons.
Montemayor, T. A. (1998). *Compaction and Strength-Deformation Characteristics of Reclaimed Asphalt Pavement*. [Master of Science Thesis, Florida Institute of Technology].
Nagaraj, T. S., Pandian, N. S., & Narashima Raju, P. S. R. (1991). An approach for prediction of compressibility and permeability behaviour of sand bentonite mixes. *Indian Geotechnical Journal*, *21*(3), 271–282.
Nokkaew, K., Tinjum, J. M., & Benson, C. H. (2012). *Hydraulic properties of recycled asphalt pavement and recycled concrete aggregate*. GeoCongress 2012: State of the Art and Practice in Geotechnical Engineering, Oakland, California. https://doi.org/10.1061/9780784412121.152
Ping, W. V., Leonard, M., & Yang, Z. (2003). *Laboratory simulation of field compaction characteristics (Phase I)* (No. FL/DOT/RMC/BB-890 (F)). Prepared for Florida Department of Transportation.
Ping, W. V, Xing, Leonard, M., & Yang, Z. (2003). *Evaluation of Laboratory Compaction*

Techniques for Simulating Field Soil Compaction (Phase II). (No. FL/DOT/RMC/BB-890(F)). Prepared for Florida Department of Transportation.
Piratheepan, J., Arulrajah, A., & Disfani, M. M. (2013). Large-scale direct shear testing of recycled construction and demolition materials. *Advances in Civil Engineering Materials*, *2*(1), 25–36.
Rahardjo, H., Vilayvong, K., & Leong, E. C. (2011). Water characteristic curves of recycled materials. *Geotechnical Testing Journal, 34*(1), 89-96. https://doi.org/10.1520/GTJ103177
Rathje, E. M., Rauch, A. F., Trejo, D., Folliard, K. J., Viyanant, C., Esfellar, M., Jain, A. & Ogalla, M. (2006). *Evaluation of crushed concrete and recycled asphalt pavement as backfill for mechanically stabilized earth walls.* (No. FHWA/TX-06/0-4177-3). Prepared for Texas Department of Transportation.
Roberts, F. L., Kim, Y. R., Lee, D. Y., & Kennedy, T. W. (2009). *Hot Mix Asphalt Materials, Mixture Design, and Construction* (2nd edition). National Center for Asphalt Technology.
Rosa, M. G. (2006). *Effect of Freeze and Thaw Cycling on Soils Stabilized Using Fly Ash*. [Master of Science Thesis, University of Wisconsin-Madison].
Sandin, C. M. (2008). *Laboratory Evaluation of the Variability of Florida's RAP Materials for Use in Earthwork Applications*. [Doctoral Dissertation, Florida Institute of Technology].
Schaefer, V. R., White, D. J., Ceylan, H., & Stevens, L. J. (2008). *Design Guide for Improved Quality of Roadway Subgrades and Subbases*. (IHRB Project TR-525). Prepared for Iowa Highway Research Board.
Sharma, A. K., & Sivapullaiah, P. V. (2016). Ground granulated blast furnace slag amended fly ash as an expansive soil stabilizer. *Soils and Foundations, 56*(2), 205-212. https://doi.org/10.1016/j.sandf.2016.02.004
Singh, A., & Mitchell James Kenneth. (1969). *Creep potential and creep rupture of soils*. Proceedings of the Seventh International Conference on Soil Mechanics and Foundation Engineering, Mexico.
Soleimanbeigi, A., Edil, T. B., & Benson, C. H. (2014). Engineering properties of recycled materials for use as embankment fill. *Geotechnical Special Publication*, *234 GSP*, 3645–3657. https://doi.org/10.1061/9780784413272.353
Soleimanbeigi, A., & Edil, T. B. (2015). Compressibility of recycled materials for use as highway embankment fill. *Journal of Geotechnical and Geoenvironmental Engineering*, *141*(5), 1–14. https://doi.org/10.1061/(ASCE)GT.1943-5606.0001285
Soleimanbeigi, A., Likos, W. J., Tanyu, B. F., Aydilek, A. H., & Florio, P. (2016). *Recycled Materials as Backfill for Mechanically Stabilized Earth Walls*. University of Wisconsin-Madison.
Soleimanbeigi, A., Shedivy, R. F., Tinjum, J. M., & Edil, T. B. (2015). Climatic effect on resilient modulus of recycled unbound aggregates. *Road Materials and Pavement Design*, *16*(4), 836–853. https://doi.org/10.1080/14680629.2015.1060250
Taha, R., Ali, G., Basma, A., & Al-Turk, O. (1999). Evaluation of reclaimed asphalt pavement aggregate in road bases and subbases. *Transportation Research Record, 1652*(1), 264-269.
Thakur, J. K., & Han, J. (2015). Recent development of recycled asphalt pavement (RAP) bases treated for roadway applications. *Transportation Infrastructure Geotechnology*, *2*(2), 68–86. https://doi.org/10.1007/s40515-015-0018-7
Ting, J. M. (1983). On the nature of the minimum creep rate–time correlation for soil, ice, and frozen soil. *Canadian Geotechnical Journal, 20*(1), 176-182. https://doi.org/10.1139/t83-017

Vennapusa, P. K. R., Keltner, L., & White, D. J. (2015). *Permeability Performance and Lateral Load for Granular Backfill Behind Abutments*. (WisDOT ID no. 0092-14-03). Prepared for Wisconsin Department of Transportation.

Viyanant, C., Rathje, E. M., & Rauch, A. F. (2007). Creep of compacted recycled asphalt pavement. *Canadian Geotechnical Journal, 44*(6), 687-697. https://doi.org/10.1139/T07-022

Wen, H., Warner, J., & Edil, T. (2008). *Laboratory comparison of crushed aggregate, recycled pavement materials with and without high carbon fly ash.* Proceedings of the 87th Transportation Research Board. Washington DC.

Wen, H., Warner, J., Edil, T., & Wang, G. (2010). Laboratory comparison of crushed aggregate and recycled pavement material with and without high carbon fly ash. *Geotechnical and Geological Engineering, 28*(4), 405-411. https://doi.org/10.1007/s10706-009-9300-1

Wen, H., Wu, M., & Uhlmeyer, J. (2011). Evaluation of the effects of climatic conditions on modulus of base materials with recycled asphalt pavement. *Journal of ASTM International*, *8*(10). https://doi.org/10.1520/JAI103701

West, R. C. (2015). *Best Practices for RAP and RAS Management*. National Asphalt Pavement Association.

Williams, B. A., Willis, J. R., & Ross, T. C. (2019). *Asphalt Pavement Industry Survey on Recycled Materials and Warm-Mix Asphalt Usage: 2018.* National Asphalt Pavement Association.

Yin, J., Soleimanbeigi, A., Likos, W. J., & Edil, T. B. (2017). Effects of temperature on creep behavior of compacted recycled asphalt pavement. *Journal of Geotechnical and Geoenvironmental Engineering*, *143*(4), 1–8. https://doi.org/10.1061/(ASCE)GT.1943-5606.0001636

Zou, C., Wang, Y., Lin, J., & Chen, Y. (2016). Creep behaviors and constitutive model for high density polyethylene geogrid and its application to reinforced soil retaining wall on soft soil foundation. *Construction and Building Materials, 114*, 763-771. https://doi.org/10.1016/j.conbuildmat.2016.03.194

Zou, L., Wang, S., & Lai, X. (2013). Creep model for unsaturated soils in sliding zone of Qianjiangping landslide. *Journal of Rock Mechanics and Geotechnical Engineering, 5*(2), 162-167. https://doi.org/10.1016/j.jrmge.2013.03.001